

CHAPTER 6 STUDY OF GROUND IMPROVEMENT USING AN AGGREGATE PIER FOUNDATION SYSTEM

The FLAC analyses were focused on two parts: the pore water pressure and the shear stress in soil matrix. The first three sections of this chapter discuss the former and the fourth section discusses the latter.

There were total of 20 cases analyzed using FLAC. The Loma Prieta and Saguenay earthquake records were used to analyze 9 cases each as shown on Table 6.1 and Figure 6.1. Cases with C indicate cases using Loma Prieta earthquake and cases with S indicate cases using Saguenay earthquake (refer to Table 5.1 for the soil, water, and aggregate pier parameters used in FLAC analyses). The last two cases were analyzed with emphasis on the shear stress in soil matrix (see Section 6.4).

Table 6.2 shows the figures that were used for each case (refer to Chapter 5 for the figures). The following sections explain the results of the studies.

6.1 Parametric Study

Before the cases presented on Table 6.1 were analyzed using FLAC, preliminary investigations were carried out to obtain a better understanding of how FLAC works. This objective was achieved by comparing FLAC and SHAKE91 (Idriss and Sun, 1992) and by conducting a parametric study using FLAC.

6.1.1 Comparison between SHAKE91 and FLAC

SHAKE91 (Idriss and Sun, 1992) is a modification of SHAKE (Schnabel, et al., 1972) a computer program that analyzes the behavior of horizontally layered soil deposits under seismic loading using equivalent linear method. SHAKE was chosen because it is still the most widely used computer program in earthquake engineering analyses. It works in frequency domain and uses iterative procedure to take partly into account the nonlinear behavior of soils.

A problem similar to Case 1C (Table 6.1 and Figure 6.1a) involving a reinforced ground with aggregate pier was created. The only difference is the value of the moduli, which are slightly lower and higher for bulk modulus and shear modulus, respectively. Table 6.3 shows the values of soil and rock parameters that were used both in SHAKE91 and FLAC analysis. It was assumed that both shear modulus and damping are strain-independent. The model consists of 14.5 feet thick of loose silty sand. In SHAKE91, the layer is divided into 29 layers with 0.5 feet thick each layer as shown Figure 6.2. While in FLAC, the model used was 1 foot by 14.5 feet divided into 4 by 29 zones as shown on Figure 6.3. Both analyses used the Loma Prieta earthquake time history. Free field boundaries and silent boundary were assigned in the FLAC analysis.

Figure 6.4 shows histories of the peak acceleration on rock outcrops (a_{ga}) and the peak acceleration on the ground surface (a_{max}). The results from SHAKE 91 were shown on black lines while those from FLAC were shown on gray lines. It can be seen that SHAKE91 results in a_{max} of 1.72g occurring at about 1.3 seconds. The value of a_{max} from FLAC is 1.61g also occurring at about 1.3 seconds. It can be concluded that both SHAKE91 and FLAC show a reasonable agreement both for the values of a_{ga} and a_{max} .

Figures 6.5 and 6.6 show the comparison of shear stress and shear strain time histories at depth of 4.5 feet, respectively, between SHAKE91 and FLAC. Figure 6.5 shows that SHAKE91 gives the maximum shear stress of 0.886 ksf while FLAC gives slightly smaller shear stress (=0.867 ksf). Figure 6.6 shows that SHAKE91 and FLAC result in maximum shear strain of 0.732% and 0.719%, respectively. All maximum shear stresses and shear strains occur at about 1.29 seconds.

Figures 6.7 and 6.8 show the comparison of shear stress and shear strain time histories at depth of 9.5 feet, respectively, between SHAKE91 and FLAC. Figure 6.7 shows that SHAKE91 results in the maximum shear stress of 1.584 ksf while FLAC results in smaller shear stress of 1.485 ksf. Figure 6.8 shows that SHAKE91 and FLAC result in maximum shear strain of 1.31% and 1.231%, respectively. All maximum shear stresses and shear strains occur at about 1.29 seconds.

Table 6.4 summarizes the results by comparing the peak ground acceleration, the shear stresses and the shear strains. FLAC shows smaller values compared to those of SHAKE91

with difference ranging from 1.81% to 6.83%. The difference is smaller for depth of 4.5 feet than for depth of 9.5 feet.

It can be concluded that both FLAC and SHAKE91 show reasonably agreement.

6.1.2 The Effects of Varying Moduli

A parametric study was conducted for Case 2C, i.e. a case with 14.5 feet thick of loose silty sand with an aggregate pier installed. Case 2Ce was created to study the effects of varying moduli with depth. The two cases are basically the same. The difference is that for Case 2Ce, the elastic modulus was varied with depth. The value of elastic modulus was calculated by using the following equation suggested by Janbu (1963):

$$E_i = K p_a \left(\frac{\sigma_0'}{p_a} \right)^n \quad (6.1)$$

where:

E_i = initial tangent modulus

K = modulus number

n = modulus exponent with typical value of 0.5

p_a = atmospheric pressure with the same unit as E_i and σ_0'

σ_0' = effective overburden pressure

At the base of the model (at depth of 14.5 feet) the value of initial tangent modulus (E_i) of 315,000 psf was to be obtained, so that Case 2Ce will be comparable to Case 2C. Hence, the value of modulus number (K) of 237 was to be used. This value is still within the range found by Duncan et al. (1980). By substituting all the known values ($K = 237$, $p_a = 2116.22$ psf, $n = 0.5$, and saturated unit weight ($\gamma_{sat}) = 120$ pcf), equation (6.1) can be written as:

$$E_i = 501,413.15 \sqrt{0.027218342 * z} \quad (6.2)$$

where:

z = depth (in feet)

E_i = initial tangent modulus (in psf)

The stiffness of the composite (E) of aggregate pier and soil is then calculated by using equation (5.8) and the fact that the elastic modulus of the aggregate pier (E_g) is eight times larger than the elastic modulus of soil (E_s).

$$E_{composite} = 2.964 * E_{soil} \quad (6.3)$$

where E_{soil} can be computed using equation (6.2)

Therefore, by substituting equation (6.2) to equation (6.3), the following equation was obtained:

$$E_{composite} = 1.486 * 10^6 \sqrt{0.027218342 * z} \quad (6.4)$$

The values of bulk modulus (K) and shear modulus (G) can be determined as a function of elastic modulus (E) and Poisson's ratio (ν) using equations (5.6) and (5.7). Hence, for soil, the elastic modulus (E) varies from 0 to 315,000 psf on the ground surface and at depth of 14.5 feet, respectively, while the bulk modulus (K) varies from 0 to 315,000 psf and the shear modulus (G) varies from 0 to 118,125 psf. For the aggregate pier, the elastic modulus (E) varies from 0 to 933,625 psf on the ground surface and at depth of 14.5 feet, respectively, while the bulk modulus (K) varies from 0 to 501,299 psf and the shear modulus (G) varies from 0 to 392,412 psf.

Before the discussion is continued, it is important to define some parameters:

- The excess pore water pressure ratio (r_u) is defined as the ratio between excess pore water pressure and the initial effective vertical stress (Section 2.1.6). There are two values that become points of interest: the peak value and the steady state value. The peak value is the maximum value of r_u . The steady state is the constant value of r_u

reached for a certain period of time at the end of shaking. In the plot of the history of excess pore water pressure, the thicker solid lines show the history points with odd numbers, while the thinner solid lines show the history points with even numbers. The points referred to here are the points mentioned in Section 5.2.1.

- To ease the discussion the ground acceleration is divided into two types: the peak acceleration on rock outcrops is designated as p_{ga} and the peak acceleration at the soil surface is designated as a_{max} . Therefore, p_{ga} is used for both earthquake records: Loma Prieta and Saguenay earthquakes and a_{max} is used for all output from FLAC analyses.
- Improvement is defined as a decrease in the values of r_u due to installation of aggregate pier.

Cases 2C and 2Ce were compared with Case 1C, which is basically the same as Case 2C but without an aggregate pier installed. Figures 6.9 to 6.11 show the results of FLAC analyses for Case 1C. The results of Case 2C are presented on Figures 6.12 to 6.14 and those of Case 2Ce can be seen on Figures 6.15 to 6.17. The comparison of these three cases is summarized on Table 6.5.

For Case 1C, Figure 6.9 shows that the values of r_u increase rapidly during the first 1 second of shaking for all depths and then remain relatively constant after about 6 seconds until the end of shaking. It can be seen that the r_u values are somewhat close to each other ranging from 0.769 to 0.872. The values of r_u decrease with depths but then increase for the deepest point, i.e. Point 4 (depth of 12.25 feet). Figure 6.10 shows that the maximum acceleration at ground surface (a_{max}) is equal to 0.163g. Figure 6.11 shows plot of contours of effective horizontal stress.

For Case 2C, Figure 6.12 shows that the values of r_u increase rapidly during the first 2 seconds of shaking for Point 1. For Points 2 and 3, the r_u values increase slightly at the beginning of shaking and then decrease to negative values and increase again until 6 seconds of shaking and then remain relatively constant until the end of shaking. The r_u values for Point 4 lie within small range between 0 and 0.4. It is apparent that the values of r_u generally decrease with depths. Figure 6.13 shows that the maximum acceleration at ground surface (a_{max}) is equal to 0.381g. Figure 6.14 shows plot of contours of effective horizontal stress. It is apparent that

the high values of horizontal stresses are concentrated at soil elements adjacent to the shaft of the aggregate pier.

For Case 2Ce, Figure 6.15 shows that the values of r_u are negative for Point 1. For Point 2, the values of r_u increase slightly at the beginning of shaking and then decrease to about -0.7 and increase again to about 0.7 after 2 seconds of shaking and then remain relatively constant until the end of shaking. For Points 3 and 4, the r_u values increase during the first 8 seconds of shaking and then remain relatively constant until the end of shaking. Figure 6.16 shows that the maximum acceleration at ground surface (a_{max}) is equal to $0.416g$. Figure 6.17 shows plot of contours of effective horizontal stress. It is apparent that the high values of horizontal stresses are concentrated at soil elements adjacent to the shaft of the aggregate pier.

By using Case 1C as the basis of comparison it can be concluded from Table 6.5 that Case 2Ce shows improvement at shallower depths (Points 1 and 2, i.e. depths of 2.25 feet and 4.75 feet) while Case 2C shows that improvement occurs at the deepest point (Point 4 - depth of 12.25 feet). The values of r_u at depth of 2.25 feet (Point 1) of Case 2Ce are somewhat negative. According to the sign convention used in FLAC, this phenomenon means tensile condition. It was suspected that the use of low moduli values close to the ground surface (equals to zero on the ground surface) caused this problem. Table 6.5 also shows that both cases result in the amplification of ground acceleration (a_{max}), that is $0.381g$ and $0.416g$ for Cases 2C and 2Ce, respectively, compared to a_{max} of $0.163g$ for Case 1C.

Based on this parametric study, it was decided to use Case 2C, i.e. constant values of moduli with depth as a base model for cases with an aggregate pier foundation system.

6.2 Cases without an Aggregate Pier Foundation System

Four cases were analyzed to study the seismic behavior of the unreinforced soils. They are Case 1C, Case 3C, Case 1S, and Case 3S. These analyses were performed to provide a base case for judging the effect of the installation of aggregate pier foundation system.

Cases 1C and 1S show the analyses of loose silty sand with the thickness of 14.5 feet as shown on Figure 6.1a while Cases 3C and 3S show the analyses of silty sand layer of 26.5 feet-thick as shown on Figure 6.1b. Another difference of these cases is that Cases 1C and 3C were

run using the Loma Prieta earthquake time history while Cases 1S and 3S were run using the Saguenay earthquake time history (see Table 6.1).

Figures 6.9 to 6.11 show the results of FLAC analyses for Case 1C. The results of Case 3C are presented on Figures 6.18 to 6.20 and those of Cases 1S and 3S can be seen on Figures 6.21 to 6.23 and Figures 6.24 to 6.26, respectively.

The results for Case 1C have already been explained in the previous section. For Case 3C, Figure 6.18 shows that the values of r_u increase rapidly during the first 1 second of shaking for all depths and then remain relatively constant until the end of shaking. It is apparent that for Point 1 (depth of 2.25 feet) initial liquefaction occurs at 2 seconds of shaking ($r_u = 1.0$). The values of r_u decrease with depths up to the depth where the aggregate pier is installed (depth of 14.5 feet). Beyond this depth, the values of r_u do not follow a consistent trend. It increases at Point 5, decreases at Point 6, and increases again at Point 7. Figure 6.19 shows that the maximum acceleration at ground surface (a_{max}) is equal to 0.155g. Figure 6.20 shows plot of contours of effective horizontal stress.

The results for Cases 1C and 3C are compared on Table 6.6. For Case 3C, the values of r_u are close to unity at shallow depths (2.25 feet and 4.75 feet). The values of r_u decrease with depth up to 14.5 feet with values smaller than those of Case 1C. As expected, due to the use of deeper model, Case 3C shows slightly smaller value of a_{max} of 0.155g than Case 1C ($a_{max} = 0.163g$). Both cases show de-amplification of input pga of 0.45g.

For Case 1S, Figure 6.21 shows that the values of r_u increase during the first 3.5 seconds of shaking for all depths and then remain relatively constant until the end of shaking. It is apparent that the values of r_u decrease with depths. Figure 6.22 shows that the maximum acceleration at ground surface (a_{max}) is equal to 0.086g. Figure 6.23 shows plot of contours of effective horizontal stress.

For Case 3S, Figure 6.24 shows that the values of r_u increase during the first 3 seconds of shaking for Points 1 and 2 and then remain relatively constant until the end of shaking for Point 2. There is somehow a sudden increase at 8 to 9 seconds of shaking for Point 1 and then remain relatively constant until the end of shaking. The values of r_u are relatively small for Points 3 to 7. It can also be seen that the values of r_u generally decrease with depths. Figure 6.25 shows that the maximum acceleration at ground surface (a_{max}) is equal to 0.0588g. Figure 6.26 shows plot of contours of effective horizontal stress.

The results for Cases 1S and 3S are summarized on Table 6.7. As noted previously, the values of r_u decrease with depth for both cases. Case 3S shows smaller values of r_u compared to those of Case 1S, except for the shallowest depth (Point 1 – depth of 2.25 feet). Similar to Cases 1C and 3C, due to the use of deeper model, Case 3S shows smaller value of a_{max} of 0.0588g than Case 1S ($a_{max} = 0.086g$). Both cases show amplification of input pga of 0.05g.

6.3 Cases with an Aggregate Pier Foundation System

Four cases were also analyzed to study the seismic response of the reinforced soils. They were Case 2C, Case 4C, Case 2S, and Case 4S. They will be compared to each other and also to the cases without aggregate pier to observe the effects of installation of aggregate pier.

Figures 6.12 to 6.14 show the results of FLAC analyses for Case 2C. The results of Case 4C are presented on Figures 6.27 to 6.29 and those of Cases 2S and 4S can be seen on Figures 6.30 to 6.32 and Figures 6.33 to 6.35, respectively.

The results for Case 2C have already been explained in the previous section. For Case 4C, Figure 6.27 shows that for Point 1 (depth of 2.25 feet) the values of r_u slightly increase and then decrease to negative values and suddenly increase to unity and then decrease again and remain relatively constant until the end of shaking. It is apparent that for Point 1 initial liquefaction ($r_u = 1.0$) occurs at about 2 seconds of shaking. For Points 2 and 3, the r_u values are relatively similar and constant throughout the shaking. The values of r_u at Point 4 are somewhat negative. According to the sign convention used in FLAC, this phenomenon means tensile condition. The values of r_u increase during the first 0.05 seconds of shaking for Points 5, 6, and 7. It can be concluded that the values of r_u generally decrease with depths up to the depth where the aggregate pier is installed (depth of 14.5 feet). Beyond this depth, the values of r_u increase for Point 5 and then decrease with depths. Figure 6.28 shows that the maximum acceleration at ground surface (a_{max}) is equal to 0.38g. Figure 6.29 shows plot of contours of effective horizontal stress. It is apparent that the high values of horizontal stresses are concentrated at soil elements adjacent to the shaft of the aggregate pier.

Table 6.8 shows the comparison between Case 2C and Case 4C, i.e. cases with Loma Prieta earthquake as the input time history. Both cases have an aggregate pier installed. The

only difference is that Case 4C uses a deeper model (26.5 feet) of silty sand as shown on Figure 6.1f while Case 2C uses 14.5 feet deep model as shown on Figure 6.1e. It can be concluded that Case 4C generally shows lower values of r_u compared to those of Case 2C except at Point 1. Both cases also show similar values of a_{max} ($\pm 0.38g$), which is de-amplification of input pga of 0.45g.

Table 6.8 can be compared to Table 6.6 to observe the effects of installation of aggregate pier, i.e. the cases with aggregate pier (Cases 2C and 4C) are compared to the ones without aggregate pier (Cases 1C and 3C). For model with 14.5 feet deep (Case 1C compared to Case 2C), improvement occurs only at the deepest point (Point 4 – depth of 12.25 feet). While for model with 26.5 feet deep (Case 2C compared to Case 4C), improvement occurs up to the depth where the aggregate pier is installed (14.5 feet). Beyond this depth, the installation of aggregate pier increases the values of r_u . It can be also concluded that the installation of aggregate pier amplifies the values of a_{max} compared to the condition without aggregate pier.

The installation of aggregate pier increases the lateral stress of the soil matrix adjacent to the pier. If Figure 6.11 is compared to Figure 6.14, i.e. Case 1C is compared to Case 2C, it can be seen that the effective horizontal stress increases by a factor of 2 to 5. If Figure 6.20 is compared to Figure 6.29, i.e. Case 3C is compared to Case 4C, it can be seen that the effective horizontal stress increases by a factor of 2 to 9.

For Case 2S, Figure 6.30 shows that the values of r_u increase during the first 3 seconds of shaking for Points 1, 2, and 4 and then remain relatively constant until the end of shaking. The values of r_u at Point 3 are somewhat negative. According to the sign convention used in FLAC, this phenomenon means tensile condition. It is apparent that the values of r_u generally decrease with depths. Figure 6.31 shows that the maximum acceleration at ground surface (a_{max}) is equal to 0.1g. Figure 6.32 shows plot of contours of effective horizontal stress. It can be seen that the contours increase slightly at soil elements adjacent to the aggregate pier.

For Case 4S, Figure 6.33 shows that the values of r_u are very small for all depths with range of 0 to about 0.15. It is apparent that the values of r_u generally decrease with depths up to the depth where the aggregate pier is installed. Beyond this depth, the values of r_u increase for Point 5 and then decrease again with depths. Figure 6.34 shows that the maximum acceleration at ground surface (a_{max}) is equal to 0.0983g. Figure 6.35 shows plot of contours of effective

horizontal stress. It can be seen that the contours increase slightly at soil elements adjacent to the aggregate pier.

The results for Saguenay earthquake are summarized on Table 6.9 for Cases 2S and 4S. Both cases use an aggregate pier foundation system with Case 2S is 14.5 feet deep of silty sand as shown on Figure 6.1e while Case 4S is 26.5 feet deep as shown Figure 6.1f. It can be concluded that Case 4S shows lower values of r_u compared to those of Case 2S. Both cases show similar values of ground acceleration ($\pm 0.1g$).

Table 6.9 can be compared to Table 6.7 to observe the effects of installation of aggregate pier, i.e. the cases with aggregate pier (Cases 2S and 4S) are compared to the ones without aggregate pier (Cases 1S and 3S). For the model with 14.5 feet deep (Case 1S compared to Case 2S), improvement occurs at all depths. While for the model with 26.5 feet deep (Case 3S compared to Case 4S), improvement occurs up to the depth where the aggregate pier is installed (14.5 feet). Beyond this depth, the installation of aggregate pier increases the values of r_u . It can be also concluded that the installation of aggregate pier amplifies the values of a_{max} .

The installation of aggregate pier increases the lateral stress of the soil matrix adjacent to the pier. If Figure 6.23 is compared to Figure 6.32, i.e. Case 1S is compared to Case 2S, it is apparent that the effective horizontal stresses are increased by a factor of 5 to 7. If Figure 6.26 is compared to Figure 6.35, i.e. Case 3S is compared to Case 4S, it can be seen that the effective horizontal stress increases by a factor of 2 to 7.

6.3.1 The Effects of Soil Stratification

The effects of soil stratification were studied by installing soft clay beyond depth of 14.5 feet up to 26.5 feet in the model as shown by Figures 6.1c and 6.1g. These are Cases 5C and 6C for Loma Prieta earthquake. Case 5C is the case without aggregate pier and Case 6C is the case with an aggregate pier foundation system. Figures 6.36 to 6.38 show the results for Case 5C while Figures 6.39 to 6.41 show the results for Case 6C.

For Case 5C, Figure 6.36 shows that the values of r_u increase rapidly during the first 1 second of shaking for all depths. The r_u values are relatively high and close to each other range from about 0.65 to 1.0. It is apparent that for Point 3 initial liquefaction ($r_u = 1.0$) occurs at about 4 and 6 seconds of shaking. Figure 6.37 shows that the maximum acceleration at ground

surface (a_{\max}) is equal to 0.134g. Figure 6.38 shows plot of contours of effective horizontal stress.

For Case 6C, Figure 6.39 shows that for Point 1 (depth of 2.25 feet) the values of r_u increase during the first 2 seconds of shaking and abruptly decrease to negative values and then show transient behavior. The values of r_u at Point 4 are somewhat negative, i.e. tensile condition. The values of r_u increase rapidly during the first 1 second of shaking for Points 5, 6, and 7. It is apparent that the r_u values in the soft clay layer (Points 5 to 7) are higher than those of the silty sand layer (Points 1 to 4). Figure 6.40 shows that the maximum acceleration at ground surface (a_{\max}) is equal to 0.419g. Figure 6.41 shows plot of contours of effective horizontal stress. It is apparent that the high values of horizontal stresses are concentrated at soil elements adjacent to the shaft of the aggregate pier.

Table 6.10 summarizes the comparison of the results of Case 5C and Case 6C. It can be concluded that improvement occurs at the last one-third of the depth of the aggregate pier that is at depth of about 9.5 feet to 14.5 feet. Beyond this depth, the values of r_u increase. The installation of aggregate pier amplifies the values of a_{\max} . It can also be concluded that the installation of aggregate pier increases the horizontal stress of soil elements adjacent to the aggregate pier by a factor of 5 to 17 as shown by comparing Figure 6.38 (Case 5C) to Figure 6.41 (Case 6C).

If Cases 5C and 6C are compared with Cases 3C and 4C, i.e. cases with silty sand underlain by 12 feet of soft clay compared to the cases with all layers are silty sand, the following phenomena were found.

The presence of soft clay increases the values of r_u at almost all depths. The ground acceleration (a_{\max}) is de-amplified for the case without aggregate pier (Case 5C compared to Case 3C). The contrary occurs for the case with aggregate pier (Case 6C compared to Case 4C). It can also be concluded that the increase of effective horizontal stress of the soil matrix is more pronounced for the cases with the presence of silty clay (Cases 5C and 6C) compared to the cases with silty sand (Cases 3C and 4C), that is 5 to 17 times compared to 2 to 9 times.

For Saguenay earthquake, Figures 6.42 to 6.44 show the results for Case 5S while Figures 6.45 to 6.47 show the results for Case 6S.

For Case 5S, Figure 6.42 shows that the values of r_u increase during about the first 4 seconds of shaking for all depths. The r_u values are relatively small with maximum value at

about 0.35. The values of r_u decrease with depths up to the depth of aggregate pier (Points 1 to 4) and then suddenly increase at Point 5 and decrease again with depths afterward. Figure 6.43 shows that the maximum acceleration at ground surface (a_{max}) is equal to 0.0384g. Figure 6.44 shows plot of contours of effective horizontal stress.

For Case 6S, Figure 6.45 shows that the values of r_u at Point 2 are somewhat negative, which means tensile condition. The values of r_u increase during the first 3.5 seconds of shaking for Points 5, 6, and 7. It is apparent that the r_u values in the soft clay layer (Points 5 to 7) are higher than those of the silty sand layer (Points 1 to 4). Figure 6.46 shows that the maximum acceleration at ground surface (a_{max}) is equal to 0.04g. Figure 6.47 shows plot of contours of effective horizontal stress. It can be seen that the contours increase slightly at soil elements adjacent to the aggregate pier.

Table 6.11 summarizes the comparison of the results of Case 5S and Case 6S for Saguenay earthquake. It can be concluded that improvement occurs along depths where the aggregate pier is installed (up to 14.5 feet). The installation of aggregate pier slightly amplifies the ground acceleration (a_{max}) compared to the condition without aggregate pier (0.0384g to 0.04g). It can also be concluded that the installation of aggregate pier increases the horizontal stress of the soil elements adjacent to the aggregate pier by a factor of 2 to 7 as shown by comparing Figure 6.44 (Case 5S) to Figure 6.47 (Case 6S).

If Cases 5S and 6S are compared with Cases 3S and 4S, i.e. cases with silty sand and underlying 12 feet soft clay compared to the cases with all layer is silty sand, the following phenomena were found.

The presence of soft clay decreases the values of r_u up to 14.5 feet (the depth of aggregate pier) but increases the values of r_u in the soft clay layer (bottom 12 feet). The ground acceleration (a_{max}) is de-amplified both for cases without aggregate pier (Case 5S compared to Case 3S) and for cases with aggregate pier (Case 6S compared to Case 4S). It can also be concluded that the increase of effective horizontal stress in the soil matrix is almost the same magnitude both for cases with the presence of silty clay (Cases 5S and 6S) and cases with silty sand (Cases 3S and 4S) that is 2 to 7 times.

6.3.2 The Effects of Soil Properties

The effects of soil properties were studied by comparing Case 4C (all layers are silty sand) to Case 8C (all layers are silt) for Loma Prieta earthquake. Aggregate pier is installed for both cases.

Figures 6.27 to 6.29 show the results for Case 4C while Figures 6.48 to 6.50 show the results for Case 8C. The results for Case 4C have been discussed previously. For Case 8C, Figure 6.48 shows that the r_u values increase rapidly during the first 1 second of shaking for all depths. Point 4 shows positive values of r_u up to 4.5 seconds of shaking and then shows negative values, i.e. tensile condition until the end of shaking. It is apparent that the r_u values beyond the depth of aggregate pier (Points 5 to 7) are higher than those along the aggregate pier (Points 1 to 4). Figure 6.49 shows that the maximum acceleration at ground surface (a_{max}) is equal to 0.416g. Figure 6.50 shows plot of contours of effective horizontal stress. It is apparent that the high values of horizontal stresses are concentrated at soil elements adjacent to the shaft of the aggregate pier.

Table 6.12 summarizes the results. Case 8C (silt) has lower moduli values than Case 4C (silty sand). From Table 6.12, it can be concluded that the presence of silt results in larger ground acceleration (a_{max}) than Case 4C (all silty sand). Both cases de-amplify the value of pga. Case 8C generally gives higher values of r_u than those of Case 4C.

Figures 6.51 to 6.53 show the results for Case 7C. Figure 6.51 shows that the r_u values increase rapidly during the first 1 second of shaking for all depths. Figure 6.52 shows that the maximum acceleration at ground surface (a_{max}) is equal to 0.269g. Figure 6.53 shows plot of contours of effective horizontal stress.

If the case with aggregate pier (Case 8C) is compared to the one without aggregate pier (Case 7C), from Table 6.12 it can be concluded that improvement occurs up to the depth where the aggregate pier is installed (14.5 feet). The installation of aggregate pier amplifies the ground acceleration (a_{max}). It can also be concluded that the installation of aggregate pier increases the horizontal stress of the soil elements adjacent to the aggregate pier by a factor of 5 to 7 as shown by comparing Figure 6.53 (Case 7C) to Figure 6.50 (Case 8C).

For Saguenay earthquake, Case 8S (all silt) was compared to Case 4S (all silty sand). Figures 6.33 to 6.35 show the results for Case 4S while Figures 6.54 to 6.56 show the results for Case 8S. Aggregate pier is installed for both cases. The results for Case 4S have been

discussed previously. For Case 8S, Figure 6.54 shows that the r_u values increase during the first 4 seconds of shaking for all depths and then remain relatively constant until the end of shaking. It is apparent that the values of r_u generally decrease with depths up to the depth where the aggregate pier is installed (depth of 14.5 feet). Beyond this depth, the values of r_u increase slightly at Point 5, decrease at Point 6, and increase again at Point 7. Figure 6.55 shows that the maximum acceleration at ground surface (a_{max}) is equal to 0.0616g. Figure 6.56 shows plot of contours of effective horizontal stress. It can be seen that the contours increase slightly at soil elements adjacent to the aggregate pier.

Table 6.13 summarizes the results. It can be concluded that the presence of silt results in smaller ground acceleration (a_{max}) than Case 4S (all silty sand). Both cases amplify the value of pga . Case 8S gives higher values of r_u than those of Case 4S.

Figures 6.57 to 6.59 show the results for Case 7S. Figure 6.57 shows that the r_u values increase during the first 3.5 seconds of shaking for all depths. The values of r_u decrease with depths but suddenly increase for Point 7. Figure 6.58 shows that the maximum acceleration at ground surface (a_{max}) is equal to 0.0562g. Figure 6.59 shows plot of contours of effective horizontal stress.

If the case with aggregate pier (Case 8S) is compared to the one without aggregate pier (Case 7S), from Table 6.13 it can be concluded that improvement occurs up to the depth of the aggregate pier. The installation of aggregate pier amplifies the value of a_{max} . It can also be concluded that the installation of aggregate pier increases the horizontal stress of soil elements adjacent to the aggregate pier by a factor of 3 to 6 as shown by comparing Figure 6.59 (Case 7S) to Figure 6.56 (Case 8S).

6.3.3 The Effects of Pore Pressure Dissipation

The effects of pore pressure dissipation were studied by comparing Case 4C (no flow) and Case 9C (with flow) for Loma Prieta earthquake and similarly, Case 4S (no flow) and Case 9S (with flow) for Saguenay earthquake. Aggregate pier is installed for all cases.

Figures 6.27 to 6.29 show the results of FLAC analyses for Case 4C. The results of Case 9C are presented on Figures 6.60 to 6.64. The results for Case 4C have been discussed previously. For Case 9C, Figure 6.60 shows that for Point 1 the values of r_u decreases with time and shows negative value at the end of shaking. It is apparent that initial liquefaction ($r_u = 1.0$)

occurs at about 3 seconds of shaking. Negative values are also shown by Points 2 to 4. The values of r_u then increase for depths beyond depth of aggregate pier (Points 5, 6, and 7). Figure 6.61 shows that the maximum acceleration at ground surface (a_{max}) is equal to 0.433g. Figure 6.62 shows plot of contours of effective horizontal stress. It is apparent that the values of horizontal stresses are relatively constant along the horizontal line. Figures 6.63 and 6.64 show the flow vectors and the flow streamlines. The flow vectors show the amount of flow discharge in unit of flow rate per unit area or for this research, in $ft^3/sec./ft^2$. The flow streamlines show the path of the water flowing from one boundary to another boundary. Figure 6.63 shows that water flows from the surrounding soil matrix to the aggregate pier. This is caused by the fact that the permeability of the aggregate pier is much larger than that of soil.

Table 6.14 summarizes the results for Loma Prieta earthquake. It can be concluded that pore pressure dissipation generally increases the values of r_u for Loma Prieta earthquake. By allowing the pore water pressure to dissipate, the ground acceleration (a_{max}) is amplified.

The results of Cases 4S and 9S can be seen on Figures 6.33 to 6.35 and Figures 6.65 to 6.69, respectively. The results for Case 4S have been discussed previously. For Case 9S, Figure 6.65 shows that for Point 2 the values of r_u increase and then decrease to almost zero after 4 seconds of shaking. The values of r_u then increase for Point 5 and then decrease with depths for depths beyond depth of aggregate pier (Points 5, 6, and 7). Figure 6.66 shows that the maximum acceleration at ground surface (a_{max}) is equal to 0.0993g. Figure 6.67 shows plot of contours of effective horizontal stress. It is apparent that the values of horizontal stresses are relatively constant along the horizontal line. Figures 6.68 and 6.69 show the flow vectors and the flow streamlines, respectively. Figure 6.68 shows that water flows from the surrounding soil matrix to the aggregate pier.

Table 6.15 summarizes the results for Saguenay earthquake. The variation of r_u values with depths does not follow a consistent trend. It decreases up to 9.75 feet, increases at 12.25 feet, decreases at 16.75 feet, increases at 19.75 feet, and decreases again at 24.25 feet. By allowing the pore water pressure to dissipate, the value of a_{max} is slightly amplified.

6.3.4 The Effects of Earthquake History

As noted in the previous section, the Saguenay earthquake has peak acceleration (pga) of 0.05g, which is much smaller compared to the Loma Prieta earthquake whose pga is 0.45g.

Beside that, the cases with Saguenay earthquake were shaken for 13 seconds while the cases with Loma Prieta earthquake were shaken for 16 seconds.

Table 6.16 shows that all cases with Loma Prieta time history de-amplify the values of p_{ga} . The contrary occurs for cases with Saguenay time history with exception for cases with silty sand layer underlain by soft clay (Cases 5S and 6S).

Tables 6.17 and 6.18 summarize the values of r_u for cases using Loma Prieta earthquake record. For cases with Saguenay earthquake, they are summarized on Tables 6.19 and 6.20.

It can be concluded that cases with Loma Prieta time history generally show much higher values of r_u compared to those with Saguenay time history. Therefore, the effects of installation aggregate pier, that is improvement, are much more significant in cases with Saguenay time history. For cases with Loma Prieta earthquake, improvement is less significant because the magnitude of p_{ga} is high, that is 0.45g.

Contradictions occur when observing the effects of soil stratification. Cases with silty sand underlain by 12 feet of soft clay were compared to the cases with all layer is silty sand, For cases with Loma Prieta time history, the presence of the underlying soft clay layer increases the values of r_u all depths. The ground acceleration (a_{max}) is de-amplified for the case without aggregate pier and is amplified for the case with aggregate pier. For cases with Saguenay time history, the presence of soft clay decreases the values of r_u up to the depth of the aggregate pier but increases the values of r_u in the soft clay layer (bottom 12 feet). The ground acceleration (a_{max}) is de-amplified for both cases with and without aggregate pier.

Contradictions also occur when the effects of soil properties were observed. The cases with silt were compared to the cases with silty sand. The presence of silt results in larger ground acceleration (a_{max}) than silty sand for Loma Prieta earthquake but smaller value of a_{max} for Saguenay earthquake. For Loma Prieta earthquake, both cases (silt and silty sand) de-amplify the value of p_{ga} . For Saguenay earthquake both cases (silt and silty sand) amplify the value of p_{ga} . Both earthquake records generally give higher values of r_u , which means no improvement occurs.

For the cases where the pore pressure dissipation is allowed, it can be concluded that the values of r_u generally increase for Loma Prieta earthquake but generally decrease for Saguenay earthquake.

6.4 Shear Stress in Soil Matrix

As noted previously, the FLAC analyses were divided into two parts. The first part was discussed in the previous three sections. This section discusses the second part, which was mainly focused on the shear stress generated in soil matrix during seismic loading. This was performed by analyzing cases with and without aggregate pier using Loma Prieta earthquake. The peak acceleration on rock outcrop (pga) was scaled down to 0.2g from 0.45g.

There were two cases analyzed: Case 1C2 (without aggregate pier) and Case 2C2 (with aggregate pier). Case 1C2 used model as shown on Figure 6.1a and Case 2C2 used model as shown on Figure 6.1e. Note that number 2 after letter C indicates the value of pga used in FLAC analyses that is 0.2g.

The reason why the study of the shear stress in soil matrix was focused on Cases 1C2 and 2C2 is because Case 1C2 results in factor of safety against liquefaction (FS_L) calculated using the Simplified Procedure (refer to Section 3.1) close to unity that is on the verge of liquefaction as shown on Table 6.21.

The peak acceleration at the ground surface (a_{max}) is shown on Figures 6.70 and 6.71 for Cases 1C2 and 2C2, respectively. The values of a_{max} are 0.138g for Case 1C2 and 0.366g for Case 2C2. It can be concluded that the value of pga (0.2g) is de-amplified for Case 1C2 and is amplified for Case 2C2. If the two cases are compared, it can be concluded that the installation of aggregate pier amplifies the ground acceleration (a_{max}).

Figures 6.72 and 6.73 show plot of the maximum shear stresses (τ_{max}) versus distance for different depths for Cases 1C2 and 2C2, respectively. Depth is defined as the depth from the ground surface and distance is the distance from the left side boundary of the model. Note that the model analyzed using FLAC has width of 8.4 feet. Hence, the distance varies from 0 to 8.4 feet.

Figure 6.72 shows that for Case 1C2 (without aggregate pier) the distribution of the shear stresses (τ_{max}) along horizontal section is reasonably uniform. Figure 6.73 shows that for Case 2C2 (with aggregate pier) the distribution of the shear stresses (τ_{max}) is concentrated in the aggregate pier. If Figure 6.73 is compared to Figure 6.72, that is case with aggregate pier (Case 2C2) is compared to case without aggregate pier (Case 1C2), it can be concluded that the

installation of aggregate pier generally results in lower shear stresses in the soil matrix and higher shear stresses in the aggregate pier.

Figures 6.74 and 6.75 present the plot of maximum shear stress (τ_{\max}) in different way that is plot of values of τ_{\max} versus depth for different distance. It can be concluded that the maximum shear stresses (τ_{\max}) generally increase with depths for case without aggregate pier (Case 1C2). For case with aggregate pier (Case 2C2) the values of τ_{\max} increase up to depth of 3 feet and then decrease up to depth of 8 feet and then increase again until the bottom of the depth of aggregate pier.

6.5 Summary

The following section summarizes the major findings including both about the excess pore water pressure ratio and about the shear stress in soil matrix generated during seismic loading.

- The installation of aggregate pier amplifies the ground motions (a_{\max}) when subjected to seismic loading. Table 6.16 summarizes the values of a_{\max} .
- The installation of aggregate pier shows that improvement occurs up to the depth where the aggregate pier is installed.
- The variation of the moduli (Case 2Ce) shows that improvement occurs at shallower depths (depths of 2.25 feet and 4.75 feet) while Case 2C (constant values of moduli) shows that the improvement occurs at the deepest point (depth of 12.25 feet). Table 6.5 shows this phenomenon. It was suspected that the use of low moduli values close to the ground surface (equals to zero on the ground surface) for Case 2Ce caused instability.
- The cases with and without aggregate pier indicate that models with 26.5 feet of silty sand show smaller ground acceleration (a_{\max}) and lower values of r_u compared to models with 14.5 feet of silty sand. This implies the effect of damping is more pronounced in the deeper model.
- Contradictions occur when observing the effects of soil stratification. The cases with silty sand and underlying 12 feet soft clay compared to the cases with all layer is silty sand. For cases with Loma Prieta time history, the presence of the underlying soft clay layer increases

the values of r_u for all depths. The ground acceleration (a_{\max}) is de-amplified for the case without aggregate pier and is amplified for the case with aggregate pier. For cases with Saguenay time history, the presence of soft clay decreases the values of r_u up to the depth of the aggregate pier but increases the values of r_u in the underlying soft clay layer. The ground acceleration (a_{\max}) is de-amplified for both cases with and without aggregate pier.

- Contradictions also occur when observing the effects of soil properties. The effects were studied by comparing cases with all layers are silty sand to cases with all layers are silt. Aggregate pier is installed in both cases. For Loma Prieta earthquake, the presence of silt results in larger ground acceleration (a_{\max}) than case with all silty sand. Both cases de-amplify the value of p_{ga} . For Saguenay earthquake, the presence of silt results in smaller ground acceleration (a_{\max}) and both cases amplify the value of p_{ga} . For both earthquakes, the presence of silt generally gives higher values of r_u , which means no improvement occurs.
- For the cases where the pore pressure dissipation is allowed, it can be concluded that pore pressure dissipation generally increases the values of r_u for Loma Prieta earthquake. For Saguenay earthquake it does not follow a consistent trend. It decreases up to 9.75 feet, increases at 12.25 feet, decreases at 16.75 feet, increases at 19.75 feet, and decreases at 24.25 feet. By allowing the pore water pressure to dissipate, the ground acceleration (a_{\max}) is amplified.
- Aggregate pier may serve as drainage system depends on the gradations of the soil matrix and aggregate pier elements. This behavior was observed from Cases 9C and 9S. From flow vectors plot that is Figures 6.63 and 6.68 for Cases 9C and 9S, respectively, it is apparent that the water flows from the surrounding soil whose permeability is three-order magnitude smaller than the permeability of the aggregate pier. This observation is valid for aggregate pier using open-graded stone since the permeability used in FLAC is a typical value of this material.
- The use of aggregate pier increases the lateral stress in soil matrix by a factor ranging from 2 to 17 with average value of 5 to 6 as shown on Table 6.22. It can be concluded that the amplification factor is larger than the coefficient of passive earth pressure applied as the initial condition.

- The distribution of the shear stresses (τ_{\max}) along horizontal section is reasonably constant for case without aggregate pier while for case with aggregate pier the distribution of the shear stresses (τ_{\max}) is concentrated in the aggregate pier. It can be concluded that the installation of aggregate pier generally results in lower shear stresses in the soil matrix and higher shear stresses in the aggregate pier.
- The maximum shear stresses (τ_{\max}) generally increase with depths for case without aggregate pier. For case with aggregate pier, the values of τ_{\max} increase up to depth of 3 feet and then decrease up to depth of 8 feet and then increase again.

Table 6.1 Analyses using FLAC

Case no.	Figures used in FLAC analyses
1C	Figure 6.1(a)
2C	Figure 6.1(e)
3C	Figure 6.1(b)
4C	Figure 6.1(f)
5C	Figure 6.1(c)
6C	Figure 6.1(g)
7C	Figure 6.1(d)
8C	Figure 6.1(h)
9C	Figure 6.1(f)
1S	Figure 6.1(a)
2S	Figure 6.1(e)
3S	Figure 6.1(b)
4S	Figure 6.1(f)
5S	Figure 6.1(c)
6S	Figure 6.1(g)
7S	Figure 6.1(d)
8S	Figure 6.1(h)
9S	Figure 6.1(f)
1C2	Figure 6.1(a)
2C2	Figure 6.1(e)

(Note: C indicates cases using Loma Prieta earthquake time history and S indicates cases using Saguenay earthquake time history)

Table 6.2 Mesh generation used for each case

Case no.	Grid generation used
1C	Figure 5.3
2C	Figure 5.4
3C	Figure 5.5
4C	Figure 5.6
5C	Figure 5.5
6C	Figure 5.6
7C	Figure 5.5
8C	Figure 5.6
9C	Figure 5.6
1S	Figure 5.3
2S	Figure 5.4
3S	Figure 5.5
4S	Figure 5.6
5S	Figure 5.5
6S	Figure 5.6
7S	Figure 5.5
8S	Figure 5.6
9S	Figure 5.6
1C2	Figure 5.3
2C2	Figure 5.4

(Note: Figures 5.3 to 5.6 are presented in Chapter 5)

Table 6.3 Soil parameters used in comparing SHAKE91 and FLAC analyses

Soil type	Parameters	Values
Silty sand	Unit weight, γ (kcf)	0.12
	Bulk Modulus (ksf)	262.5
	Shear Modulus (ksf)	121
	Damping (%)	5
Rock	Unit weight, γ (kcf)	0.15
	Shear wave velocity (fps)	5000
	Damping (%)	2

Table 6.4 Results of comparison study between SHAKE91 and FLAC analyses

Parameter	SHAKE91	FLAC	Difference (%)
Max. acceleration, a_{\max} (g)	1.72	1.61	6.83
Depth 4.5 feet			
- Max. shear stress (ksf)	0.886	0.867	2.19
- Max. shear strain (%)	0.732	0.719	1.81
Depth 9.5 feet			
- Max. shear stress (ksf)	1.584	1.485	6.67
- Max. shear strain (%)	1.310	1.231	6.42

Table 6.5 The effects of varying moduli with depth

Parameters		Case 1C		Case 2C		Case 2Ce	
		Peak	Steady state	Peak	Steady state	Peak	Steady state
r_u	Point 1 (2.25 ft)	0.872	0.751	0.989	N/A	-0.719	N/A
	Point 2 (4.75 ft)	0.829	0.747	0.961	N/A	0.756	N/A
	Point 3 (9.75 ft)	0.769	0.718	0.813	N/A	0.980	N/A
	Point 4 (12.25 ft)	0.842	0.776	0.449	N/A	0.969	N/A
a_{max} (g)		0.163		0.381		0.416	

(Note: The excess pore water pressure ratio (r_u) is the ratio between excess pore water pressure and the initial effective vertical stress)

Table 6.6 The effects of no aggregate pier (Loma Prieta earthquake)

Parameters		Case 1C		Case 3C	
		Peak	Steady state	Peak	Steady state
r _u	Point 1 (2.25 ft)	0.872	0.751	0.999	0.966
	Point 2 (4.75 ft)	0.829	0.747	0.907	0.7
	Point 3 (9.75 ft)	0.769	0.718	0.752	0.62
	Point 4 (12.25 ft)	0.842	0.776	0.591	0.55
	Point 5 (16.75 ft)	N/A	N/A	0.644	0.62
	Point 6 (19.75 ft)	N/A	N/A	0.567	0.54
	Point 7 (24.25 ft)	N/A	N/A	0.820	0.79
a _{max} (g)		0.163		0.155	

Table 6.7 The effects of no aggregate pier (Saguenay earthquake)

Parameters		Case 1S		Case 3S	
		Peak	Steady state	Peak	Steady state
r _u	Point 1 (2.25 ft)	0.894	0.87	0.958	0.92
	Point 2 (4.75 ft)	0.668	0.65	0.596	0.57
	Point 3 (9.75 ft)	0.336	0.33	0.272	0.26
	Point 4 (12.25 ft)	0.246	0.24	0.174	0.17
	Point 5 (16.75 ft)	N/A	N/A	0.0952	0.091
	Point 6 (19.75 ft)	N/A	N/A	0.0827	0.08
	Point 7 (24.25 ft)	N/A	N/A	0.0864	0.085
a _{max} (g)		0.086		0.0588	

Table 6.8 The effects of aggregate pier (Loma Prieta earthquake)

Parameters		Case 2C		Case 4C	
		Peak	Steady state	Peak	Steady state
r _u	Point 1 (2.25 ft)	0.989	N/A	0.999	0.76
	Point 2 (4.75 ft)	0.961	N/A	-0.473	-0.145
	Point 3 (9.75 ft)	0.813	N/A	0.279	0.07
	Point 4 (12.25 ft)	0.449	N/A	0.214	0.06
	Point 5 (16.75 ft)	N/A	N/A	0.933	0.84
	Point 6 (19.75 ft)	N/A	N/A	0.686	0.67
	Point 7 (24.25 ft)	N/A	N/A	0.753	0.45
a _{max} (g)		0.381		0.380	

Table 6.9 The effects of aggregate pier (Saguenay earthquake)

Parameters		Case 2S		Case 4S	
		Peak	Steady state	Peak	Steady state
r _u	Point 1 (2.25 ft)	0.332	0.31	0.144	0.088
	Point 2 (4.75 ft)	0.146	0.14	0.141	0.076
	Point 3 (9.75 ft)	-0.0958	-0.093	0.076	0.072
	Point 4 (12.25 ft)	0.0635	0.055	0.0348	0.032
	Point 5 (16.75 ft)	N/A	N/A	0.141	0.139
	Point 6 (19.75 ft)	N/A	N/A	0.104	0.103
	Point 7 (24.25 ft)	N/A	N/A	0.0984	0.098
a _{max} (g)		0.1		0.0983	

Table 6.10 The effects of soil stratification (Loma Prieta earthquake)

Parameters		Case 5C		Case 6C	
		Peak	Steady state	Peak	Steady state
r _u	Point 1 (2.25 ft)	0.92	0.78	0.984	N/A
	Point 2 (4.75 ft)	0.824	0.68	0.885	N/A
	Point 3 (9.75 ft)	0.996	0.95	0.326	N/A
	Point 4 (12.25 ft)	0.993	0.75	-0.36	N/A
	Point 5 (16.75 ft)	0.994	0.94	0.999	N/A
	Point 6 (19.75 ft)	0.952	0.87	0.991	N/A
	Point 7 (24.25 ft)	0.958	0.88	0.976	N/A
a _{max} (g)		0.134		0.419	

Table 6.11 The effects of soil stratification (Saguenay earthquake)

Parameters		Case 5S		Case 6S	
		Peak	Steady state	Peak	Steady state
r _u	Point 1 (2.25 ft)	0.322	0.322	0.0979	0.065
	Point 2 (4.75 ft)	0.277	0.277	-0.0337	-0.031
	Point 3 (9.75 ft)	0.125	0.125	0.0253	0.02
	Point 4 (12.25 ft)	0.0932	0.093	0.0325	0.024
	Point 5 (16.75 ft)	0.336	0.336	0.371	0.37
	Point 6 (19.75 ft)	0.24	0.24	0.18	0.18
	Point 7 (24.25 ft)	0.188	0.187	0.253	0.252
a _{max} (g)		0.0384		0.04	

Table 6.12 The effects of soil properties (Loma Prieta earthquake)

Parameters		Case 4C		Case 8C		Case 7C	
		Peak	Steady state	Peak	Steady state	Peak	Steady state
r _u	Point 1 (2.25 ft)	0.999	0.76	0.949	0.4	0.806	0.753
	Point 2 (4.75 ft)	-0.473	-0.145	0.729	0.66	0.804	0.721
	Point 3 (9.75 ft)	0.279	0.07	0.459	0.42	0.794	0.76
	Point 4 (12.25 ft)	0.214	0.06	-0.093	-0.073	0.869	0.861
	Point 5 (16.75 ft)	0.933	0.84	0.915	0.84	0.743	0.728
	Point 6 (19.75 ft)	0.686	0.67	0.994	0.96	0.919	0.892
	Point 7 (24.25 ft)	0.753	0.45	0.961	0.918	0.983	0.917
a _{max} (g)		0.380		0.416		0.269	

Table 6.13 The effects of soil properties (Saguenay earthquake)

Parameters		Case 4S		Case 8S		Case 7S	
		Peak	Steady state	Peak	Steady state	Peak	Steady state
r _u	Point 1 (2.25 ft)	0.144	0.088	0.718	0.71	0.854	0.853
	Point 2 (4.75 ft)	0.141	0.076	0.292	0.28	0.606	0.605
	Point 3 (9.75 ft)	0.076	0.072	0.168	0.166	0.334	0.334
	Point 4 (12.25 ft)	0.0348	0.032	0.14	0.14	0.221	0.221
	Point 5 (16.75 ft)	0.141	0.139	0.145	0.146	0.127	0.127
	Point 6 (19.75 ft)	0.104	0.103	0.123	0.12	0.0781	0.0779
	Point 7 (24.25 ft)	0.0984	0.098	0.142	0.141	0.133	0.133
a _{max} (g)		0.0983		0.0616		0.0562	

Table 6.14 The effects of pore pressure generation (Loma Prieta earthquake)

Parameters		Case 4C		Case 9C	
		Peak	Steady state	Peak	Steady state
r _u	Point 1 (2.25 ft)	0.999	0.76	0.999	N/A
	Point 2 (4.75 ft)	-0.473	-0.145	-0.667	N/A
	Point 3 (9.75 ft)	0.279	0.07	-0.299	-0.07
	Point 4 (12.25 ft)	0.214	0.06	-0.298	-0.08
	Point 5 (16.75 ft)	0.933	0.84	0.686	0.62
	Point 6 (19.75 ft)	0.686	0.67	0.868	0.79
	Point 7 (24.25 ft)	0.753	0.45	0.999	0.96
a _{max} (g)		0.380		0.433	

Table 6.15 The effects of pore pressure generation (Saguenay earthquake)

Parameters		Case 4S		Case 9S	
		Peak	Steady state	Peak	Steady state
r _u	Point 1 (2.25 ft)	0.144	0.088	0.182	0.11
	Point 2 (4.75 ft)	0.141	0.076	0.0877	0.01
	Point 3 (9.75 ft)	0.076	0.072	0.0641	0.042
	Point 4 (12.25 ft)	0.0348	0.032	0.053	0.015
	Point 5 (16.75 ft)	0.141	0.139	0.129	0.125
	Point 6 (19.75 ft)	0.104	0.103	0.11	0.107
	Point 7 (24.25 ft)	0.0984	0.098	0.0921	0.09
a _{max} (g)		0.0983		0.0993	

Table 6.16 Values of ground acceleration from FLAC analyses

Case	pga	a _{max}		Note
		(ft/sec ²)	(g)	
1C	0.45 g	5.25	0.163	De-amplification
2C	0.45 g	12.26	0.381	De-amplification
3C	0.45 g	4.99	0.155	De-amplification
4C	0.45 g	12.23	0.380	De-amplification
5C	0.45 g	4.31	0.134	De-amplification
6C	0.45 g	13.48	0.419	De-amplification
7C	0.45 g	8.66	0.269	De-amplification
8C	0.45 g	13.39	0.416	De-amplification
9C	0.45 g	13.94	0.433	De-amplification
1S	0.05 g	2.77	0.086	Amplification
2S	0.05 g	3.22	0.100	Amplification
3S	0.05 g	1.89	0.059	Amplification
4S	0.05 g	3.16	0.098	Amplification
5S	0.05 g	1.24	0.0384	De-amplification
6S	0.05 g	1.29	0.040	De-amplification
7S	0.05 g	1.81	0.0562	Amplification
8S	0.05 g	1.98	0.0616	Amplification
9S	0.05 g	3.20	0.0993	Amplification

Table 6.17 Values of r_u – peak (Loma Prieta earthquake)

Case	Excess pore water pressure ratio, r_u (peak)						
	Point 1	Point 2	Point 3	Point 4	Point 5	Point 6	Point 7
1C	0.872	0.829	0.769	0.842	N/A	N/A	N/A
2C	0.989	0.961	0.813	0.449	N/A	N/A	N/A
3C	0.999	0.907	0.752	0.591	0.644	0.567	0.820
4C	0.999	-0.473	0.279	0.214	0.933	0.686	0.753
5C	0.92	0.824	0.996	0.993	0.994	0.952	0.958
6C	0.984	0.885	0.326	-0.36	0.999	0.991	0.976
7C	0.806	0.804	0.794	0.869	0.743	0.919	0.983
8C	0.949	0.729	0.459	-0.093	0.915	0.994	0.961
9C	0.999	-0.667	-0.299	-0.298	0.686	0.868	0.999

Table 6.18 Values of r_u – steady state (Loma Prieta earthquake)

Case	Excess pore water pressure ratio, r_u (steady state)						
	Point 1	Point 2	Point 3	Point 4	Point 5	Point 6	Point 7
1C	0.751	0.747	0.718	0.776	N/A	N/A	N/A
2C	N/A	N/A	N/A	N/A	N/A	N/A	N/A
3C	0.966	0.7	0.62	0.55	0.62	0.54	0.79
4C	0.76	-0.145	0.07	0.06	0.84	0.67	0.45
5C	0.78	0.68	0.95	0.75	0.94	0.87	0.88
6C	N/A	N/A	N/A	N/A	N/A	N/A	N/A
7C	0.753	0.721	0.76	0.861	0.728	0.892	0.917
8C	0.4	0.66	0.42	-0.073	0.84	0.96	0.918
9C	N/A	N/A	-0.07	-0.08	0.62	0.79	0.96

Table 6.19 Values of r_u – peak (Saguenay earthquake)

Case	Excess pore water pressure ratio, r_u (peak)						
	Point 1	Point 2	Point 3	Point 4	Point 5	Point 6	Point 7
1S	0.894	0.668	0.336	0.246	N/A	N/A	N/A
2S	0.332	0.146	-0.0958	0.0635	N/A	N/A	N/A
3S	0.958	0.596	0.272	0.174	0.0952	0.0827	0.0864
4S	0.144	0.141	0.076	0.0348	0.141	0.104	0.0984
5S	0.322	0.277	0.125	0.0932	0.336	0.24	0.188
6S	0.0979	-0.0337	0.0253	0.0325	0.371	0.18	0.253
7S	0.854	0.606	0.334	0.221	0.127	0.0781	0.133
8S	0.718	0.292	0.168	0.14	0.145	0.123	0.142
9S	0.182	0.0877	0.0641	0.053	0.129	0.11	0.0921

Table 6.20 Values of r_u – steady state (Saguenay earthquake)

Case	Excess pore water pressure ratio, r_u (steady state)						
	Point 1	Point 2	Point 3	Point 4	Point 5	Point 6	Point 7
1S	0.87	0.65	0.33	0.24	N/A	N/A	N/A
2S	0.31	0.14	-0.093	0.055	N/A	N/A	N/A
3S	0.92	0.57	0.26	0.17	0.091	0.08	0.085
4S	0.088	0.076	0.072	0.032	0.139	0.103	0.098
5S	0.322	0.277	0.125	0.093	0.336	0.24	0.187
6S	0.0979	-0.0337	0.0253	0.0325	0.371	0.18	0.253
7S	0.853	0.605	0.334	0.221	0.127	0.0779	0.133
8S	0.71	0.28	0.166	0.14	0.146	0.12	0.141
9S	0.11	0.01	0.042	0.015	0.125	0.107	0.09

Table 6.21 Calculation of factor of safety against liquefaction (FS_L) for Case 1C2

z (ft)	z (m)	r _d	σ _o (tsf)	σ _o ' (tsf)	CSR	N _m	C _N	(N ₁) ₆₀	α	β	(N ₁) _{60CS}	CRR _{M=7.5}	K _σ	MSF	CRR _{M=7.1}	FS _L
0.0	0.000	1.000	0.00	0.00	-	-	-	-	-	-	-	-	-	-	-	-
0.5	0.152	0.999	0.03	0.01	0.1867	6	1.70	10	3.615	1.0794	14	0.15418	1.00	1.174	0.1810	0.97
1.0	0.305	0.998	0.06	0.03	0.1864	6	1.70	10	3.615	1.0794	14	0.15418	1.00	1.174	0.1810	0.97
1.5	0.457	0.997	0.09	0.04	0.1862	6	1.70	10	3.615	1.0794	14	0.15418	1.00	1.174	0.1810	0.97
2.0	0.610	0.995	0.12	0.06	0.1860	6	1.70	10	3.615	1.0794	14	0.15418	1.00	1.174	0.1810	0.97
2.5	0.762	0.994	0.15	0.07	0.1858	6	1.70	10	3.615	1.0794	14	0.15418	1.00	1.174	0.1810	0.97
3.0	0.914	0.993	0.18	0.09	0.1856	6	1.70	10	3.615	1.0794	14	0.15418	1.00	1.174	0.1810	0.98
3.5	1.067	0.992	0.21	0.10	0.1853	6	1.70	10	3.615	1.0794	14	0.15418	1.00	1.174	0.1810	0.98
4.0	1.219	0.991	0.24	0.12	0.1851	6	1.70	10	3.615	1.0794	14	0.15418	1.00	1.174	0.1810	0.98
4.5	1.372	0.990	0.27	0.13	0.1849	6	1.70	10	3.615	1.0794	14	0.15418	1.00	1.174	0.1810	0.98
5.0	1.524	0.988	0.30	0.14	0.1847	6	1.70	10	3.615	1.0794	14	0.15418	1.00	1.174	0.1810	0.98
5.5	1.676	0.987	0.33	0.16	0.1845	6	1.70	10	3.615	1.0794	14	0.15418	1.00	1.174	0.1810	0.98
6.0	1.829	0.986	0.36	0.17	0.1843	6	1.70	10	3.615	1.0794	14	0.15418	1.00	1.174	0.1810	0.98
6.5	1.981	0.985	0.39	0.19	0.1840	6	1.70	10	3.615	1.0794	14	0.15418	1.00	1.174	0.1810	0.98
7.0	2.134	0.984	0.42	0.20	0.1838	6	1.70	10	3.615	1.0794	14	0.15418	1.00	1.174	0.1810	0.98
7.5	2.286	0.983	0.45	0.22	0.1836	6	1.70	10	3.615	1.0794	14	0.15418	1.00	1.174	0.1810	0.99
8.0	2.438	0.981	0.48	0.23	0.1834	6	1.70	10	3.615	1.0794	14	0.15418	1.00	1.174	0.1810	0.99
8.5	2.591	0.980	0.51	0.24	0.1832	6	1.70	10	3.615	1.0794	14	0.15418	1.00	1.174	0.1810	0.99
9.0	2.743	0.979	0.54	0.26	0.1830	6	1.70	10	3.615	1.0794	14	0.15418	1.00	1.174	0.1810	0.99
9.5	2.896	0.978	0.57	0.27	0.1827	6	1.70	10	3.615	1.0794	14	0.15418	1.00	1.174	0.1810	0.99
10.0	3.048	0.977	0.60	0.29	0.1825	6	1.70	10	3.615	1.0794	14	0.15418	1.00	1.174	0.1810	0.99
10.5	3.200	0.976	0.63	0.30	0.1823	6	1.70	10	3.615	1.0794	14	0.15418	1.00	1.174	0.1810	0.99
11.0	3.353	0.974	0.66	0.32	0.1821	6	1.70	10	3.615	1.0794	14	0.15418	1.00	1.174	0.1810	0.99
11.5	3.505	0.973	0.69	0.33	0.1819	6	1.70	10	3.615	1.0794	14	0.15418	1.00	1.174	0.1810	1.00
12.0	3.658	0.972	0.72	0.35	0.1816	6	1.70	10	3.615	1.0794	14	0.15418	1.00	1.174	0.1810	1.00
12.5	3.810	0.971	0.75	0.36	0.1814	6	1.67	10	3.615	1.0794	14	0.15418	1.00	1.174	0.1810	1.00
13.0	3.962	0.970	0.78	0.37	0.1812	6	1.63	10	3.615	1.0794	14	0.15418	1.00	1.174	0.1810	1.00
13.5	4.115	0.969	0.81	0.39	0.1810	6	1.60	10	3.615	1.0794	14	0.15418	1.00	1.174	0.1810	1.00
14.0	4.267	0.967	0.84	0.40	0.1808	6	1.57	10	3.615	1.0794	14	0.15418	1.00	1.174	0.1810	1.00
14.5	4.420	0.966	0.87	0.42	0.1806	6	1.55	10	3.615	1.0794	14	0.15418	1.00	1.174	0.1810	1.00

Table 6.22 Increase in lateral stress

Earthquake	No aggregate pier	With aggregate pier	Magnification factor in lateral stress
Loma Prieta	Case 1C	Case 2C	2 to 5
	Case 3C	Case 4C	2 to 9
	Case 5C	Case 6C	5 to 17
	Case 7C	Case 8C	5 to 7
Saguenay	Case 1S	Case 2S	5 to 7
	Case 3S	Case 4S	2 to 7
	Case 5S	Case 6S	2 to 7
	Case 7S	Case 8S	3 to 6

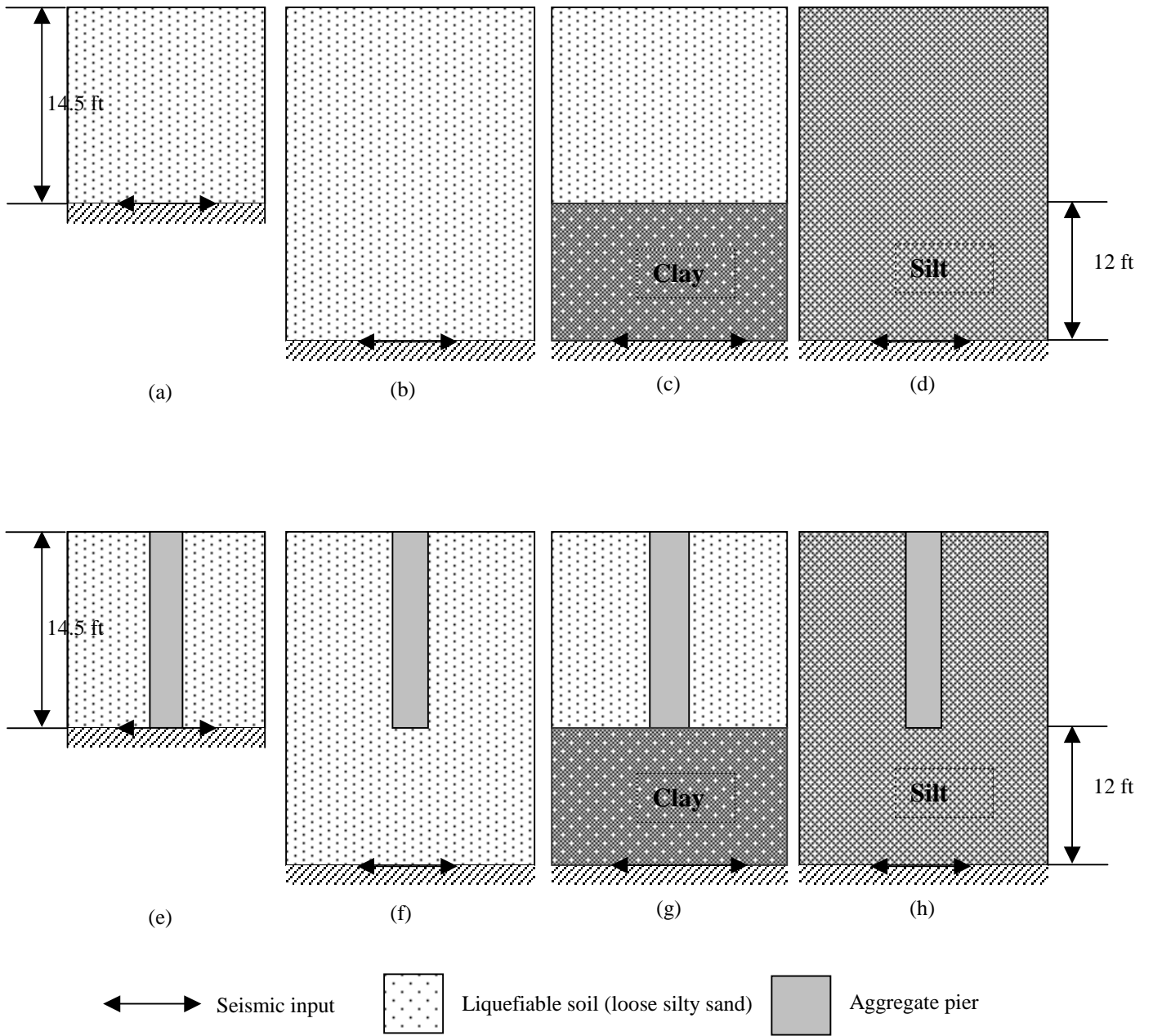


Figure 6.1 Models used in FLAC analyses

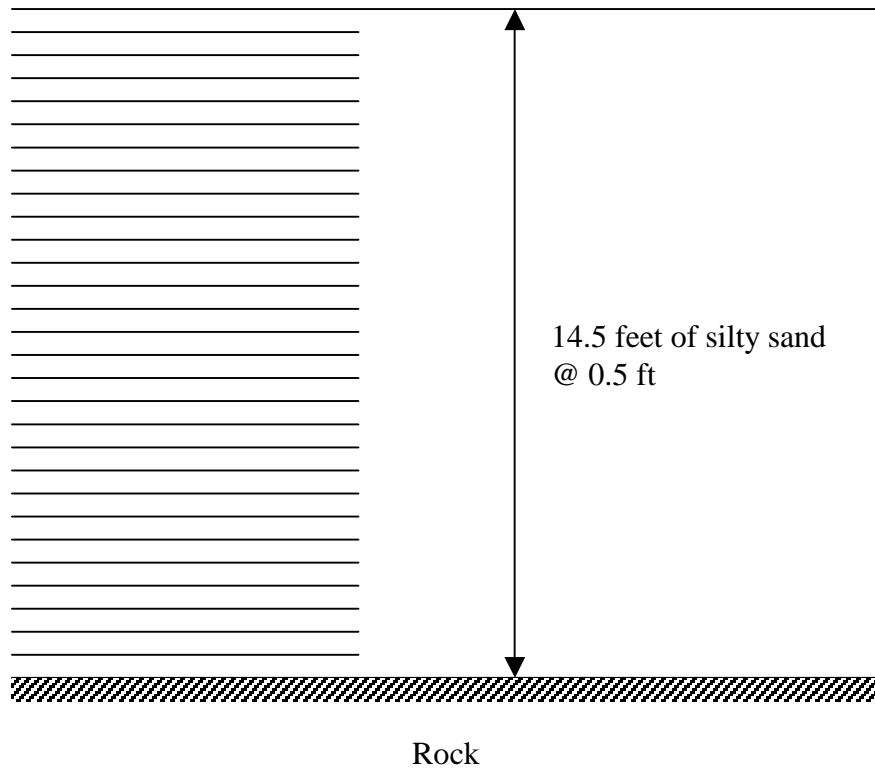


Figure 6.2 Model used in SHAKE91 analysis to compare with FLAC analysis

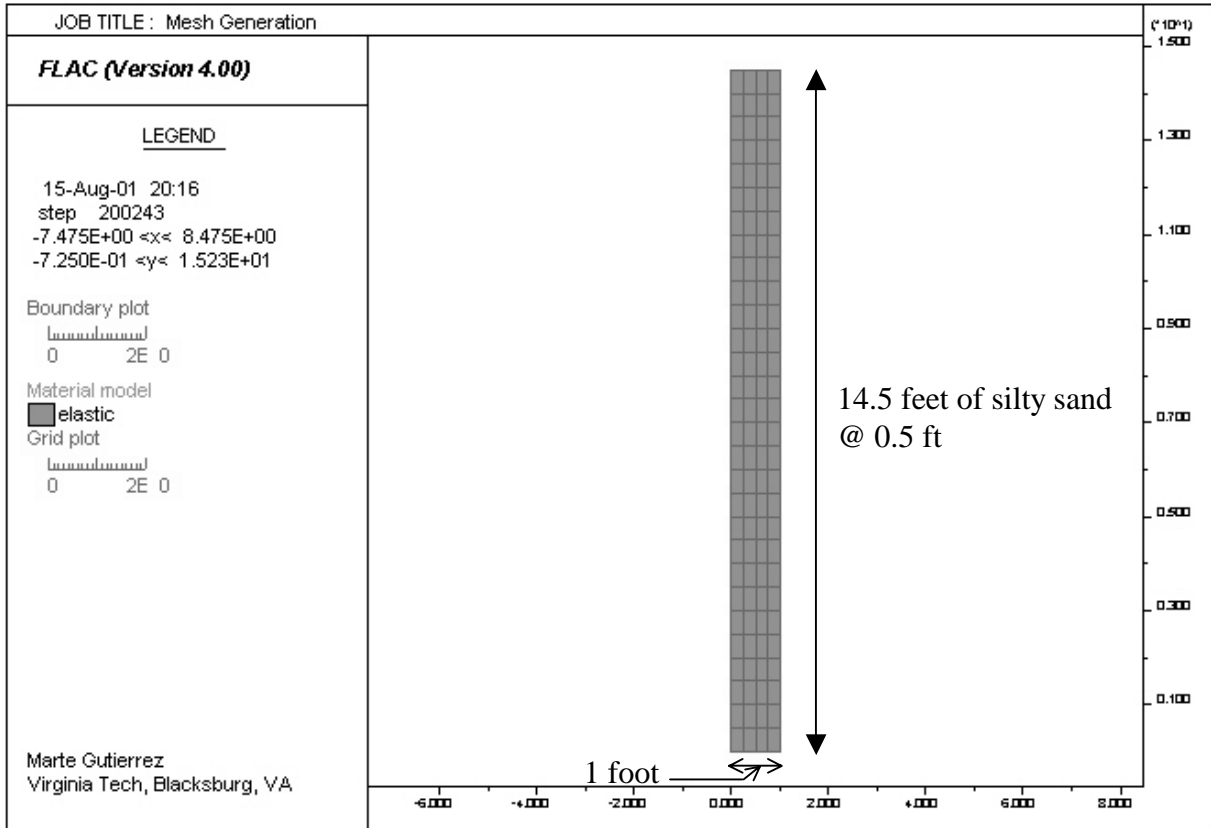


Figure 6.3 Model used in FLAC analysis to compare with SHAKE91 analysis

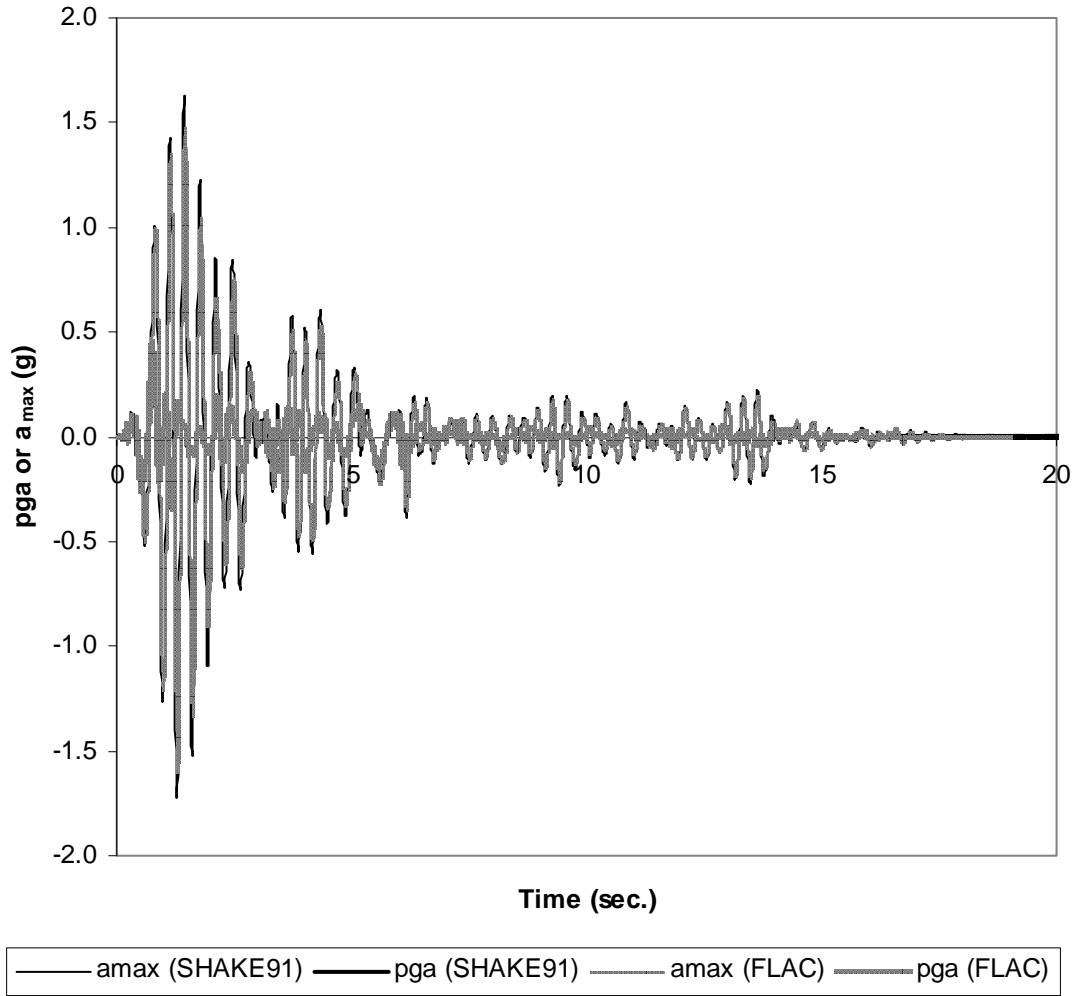


Figure 6.4 Comparison of time histories of pga and a_{max} between SHAKE91 and FLAC

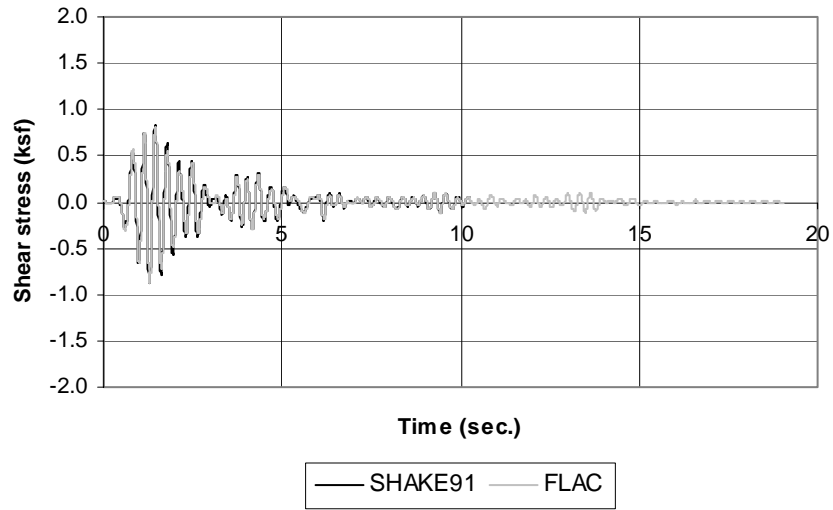


Figure 6.5 Comparison of shear stress time history at depth of 4.5 feet between SHAKE91 and FLAC

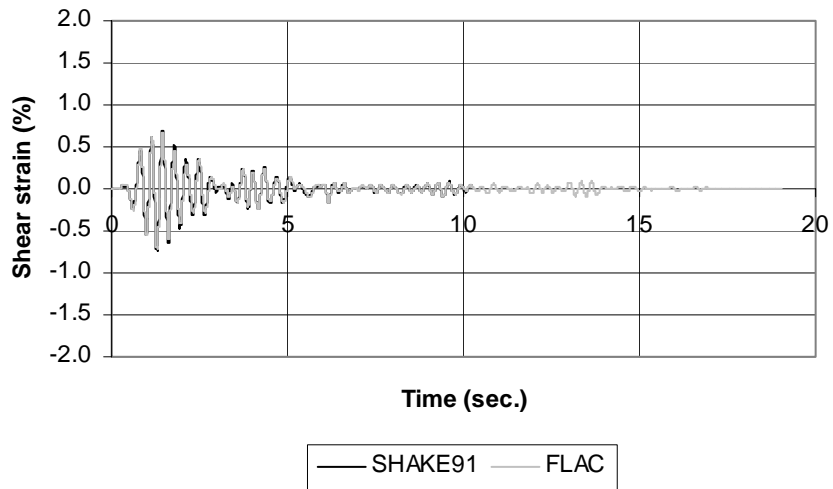


Figure 6.6 Comparison of shear strain time history at depth of 4.5 feet between SHAKE91 and FLAC

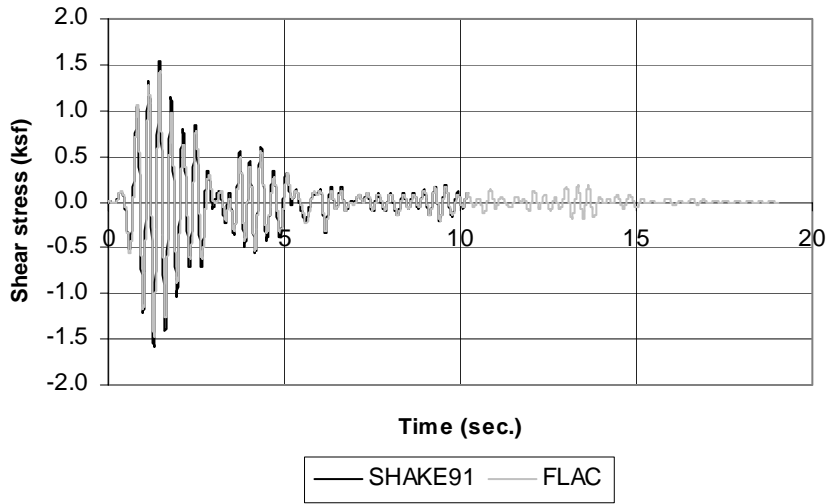


Figure 6.7 Comparison of shear stress time history at depth of 9.5 feet between SHAKE91 and FLAC

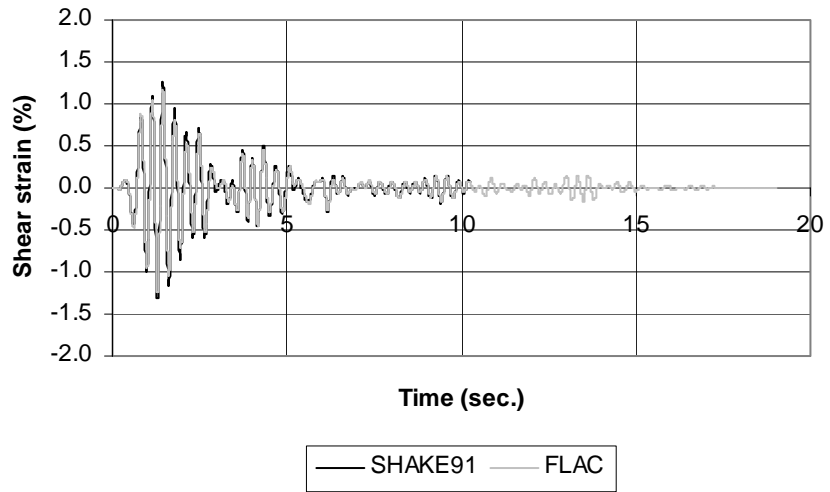


Figure 6.8 Comparison of shear strain time history at depth of 9.5 feet between SHAKE91 and FLAC

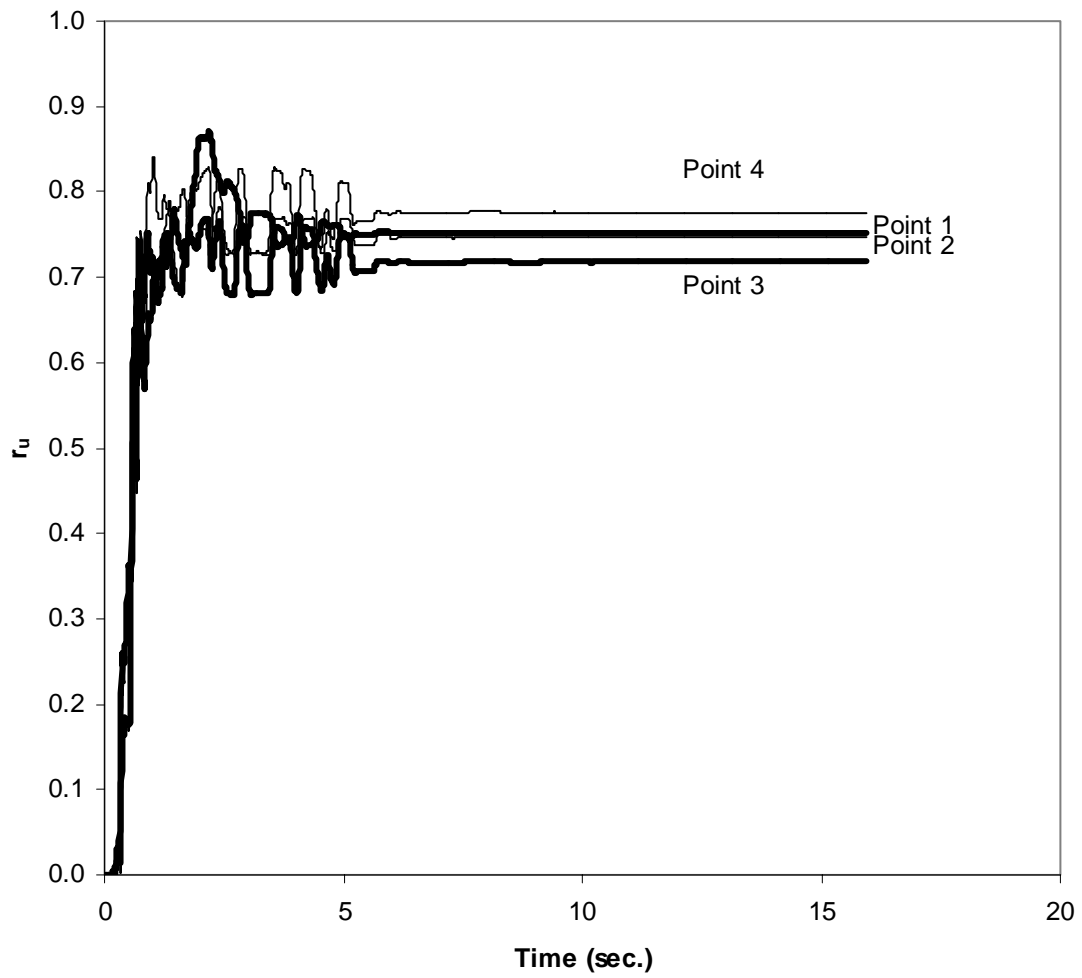


Figure 6.9 History of excess pore pressure ratio (r_u) for Case 1C

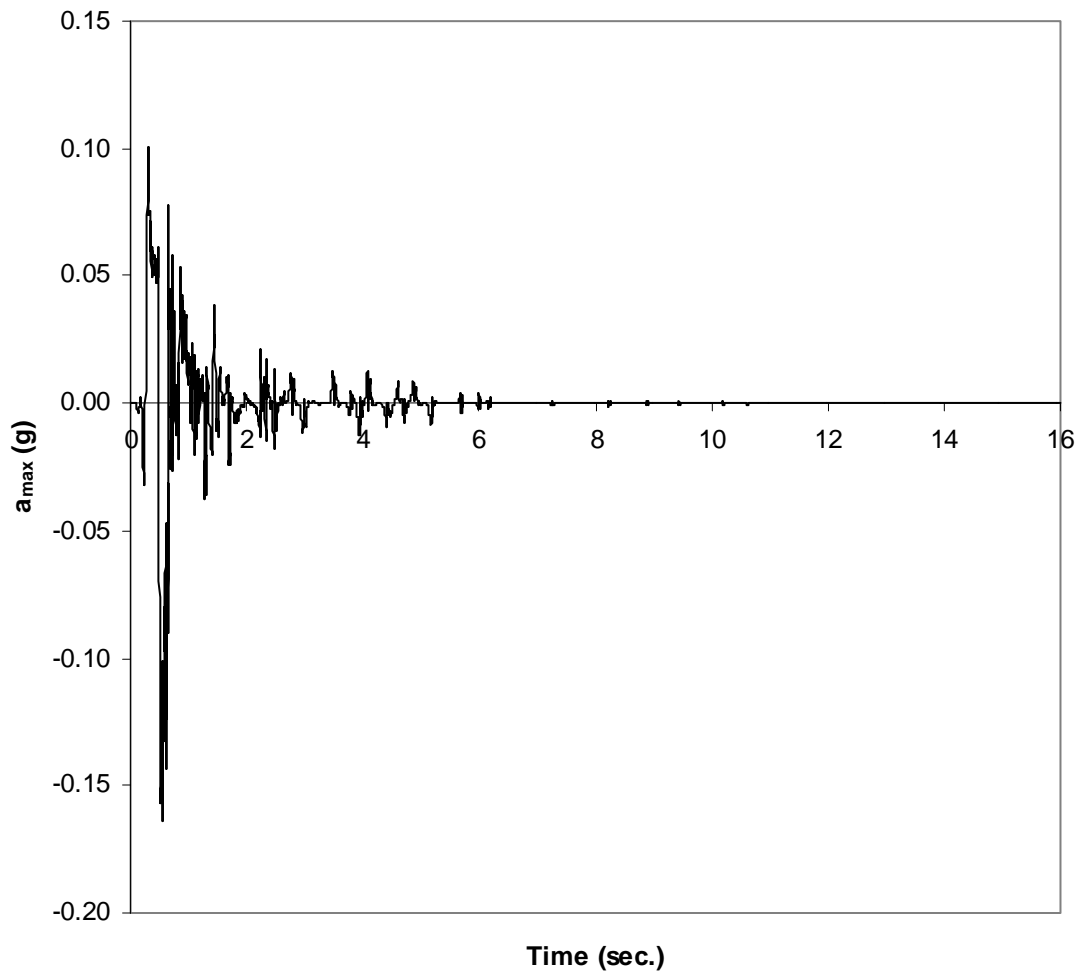


Figure 6.10 Acceleration time history (a_{\max}) for Case 1C

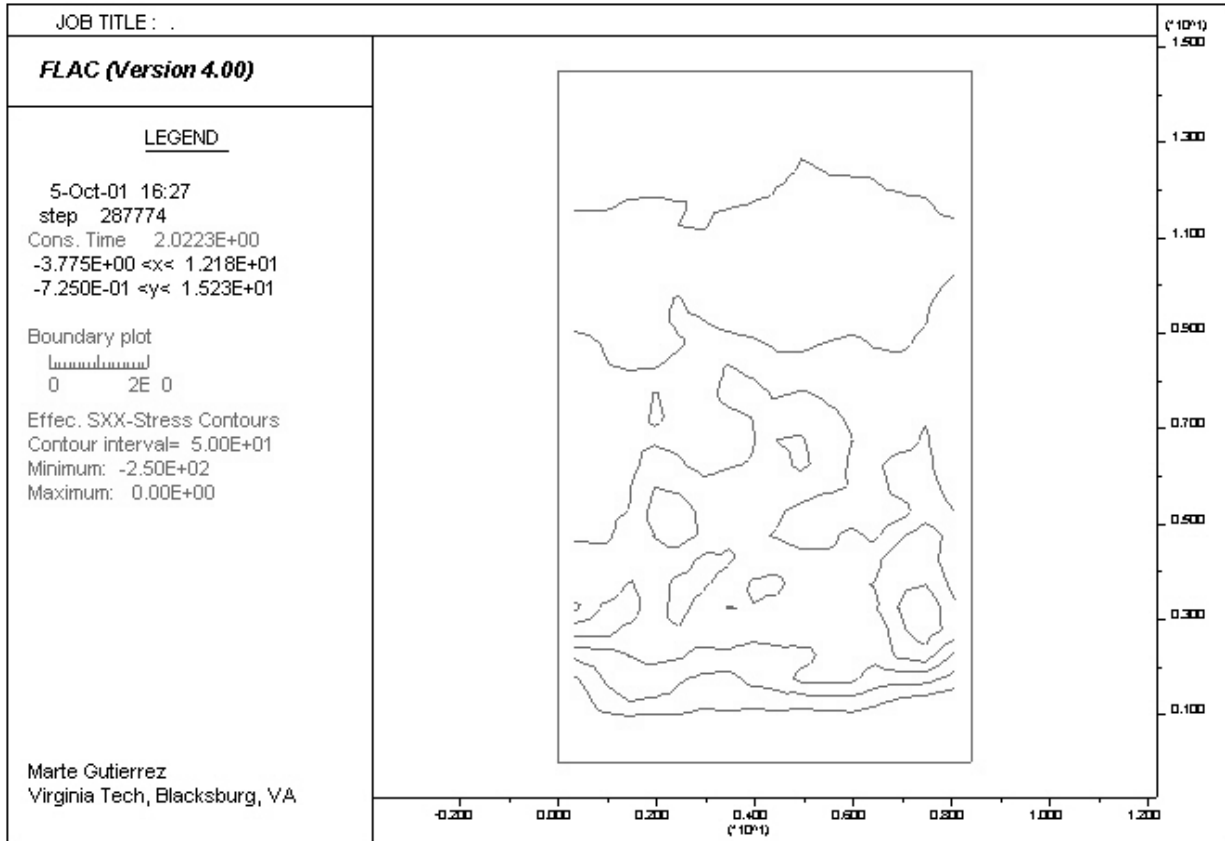


Figure 6.11 Contours of effective horizontal stress for Case 1C

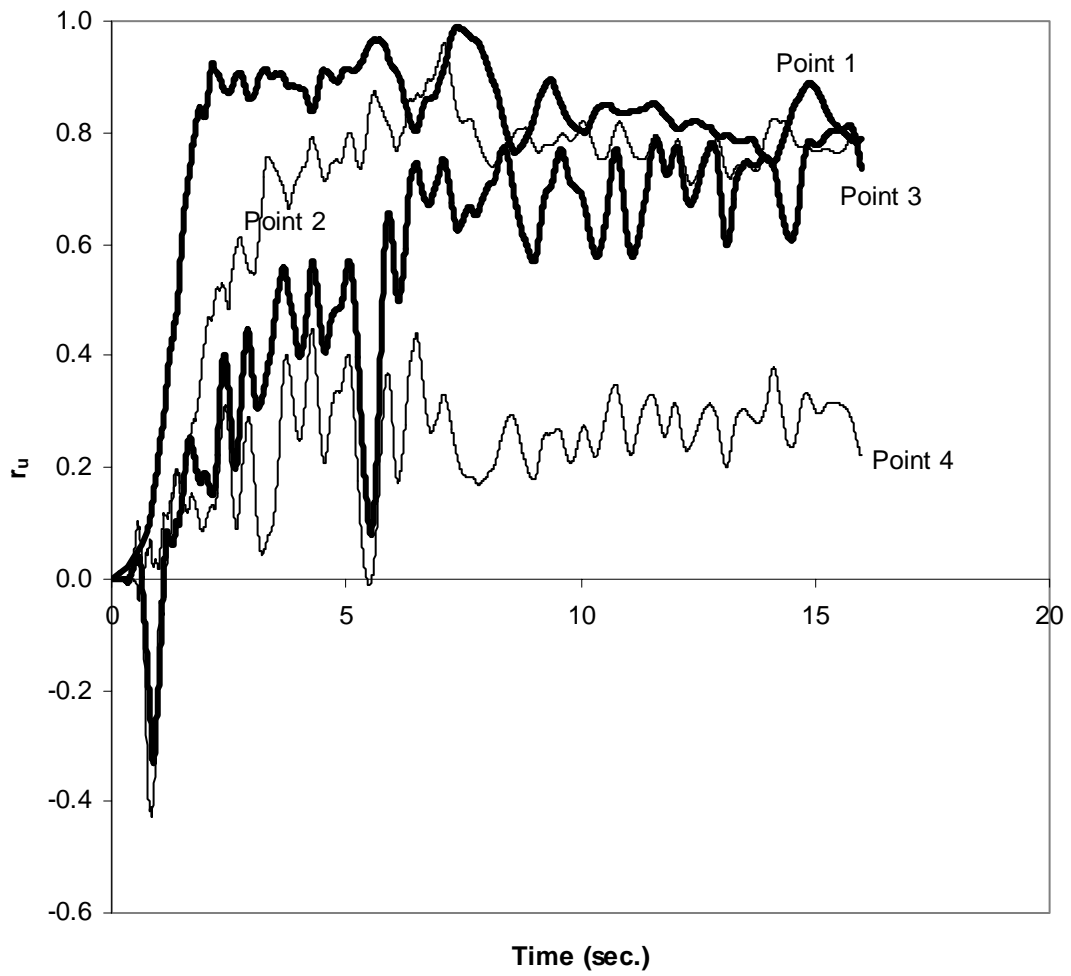


Figure 6.12 History of excess pore pressure ratio (r_u) for Case 2C

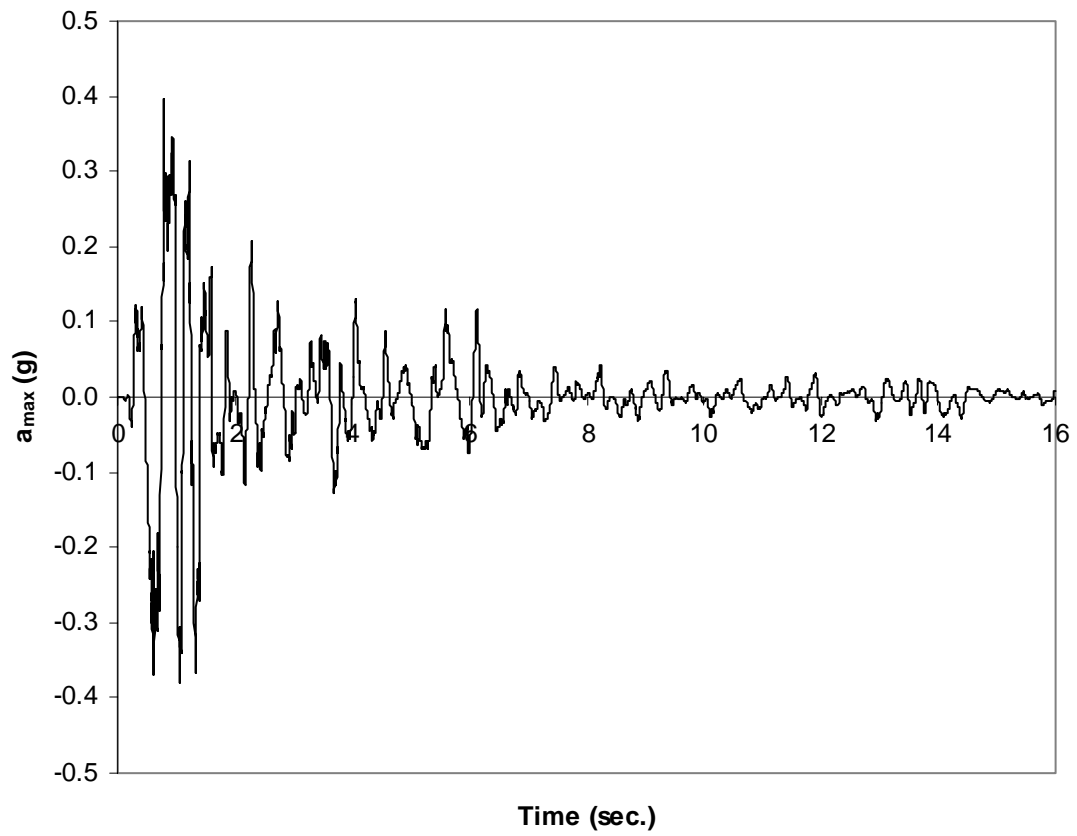


Figure 6.13 Acceleration time history (a_{\max}) for Case 2C

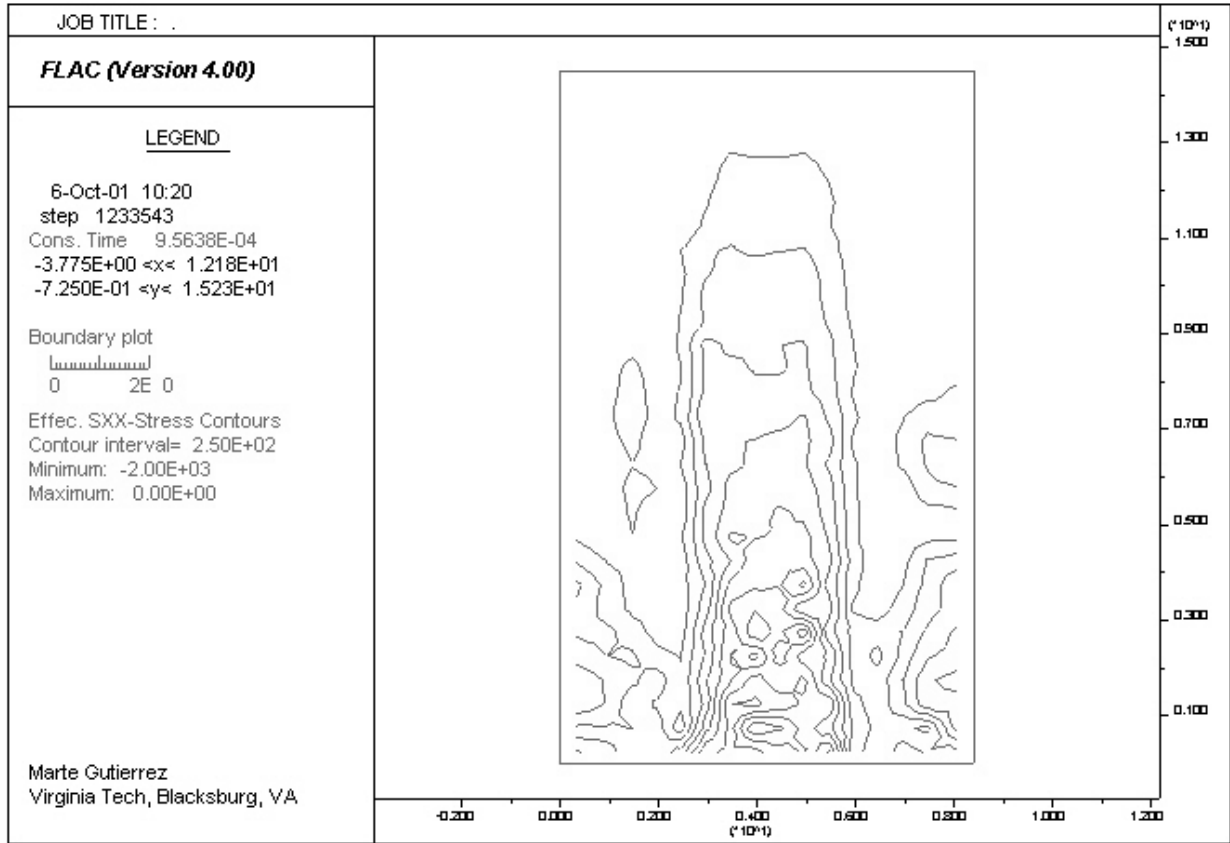


Figure 6.14 Contours of effective horizontal stress for Case 2C

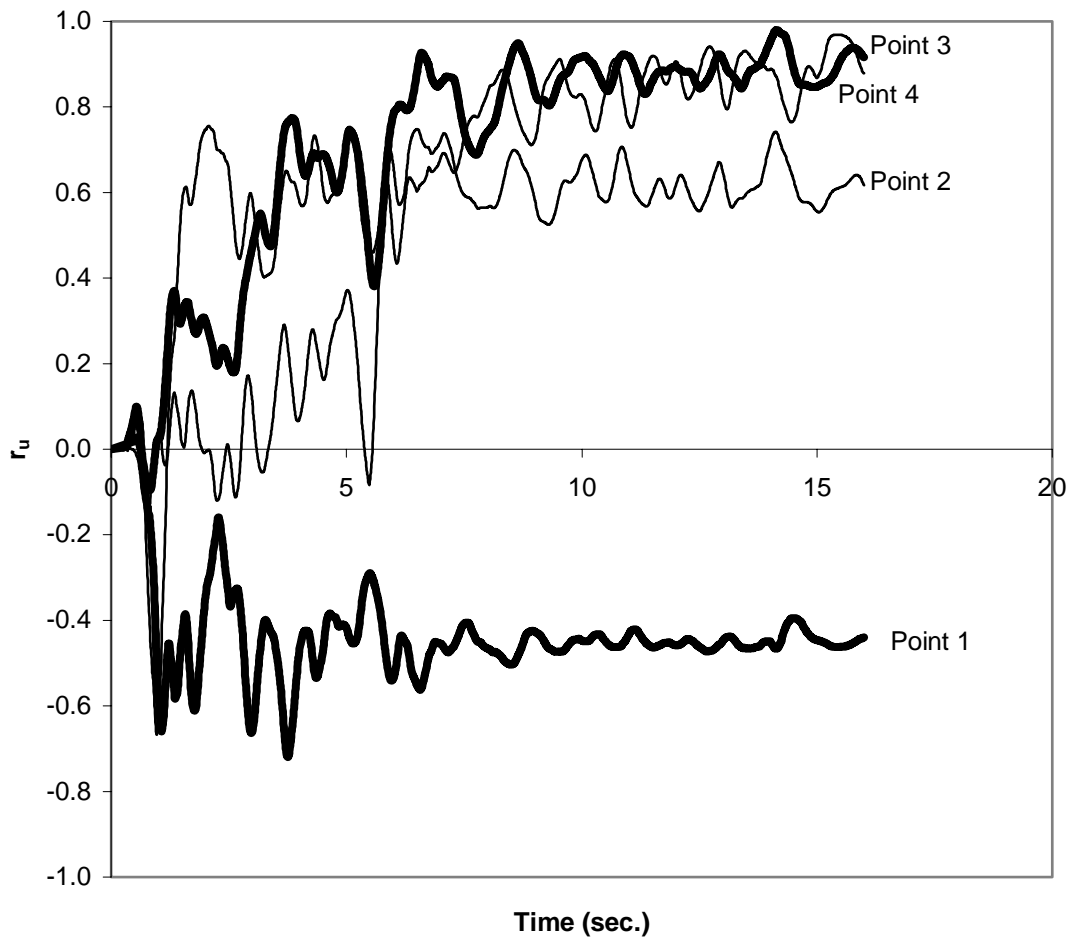


Figure 6.15 History of excess pore pressure ratio (r_u) for Case 2Ce

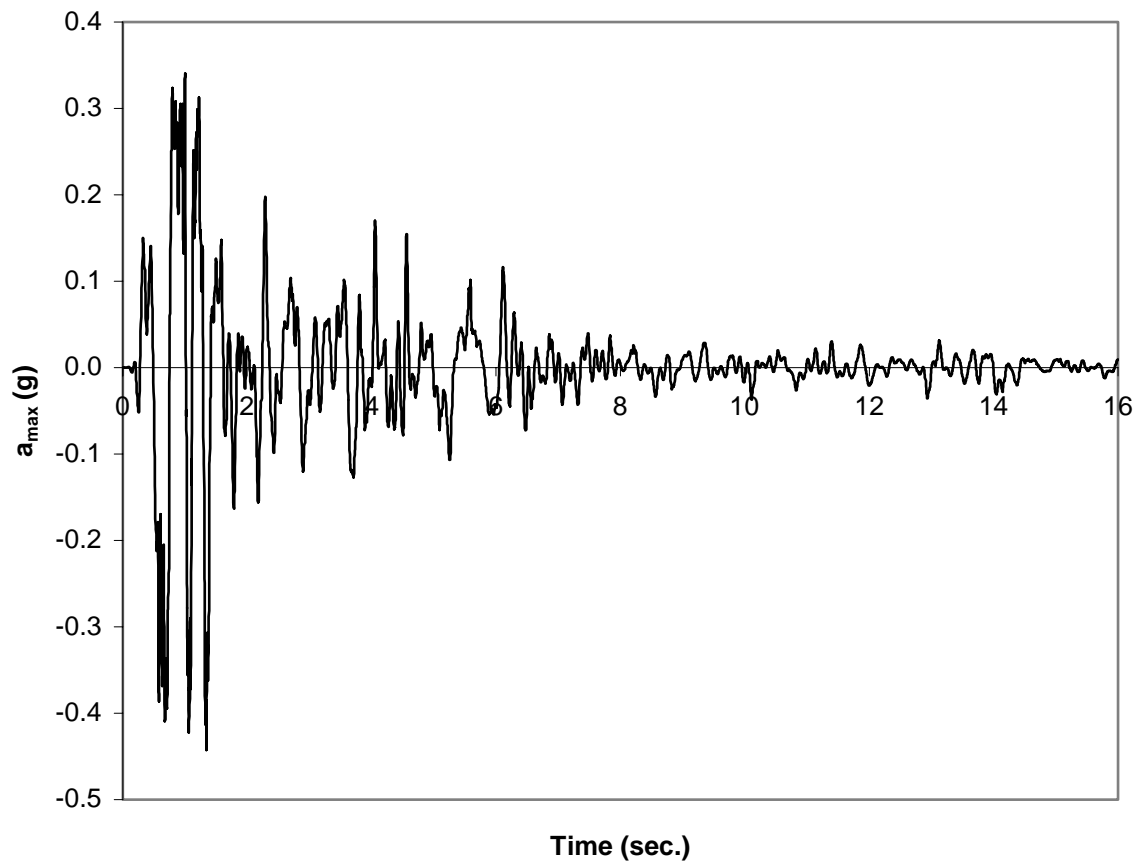


Figure 6.16 Acceleration time history (a_{\max}) for Case 2Ce

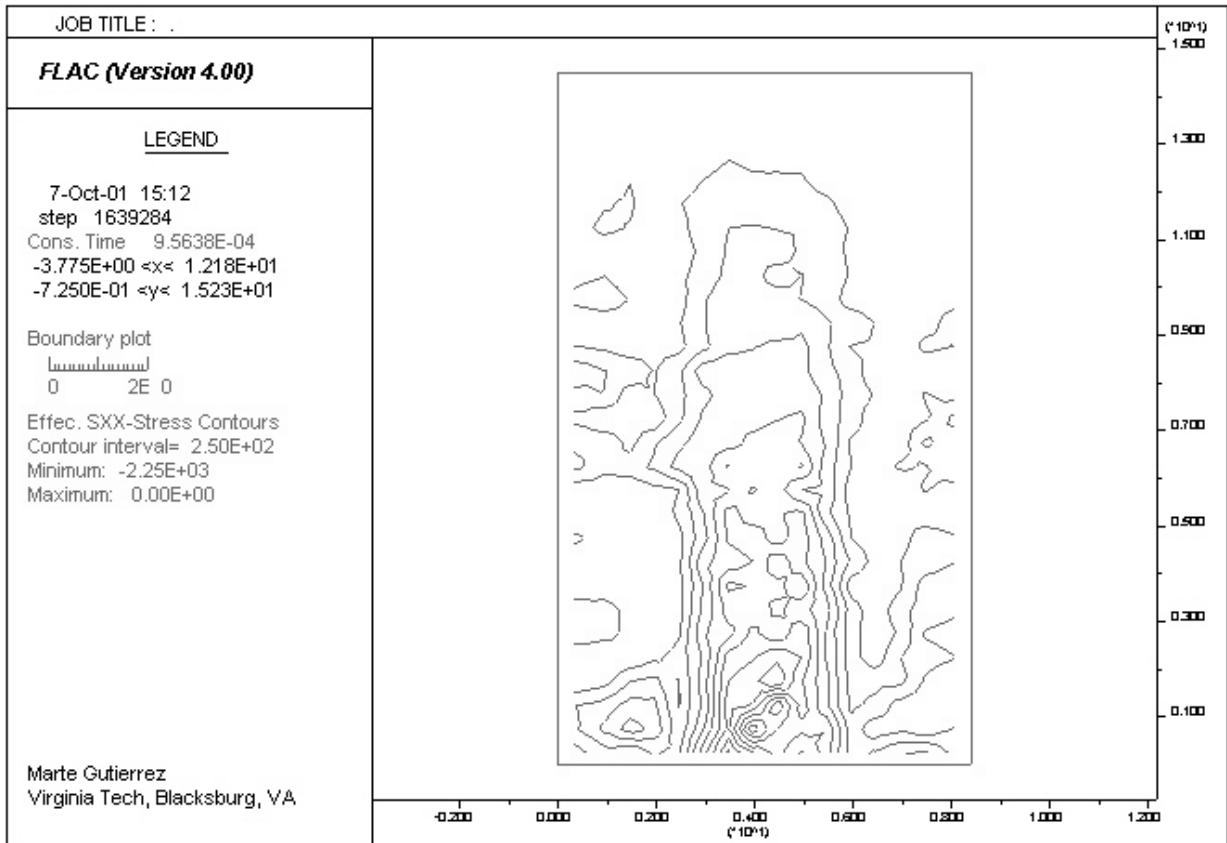


Figure 6.17 Contours of effective horizontal stress for Case 2Ce

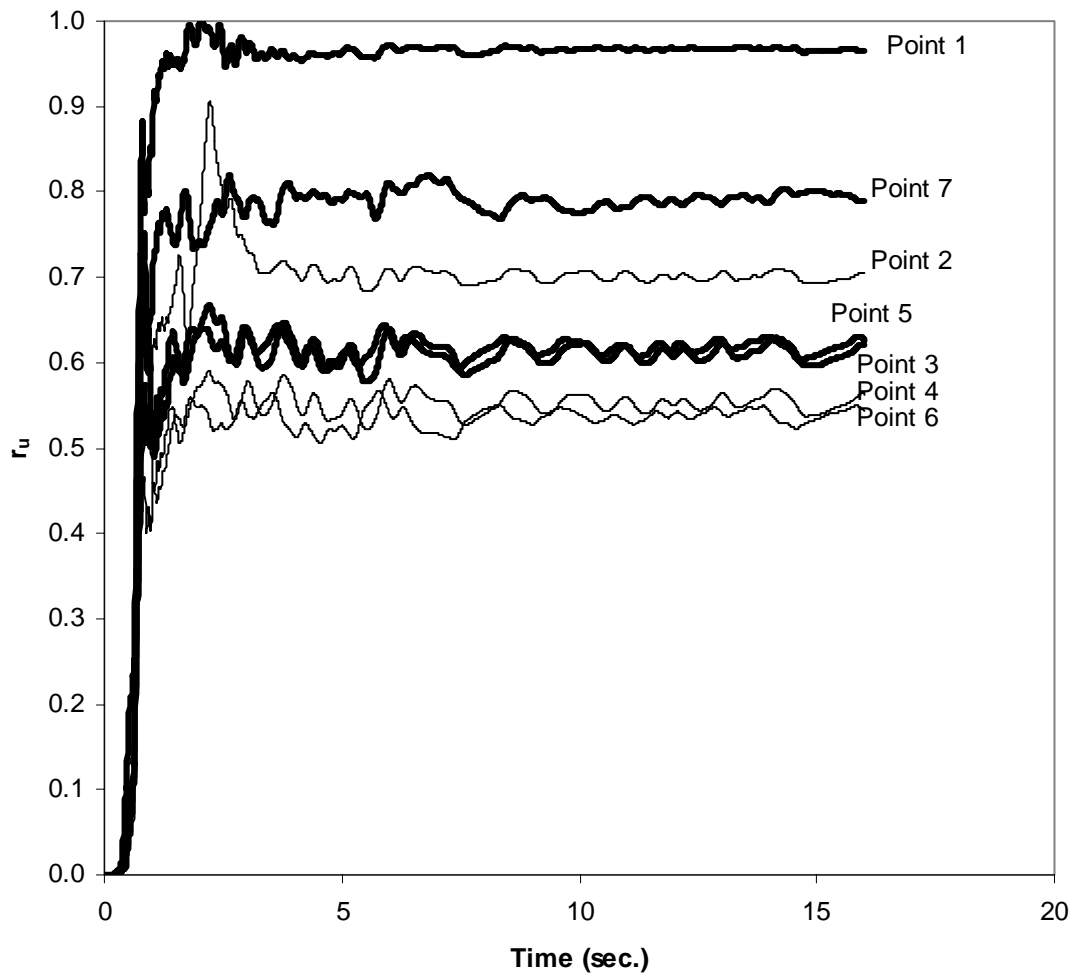


Figure 6.18 History of excess pore pressure ratio (r_u) for Case 3C

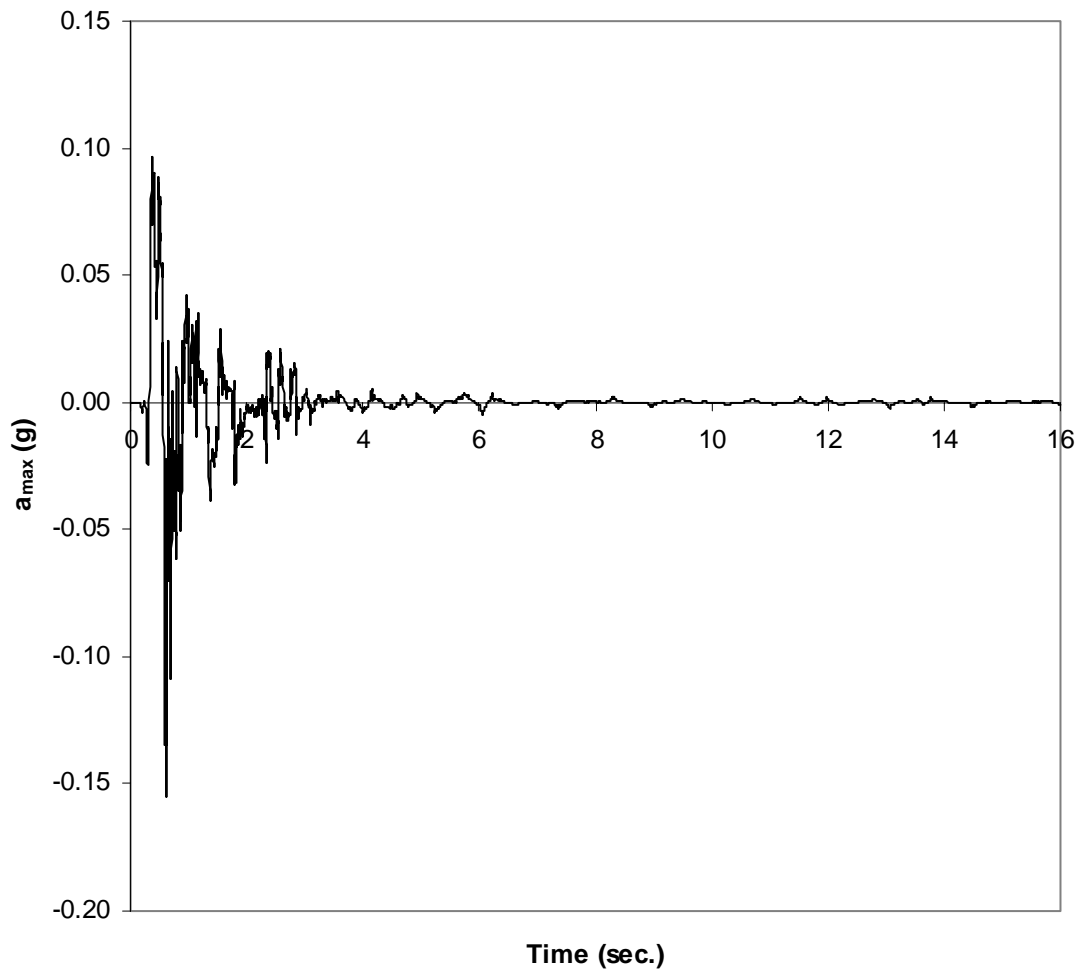


Figure 6.19 Acceleration time history (a_{\max}) for Case 3C

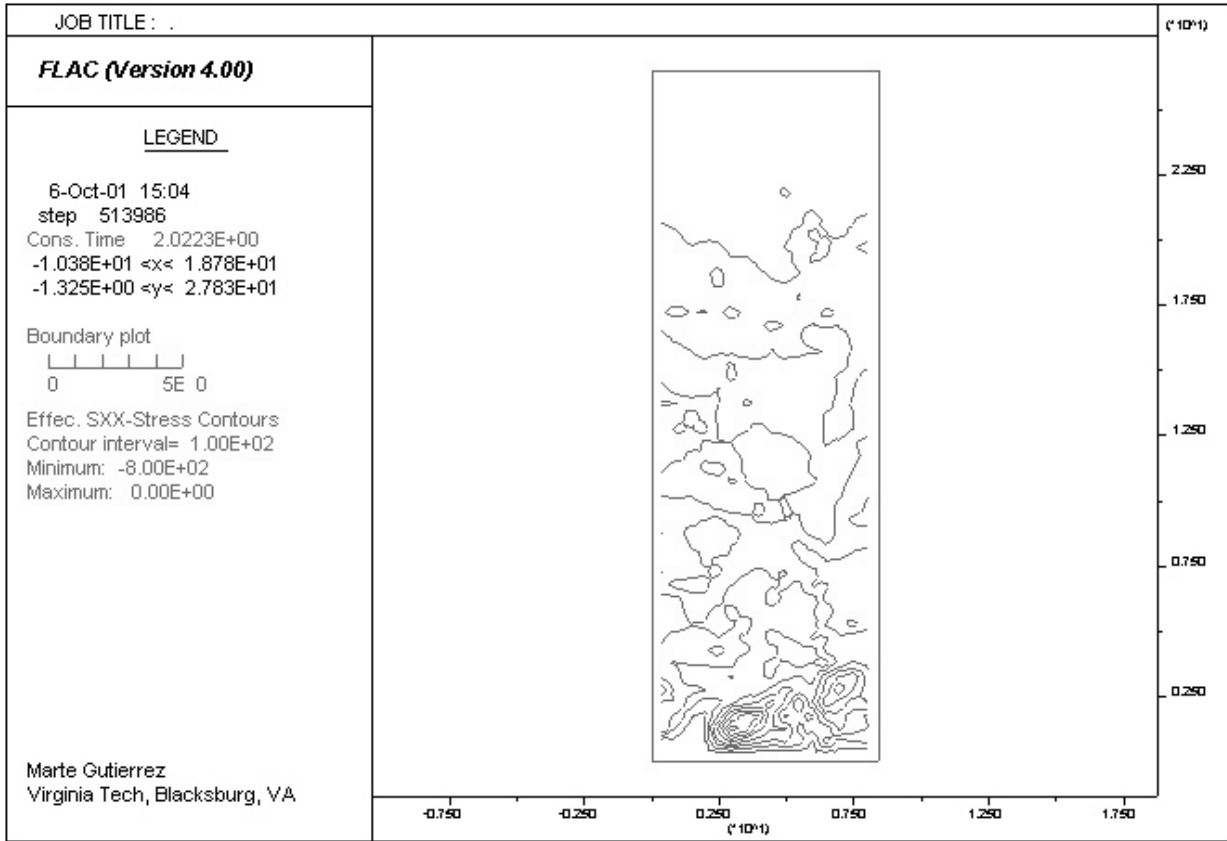


Figure 6.20 Contours of effective horizontal stress for Case 3C

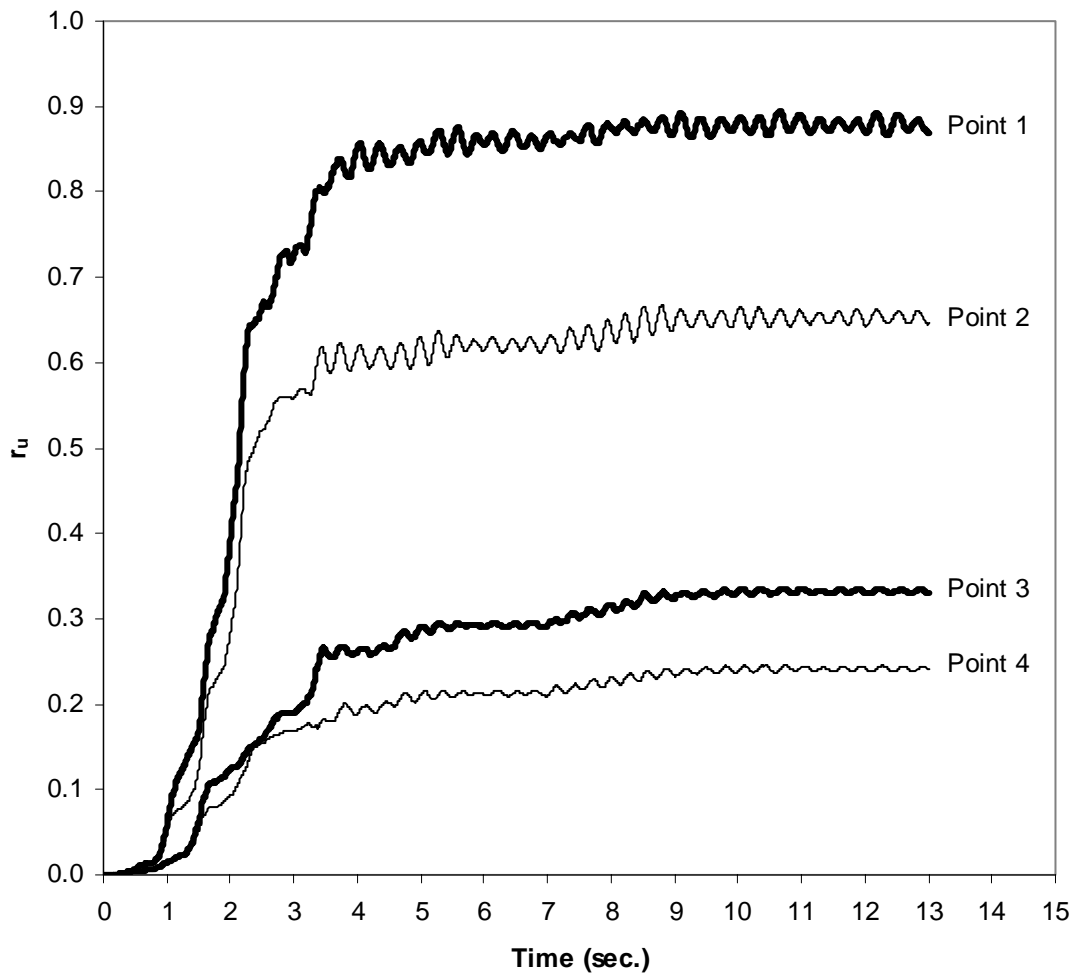


Figure 6.21 History of excess pore pressure ratio (r_u) for Case 1S

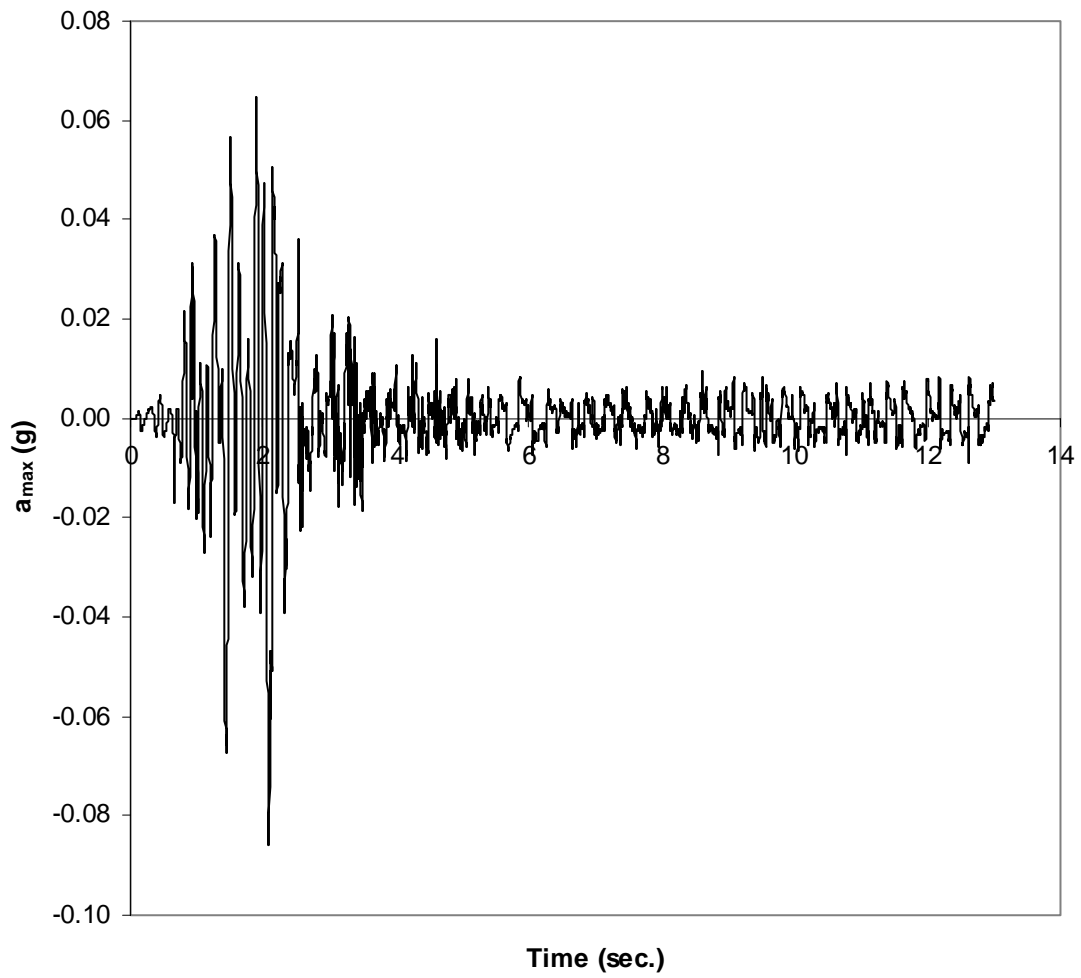


Figure 6.22 Acceleration time history (a_{\max}) for Case 1S

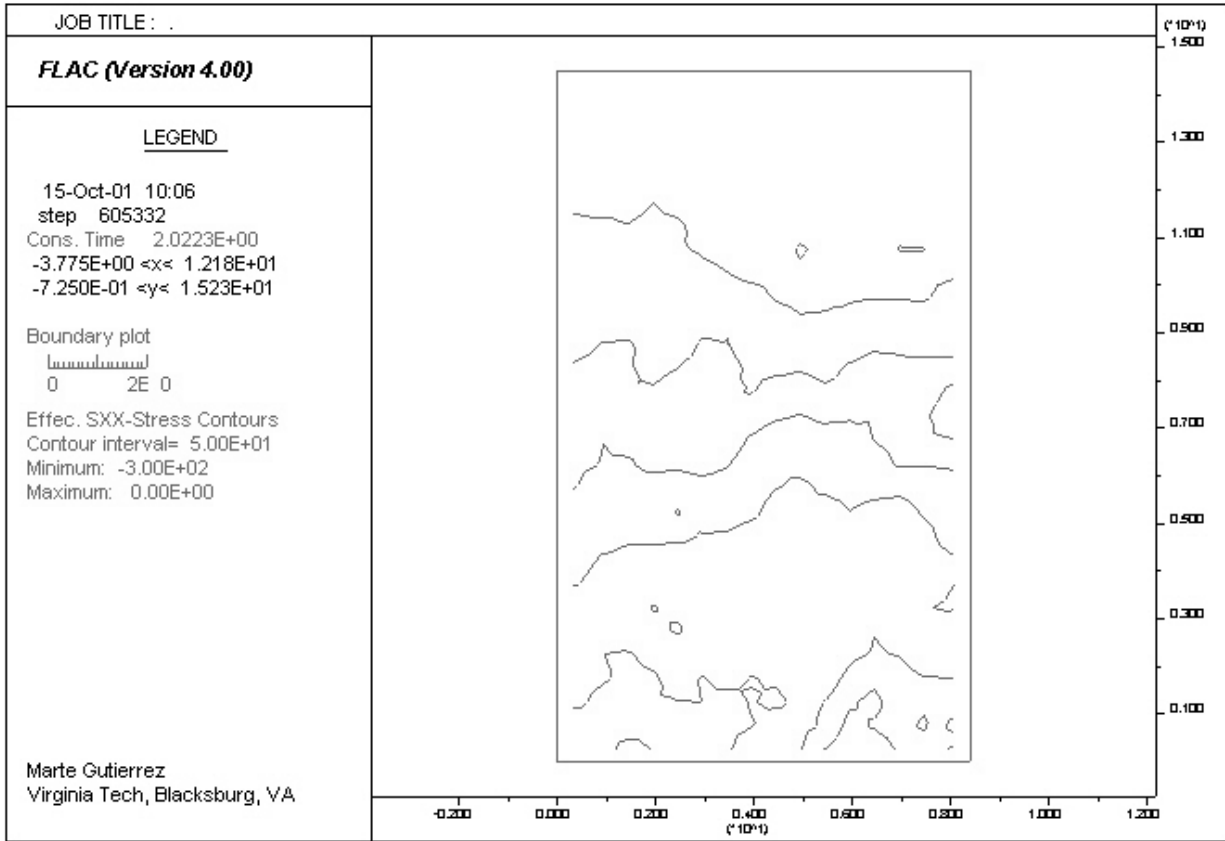


Figure 6.23 Contours of effective horizontal stress for Case 1S

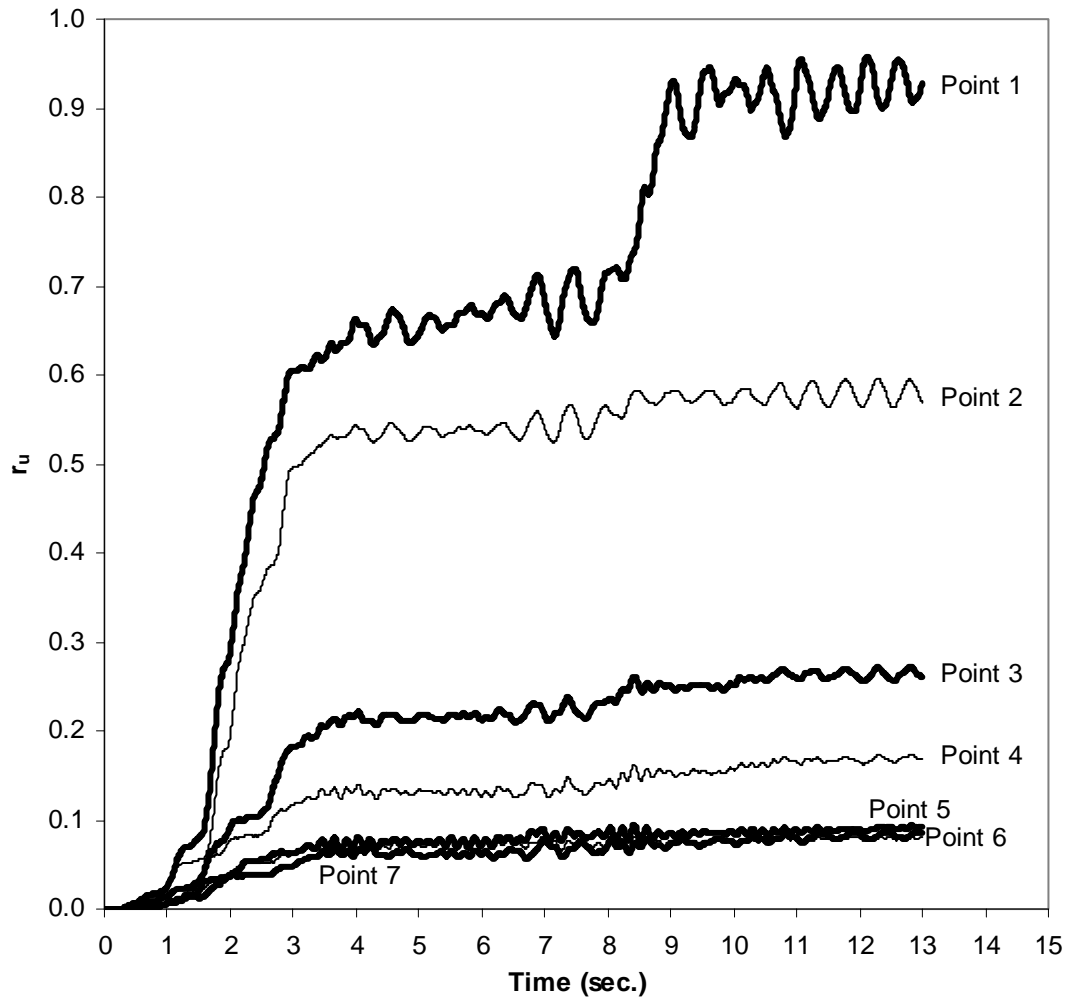


Figure 6.24 History of excess pore pressure ratio (r_u) for Case 3S

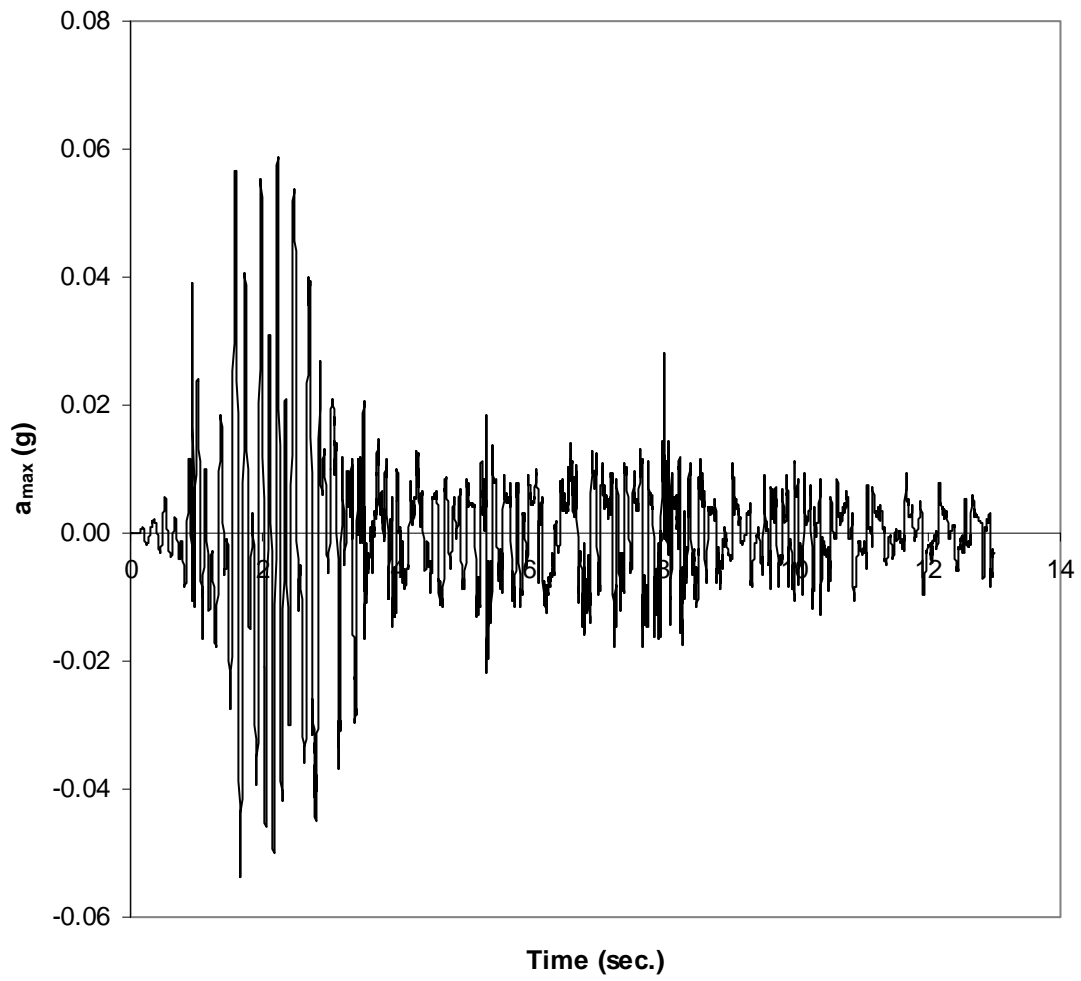


Figure 6.25 Acceleration time history (a_{max}) for Case 3S

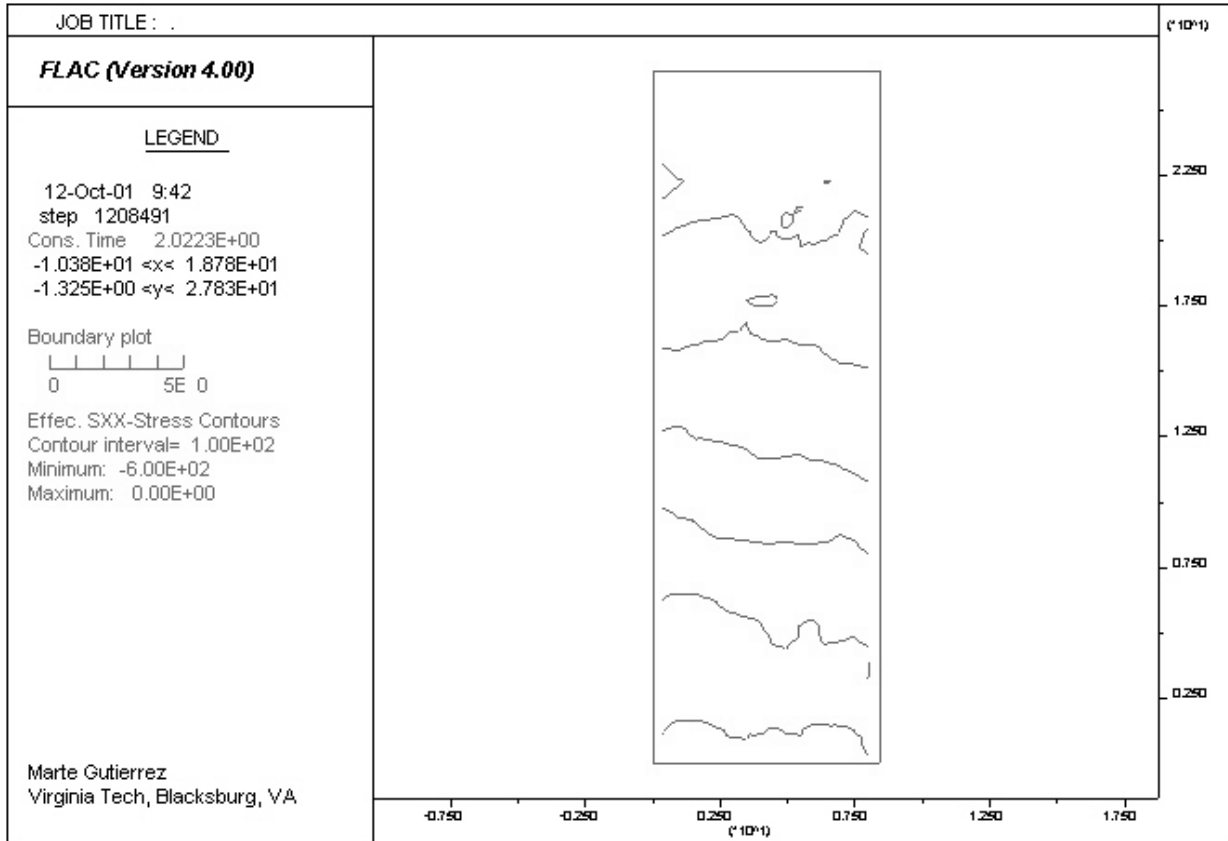


Figure 6.26 Contours of effective horizontal stress for Case 3S

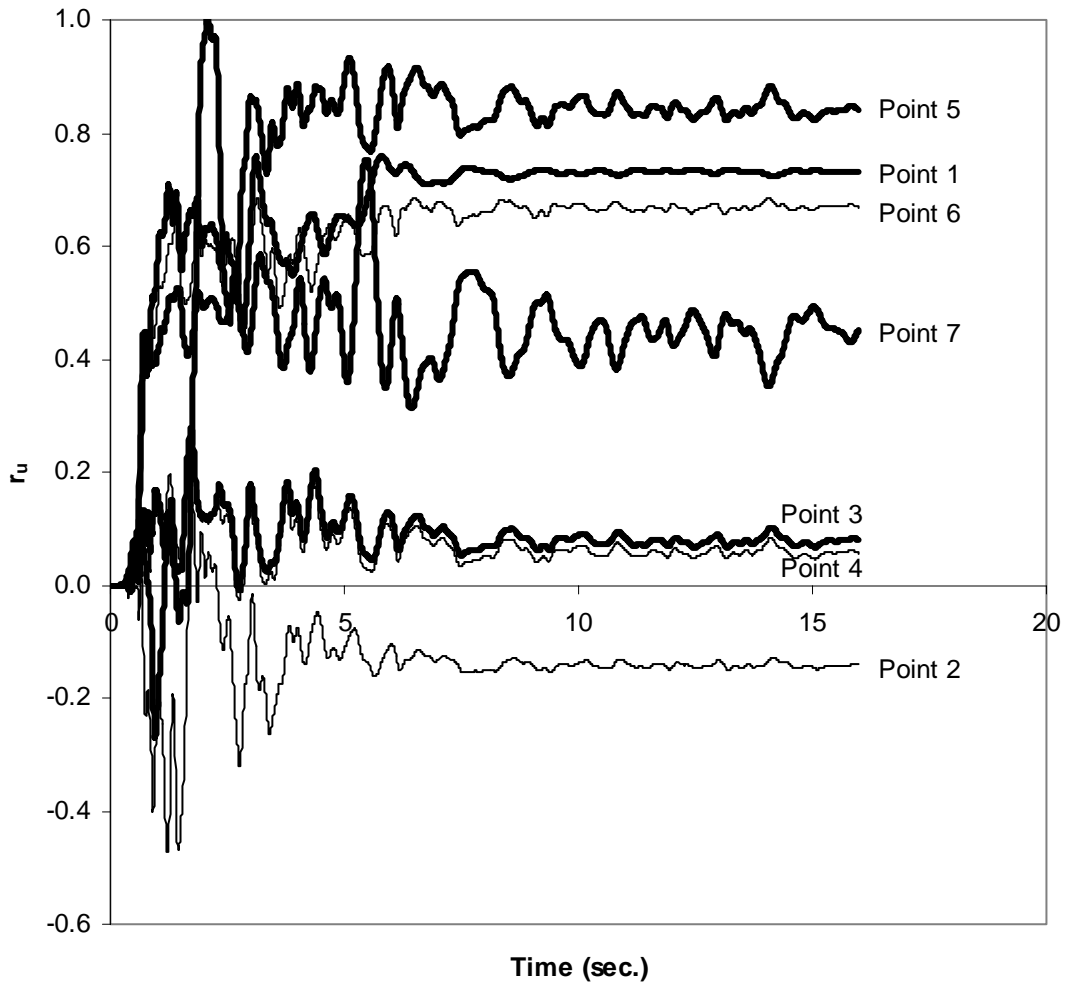


Figure 6.27 History of excess pore pressure ratio (r_u) for Case 4C

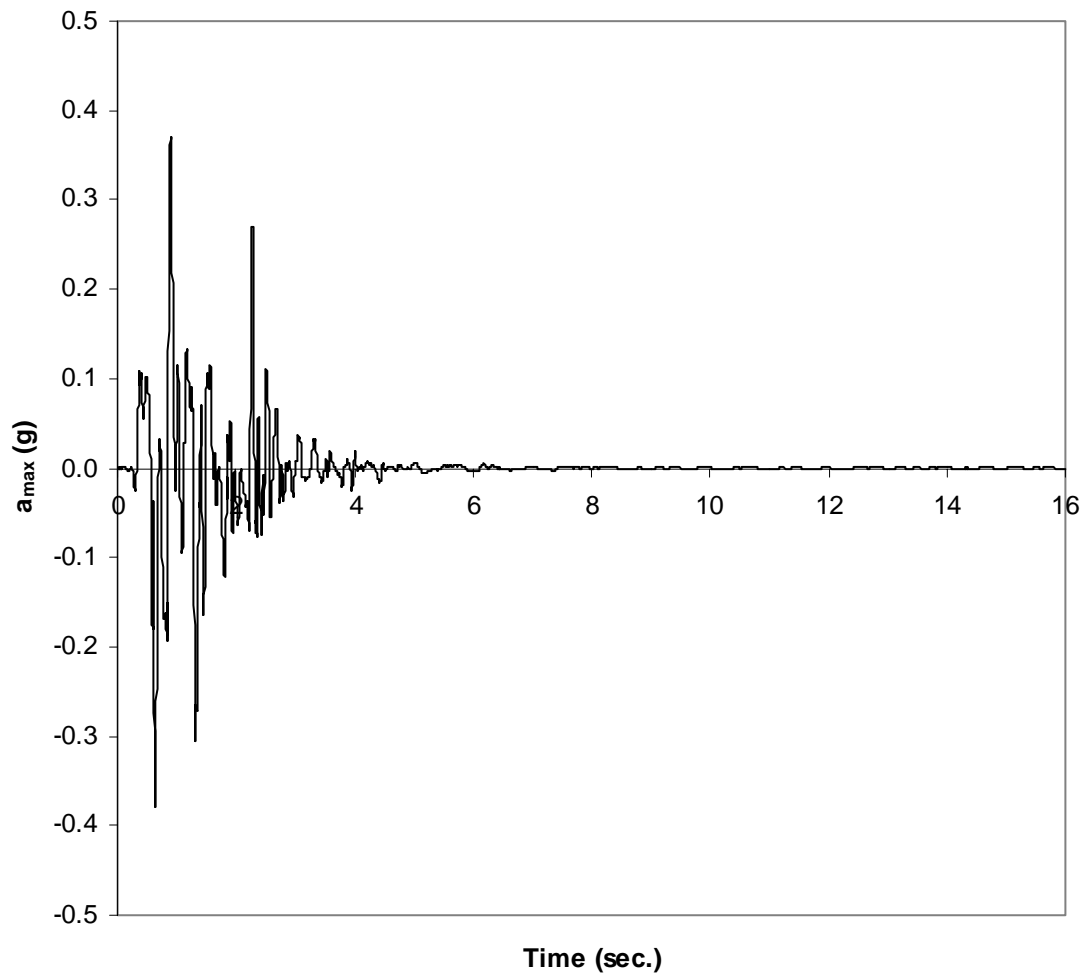


Figure 6.28 Acceleration time history (a_{\max}) for Case 4C

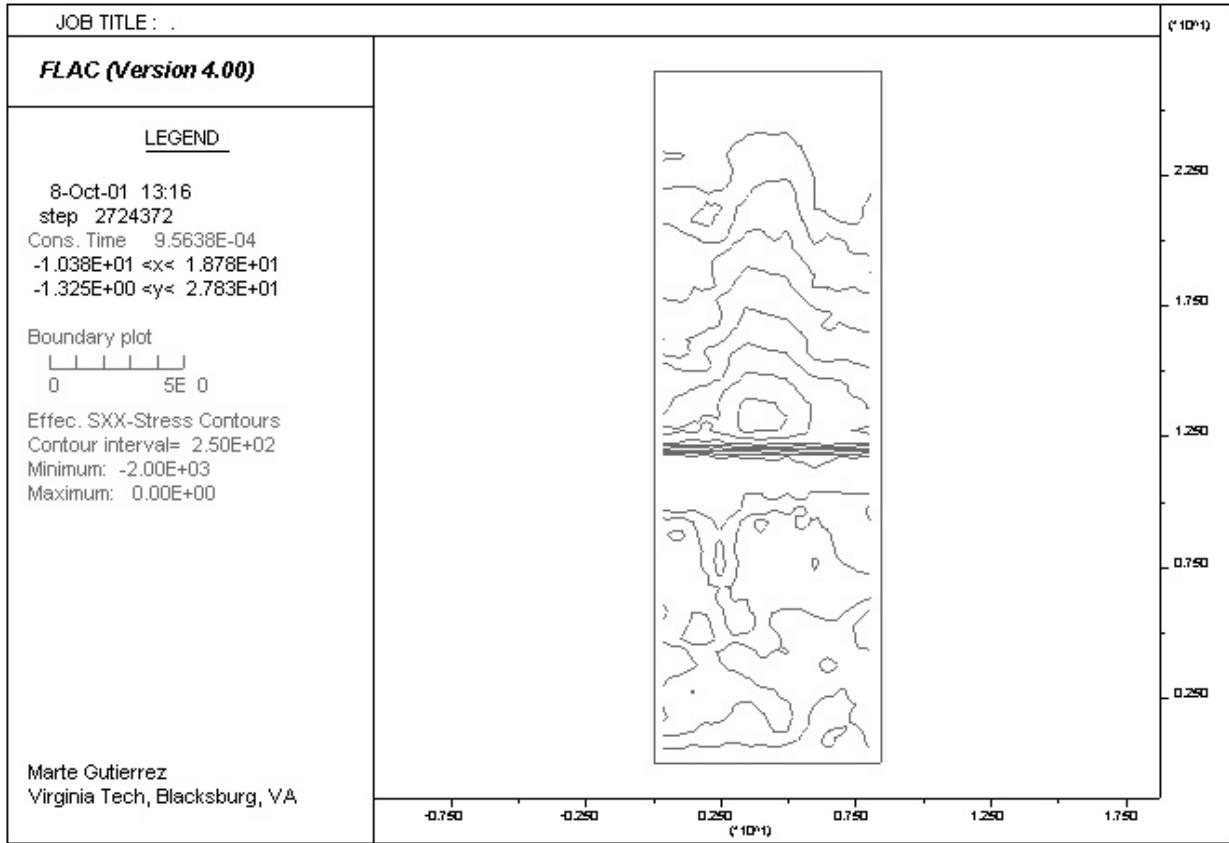


Figure 6.29 Contours of effective horizontal stress for Case 4C

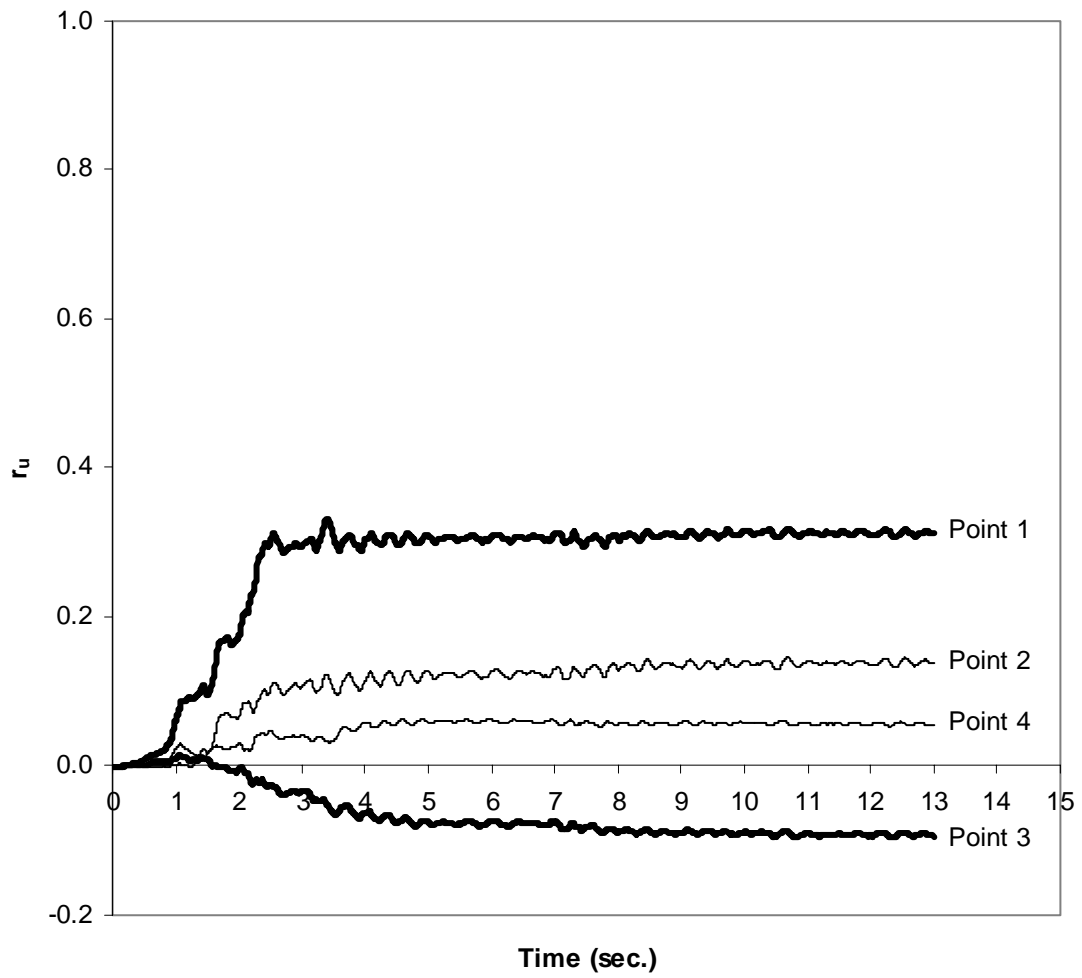


Figure 6.30 History of excess pore pressure ratio (r_u) for Case 2S

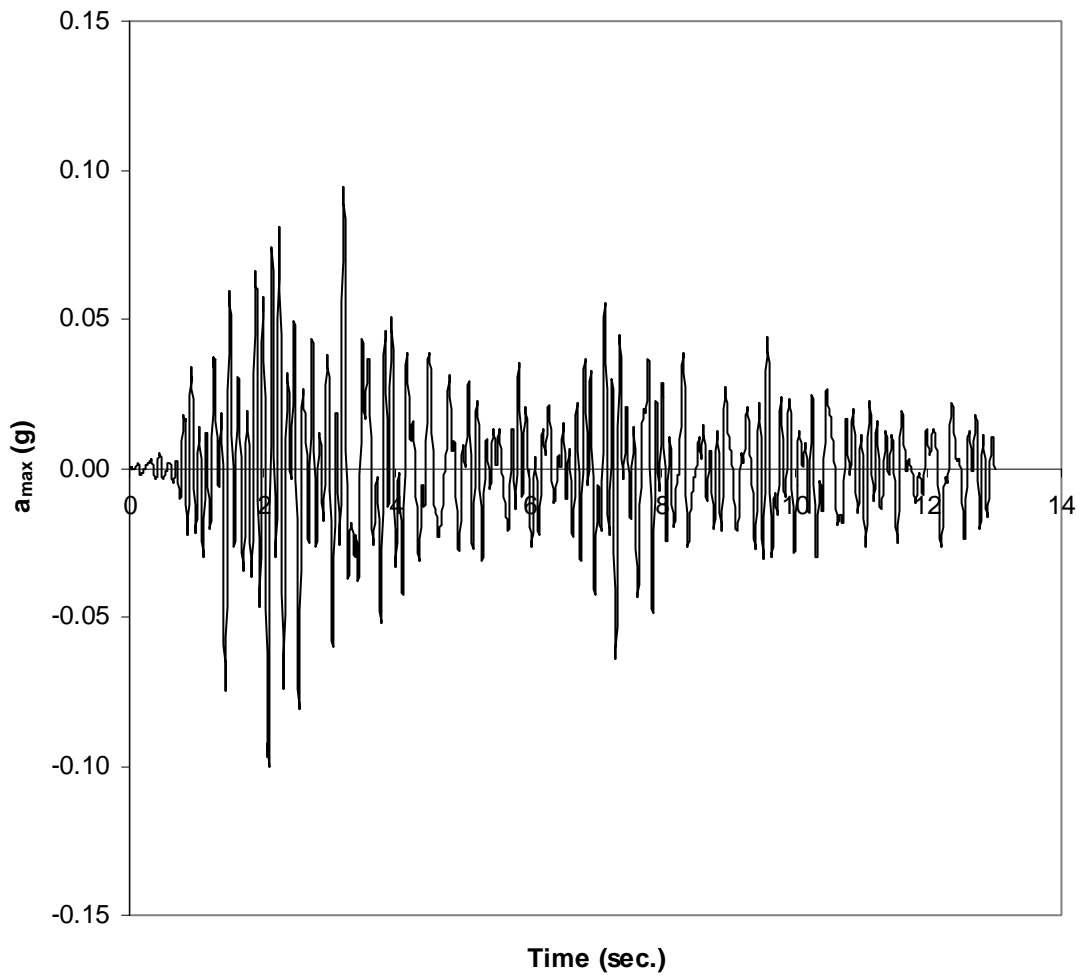


Figure 6.31 Acceleration time history (a_{\max}) for Case 2S

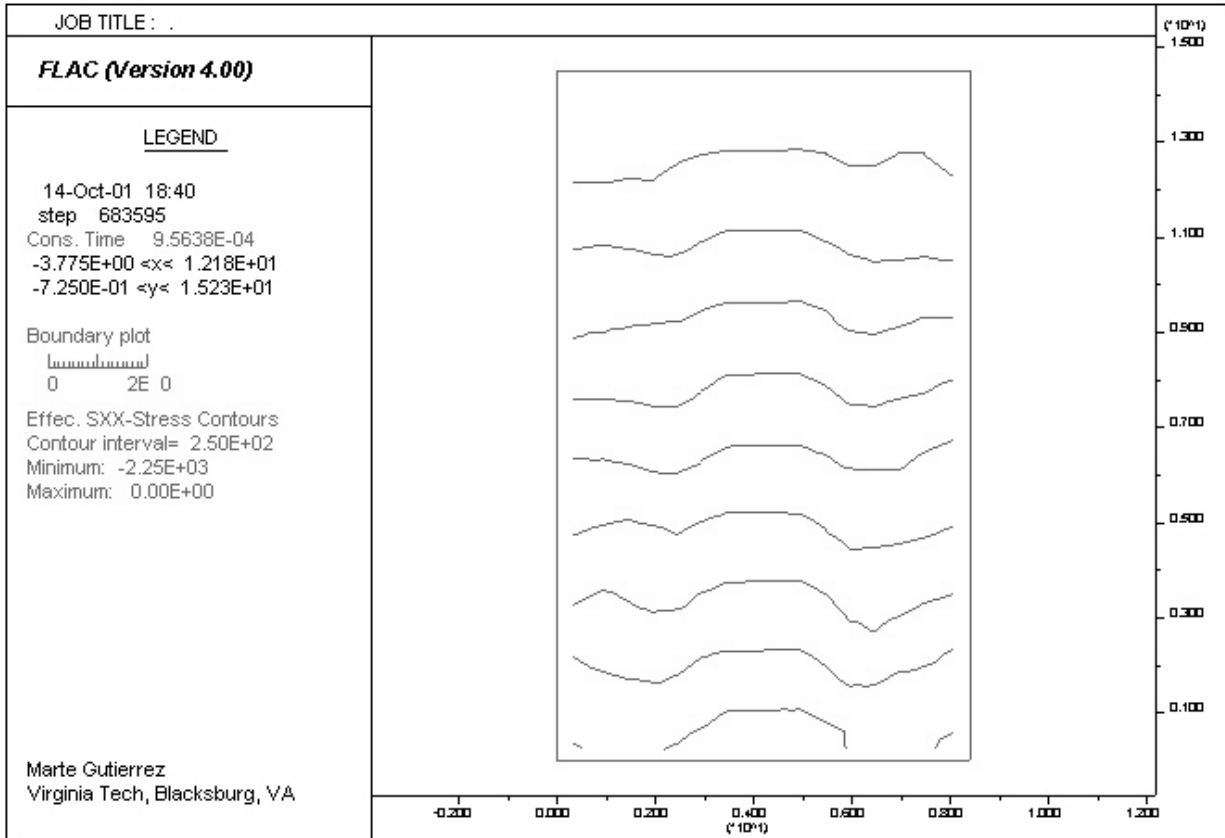


Figure 6.32 Contours of effective horizontal stress for Case 2S

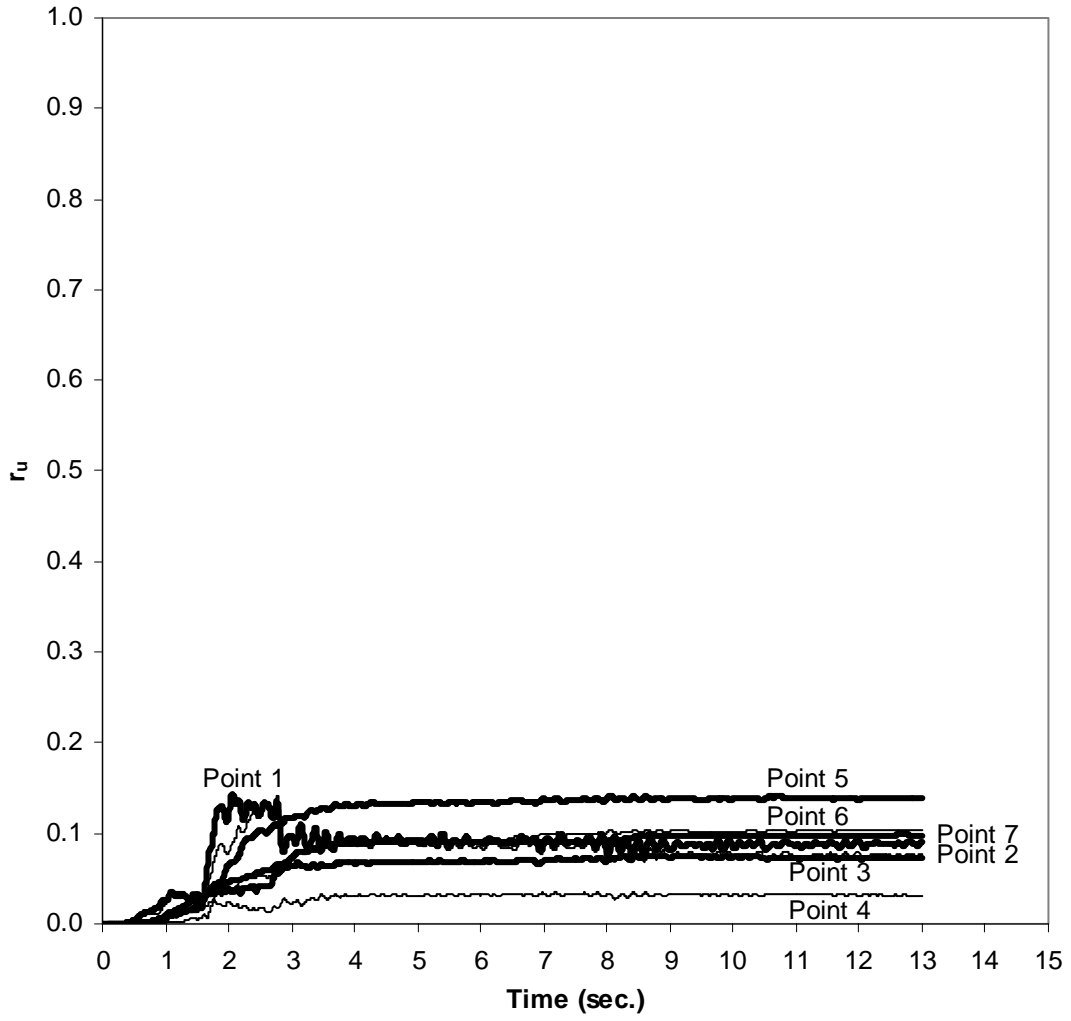


Figure 6.33 History of excess pore pressure ratio (r_u) for Case 4S

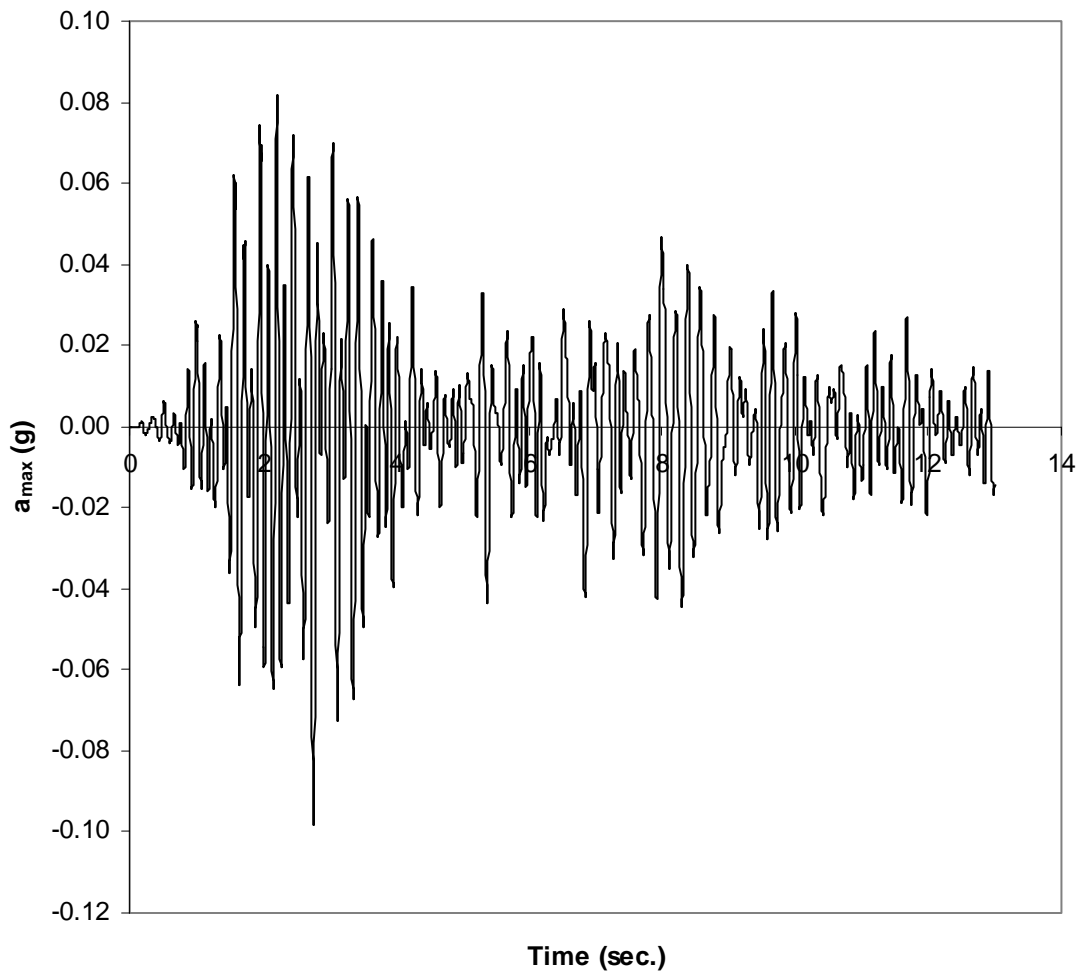


Figure 6.34 Acceleration time history (a_{\max}) for Case 4S

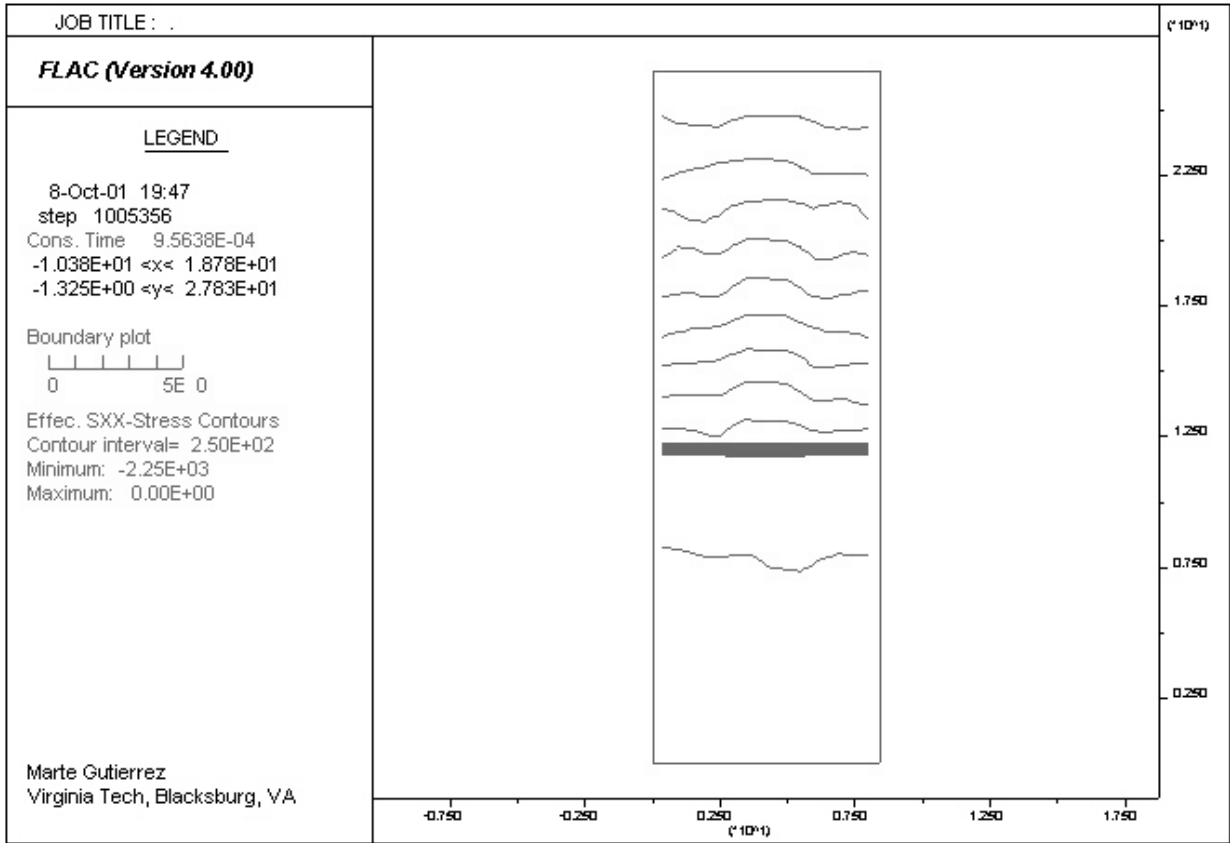


Figure 6.35 Contours of effective horizontal stress for Case 4S

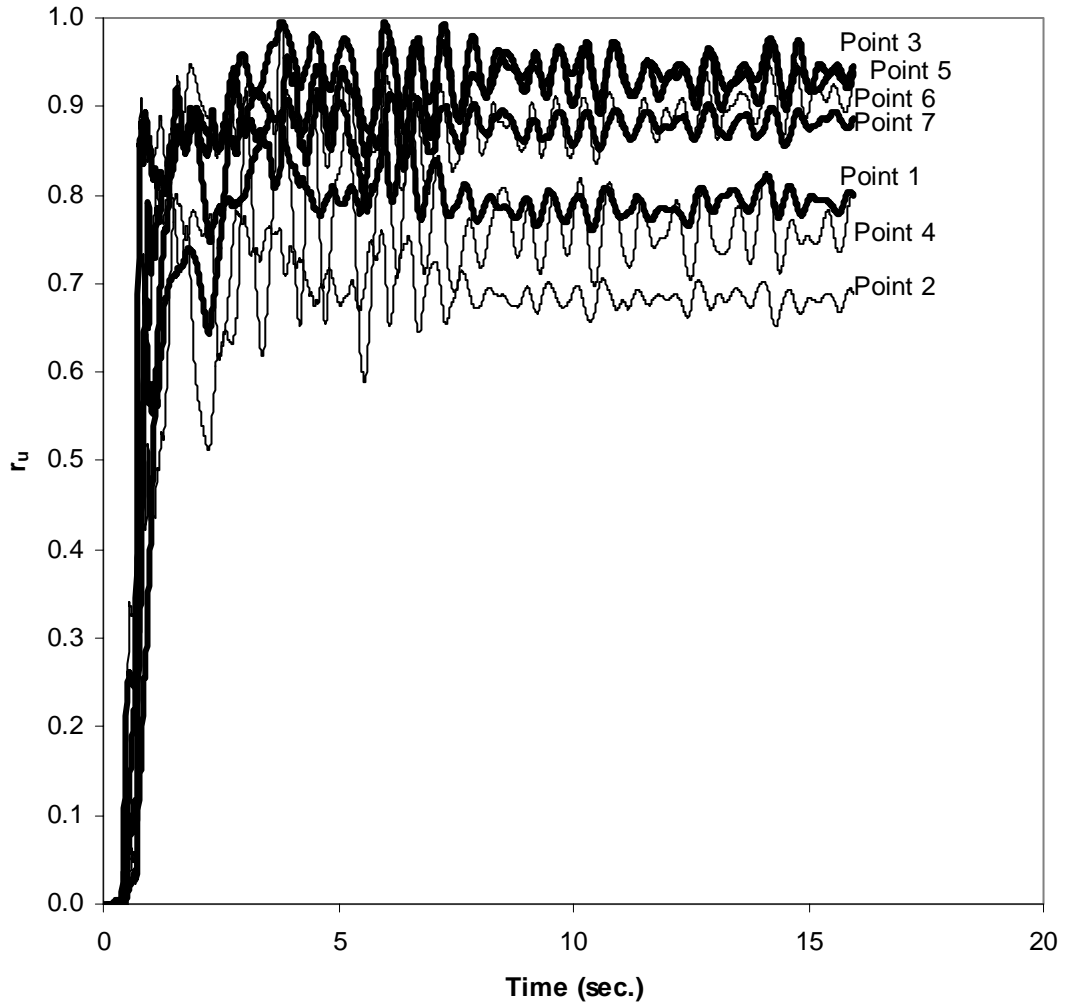


Figure 6.36 History of excess pore pressure ratio (r_u) for Case 5C

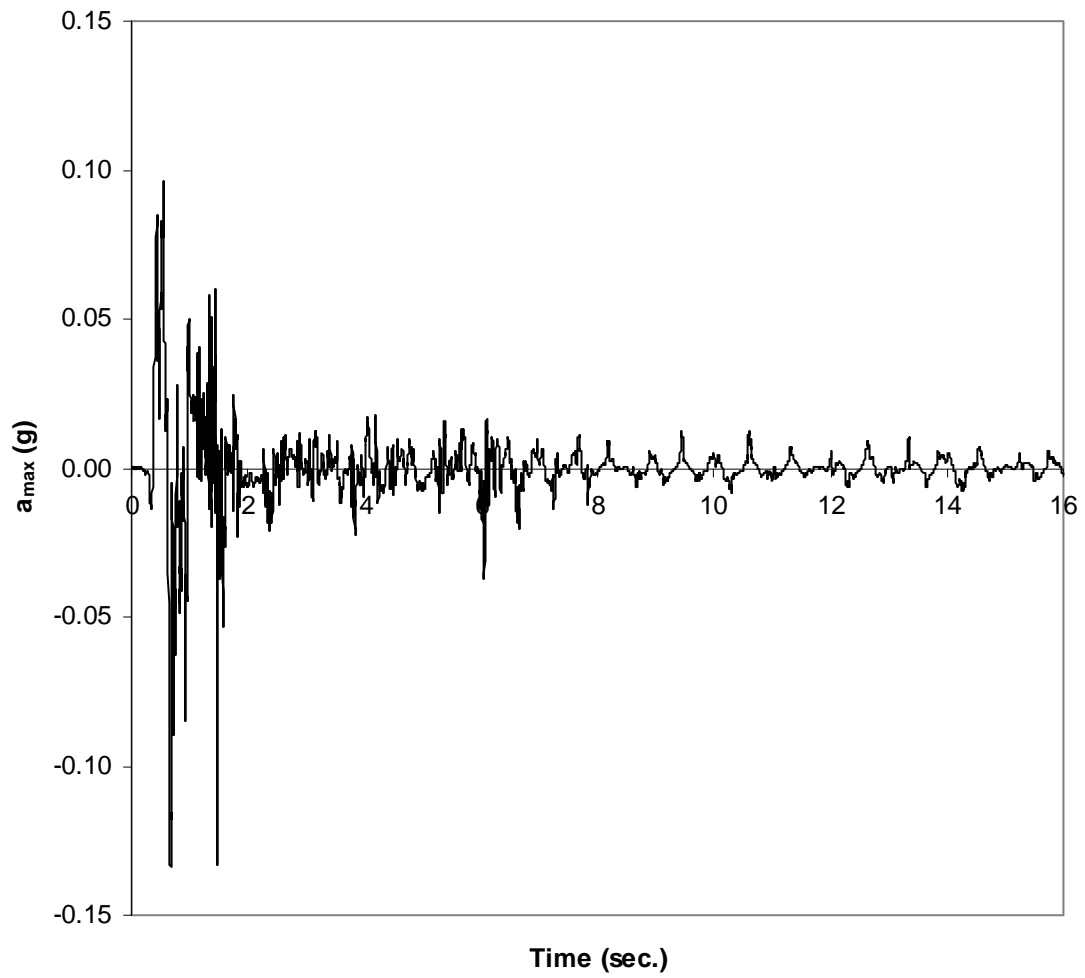


Figure 6.37 Acceleration time history (a_{\max}) for Case 5C

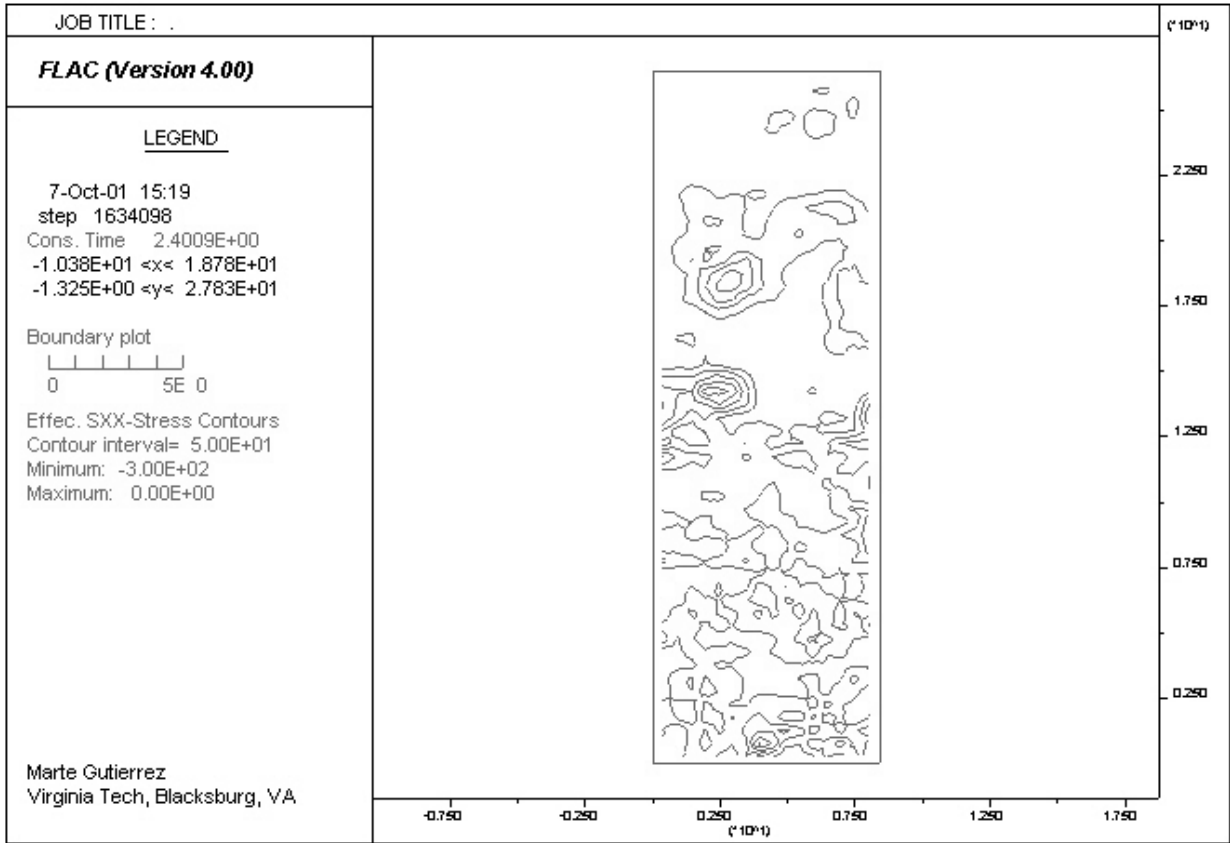


Figure 6.38 Contours of effective horizontal stress for Case 5C

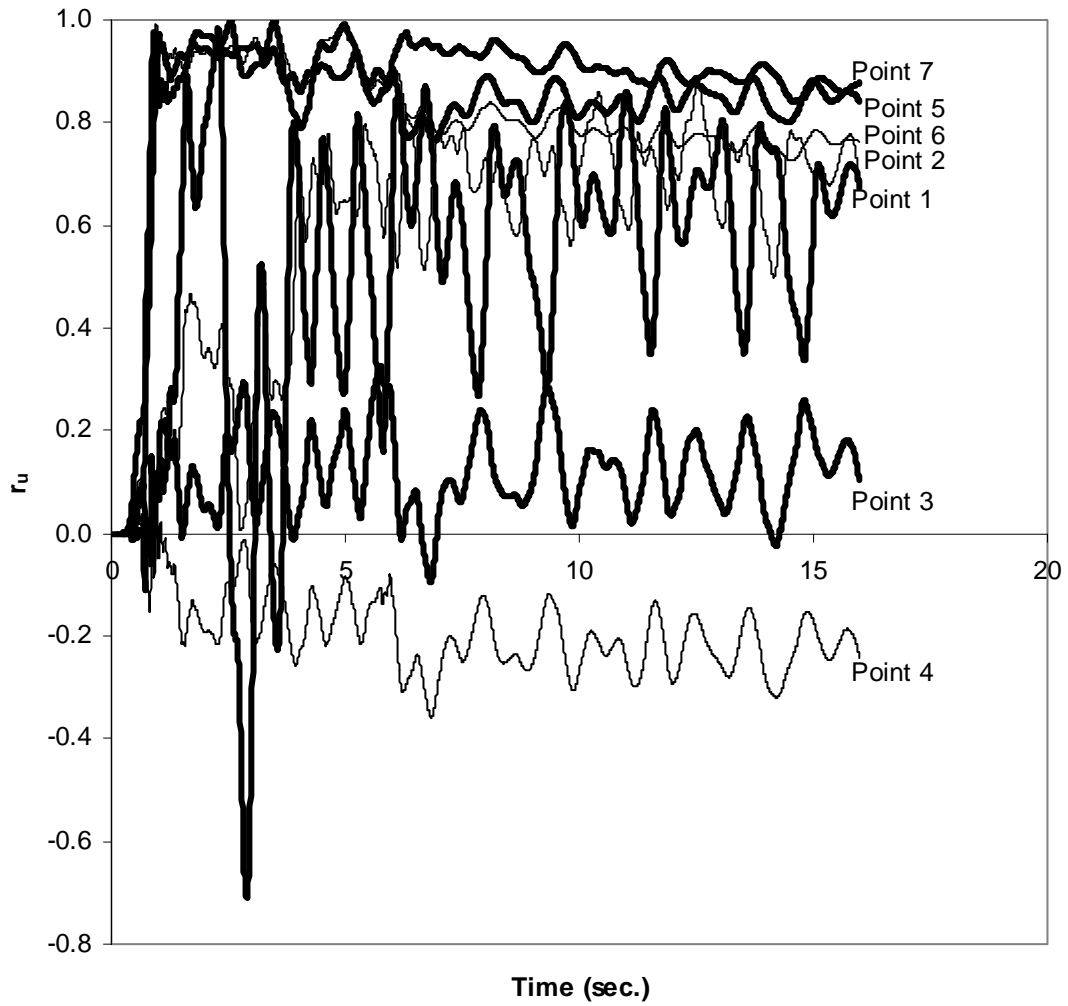


Figure 6.39 History of excess pore pressure ratio (r_u) for Case 6C

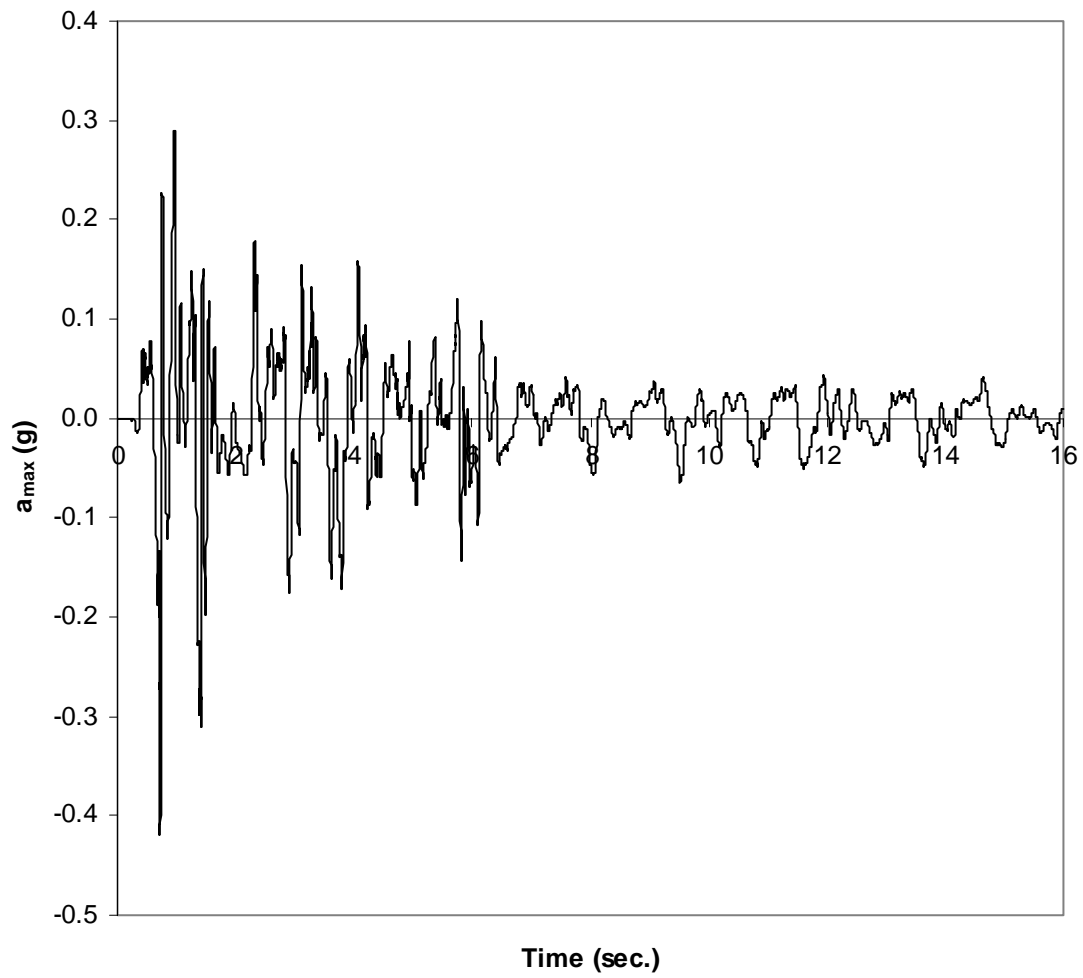


Figure 6.40 Acceleration time history (a_{\max}) for Case 6C

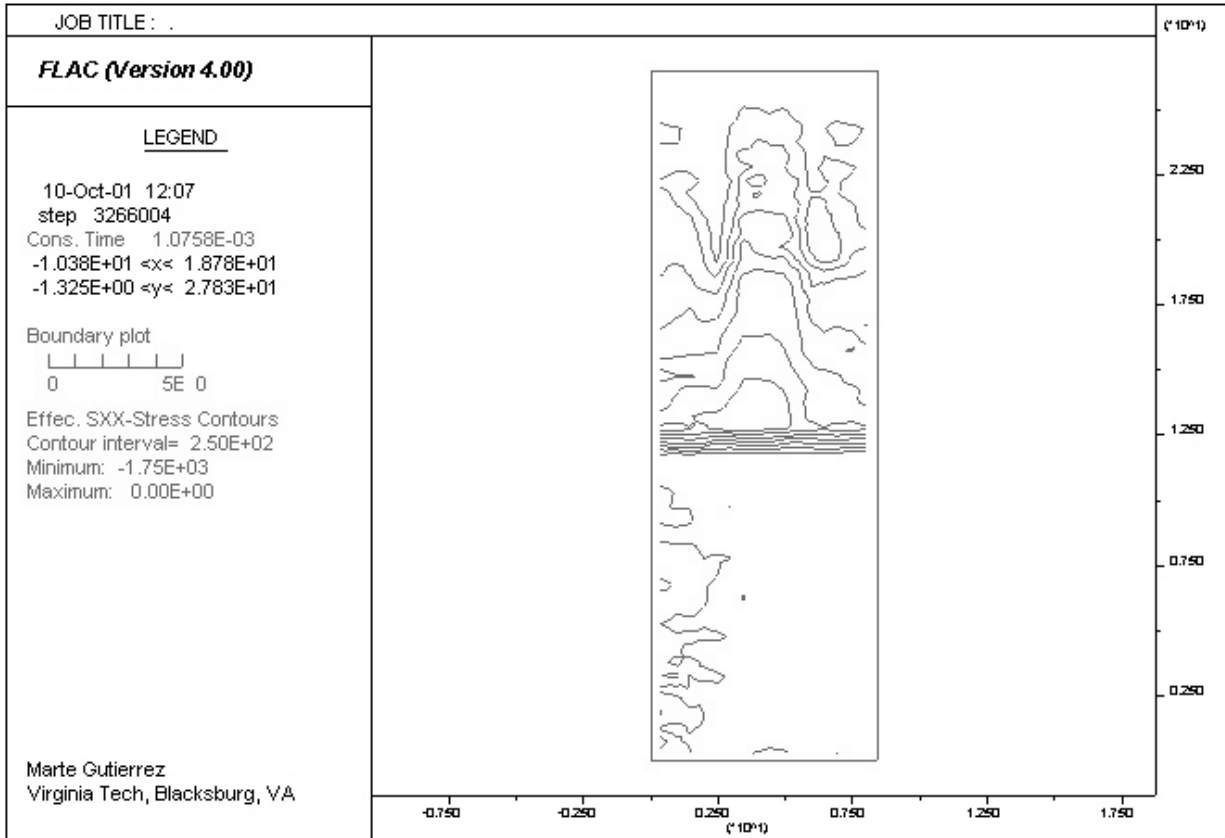


Figure 6.41 Contours of effective horizontal stress for Case 6C

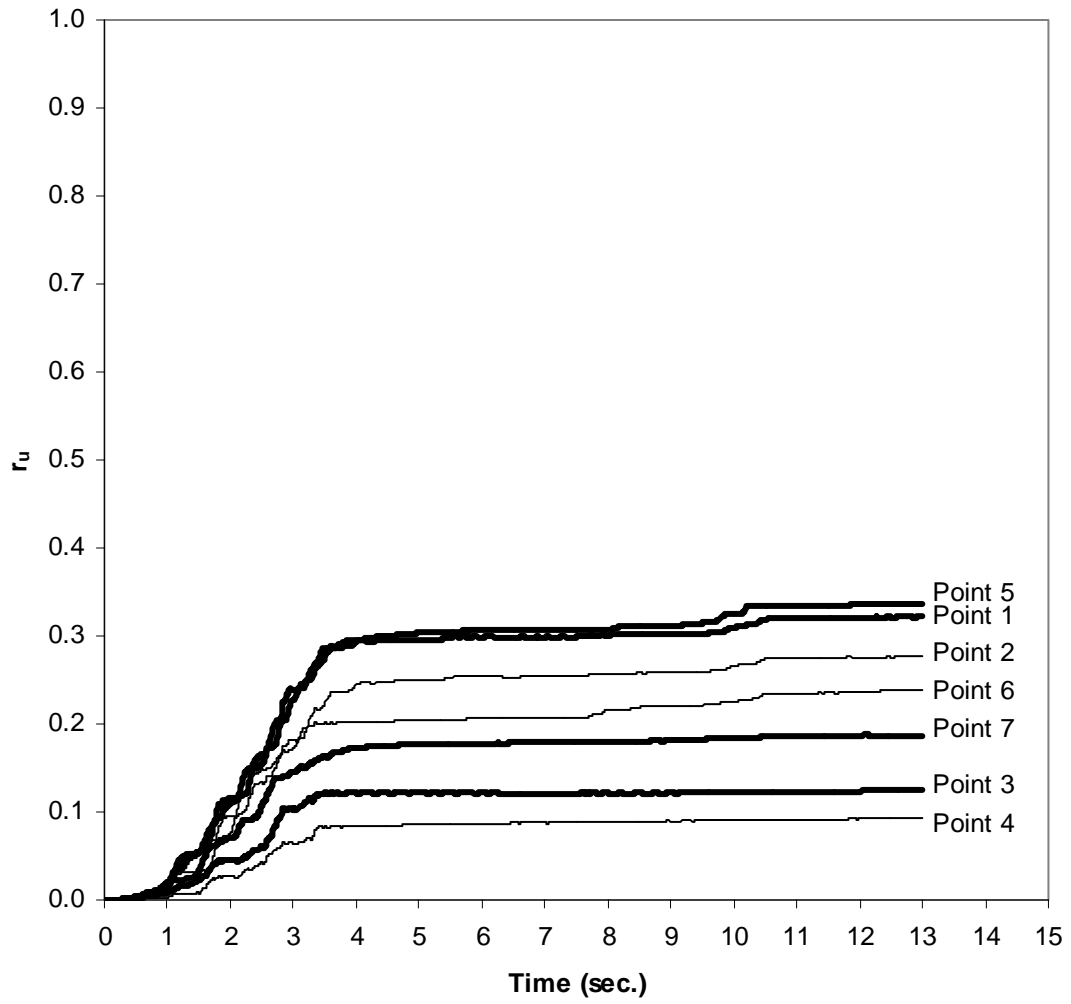


Figure 6.42 History of excess pore pressure ratio (r_u) for Case 5S

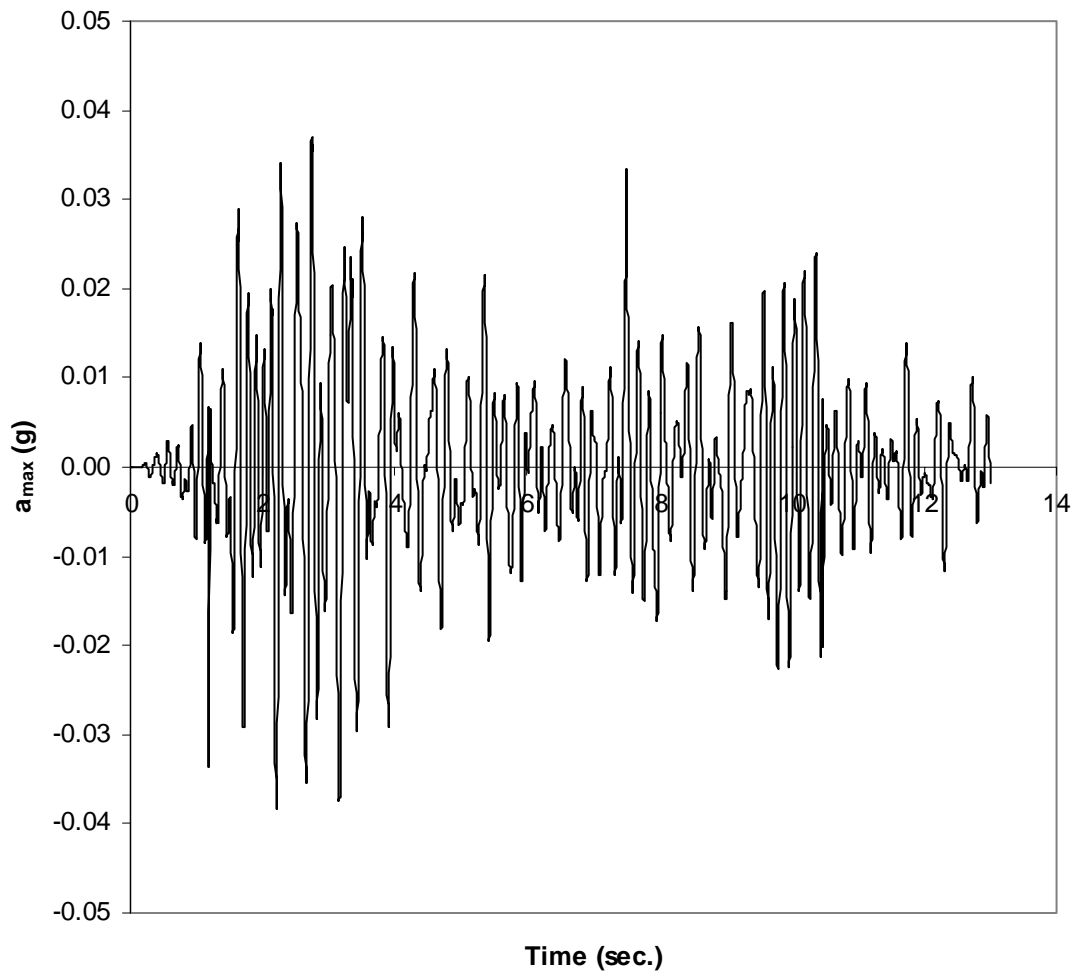


Figure 6.43 Acceleration time history (a_{max}) for Case 5S

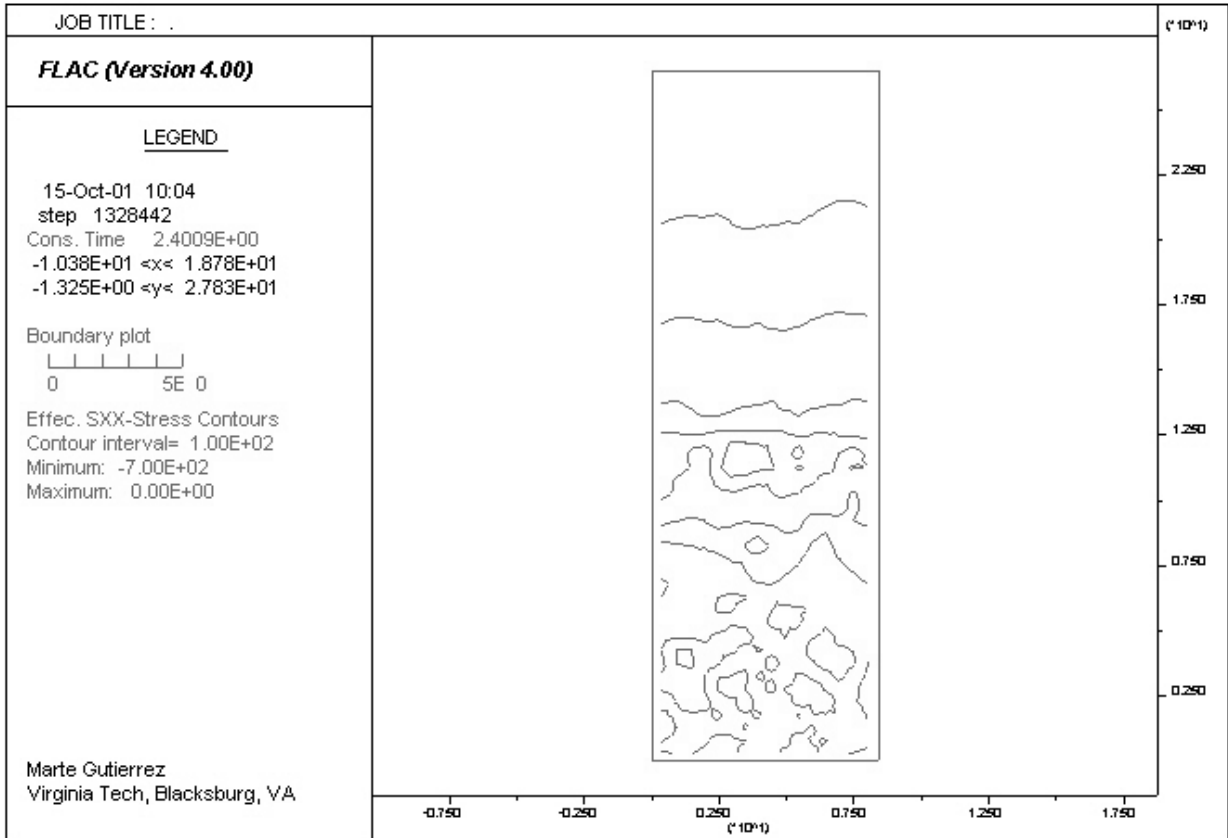


Figure 6.44 Contours of effective horizontal stress for Case 5S

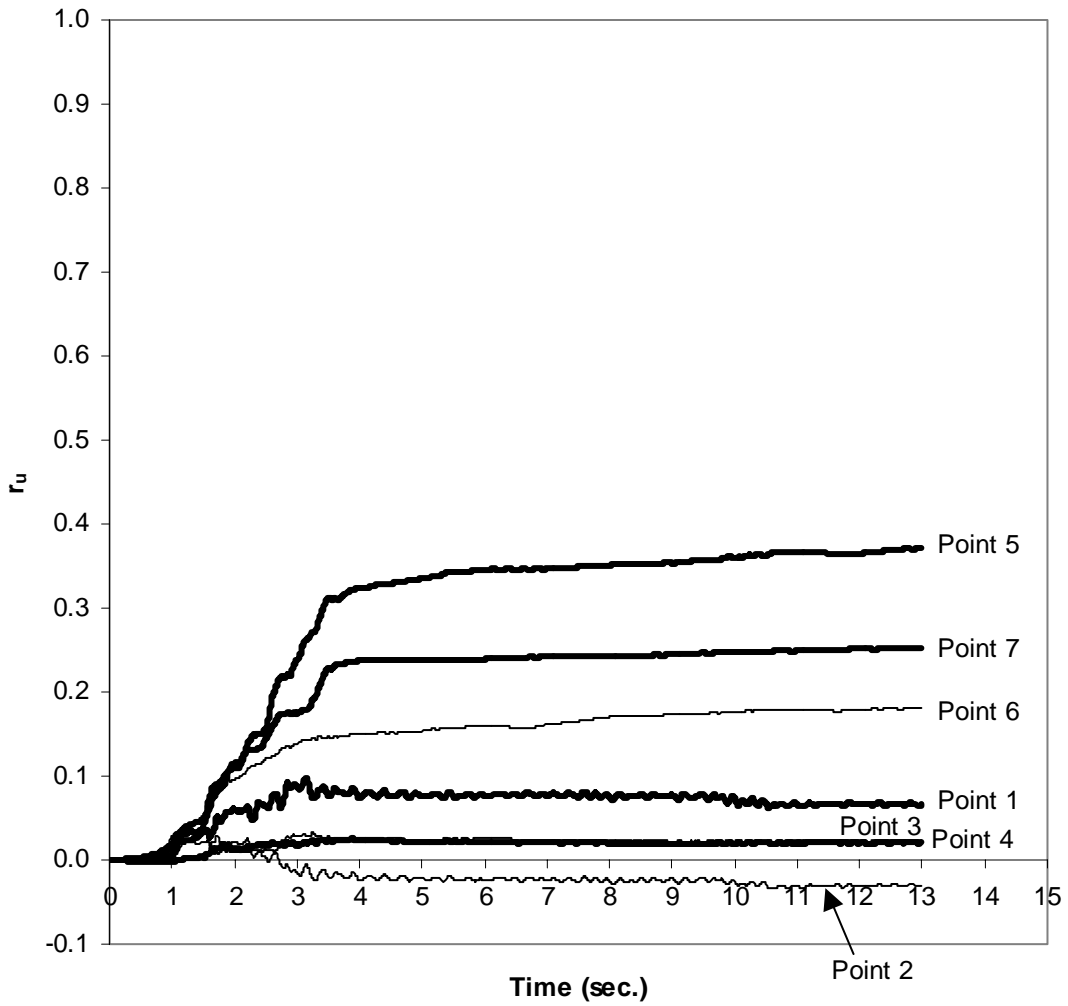


Figure 6.45 History of excess pore pressure ratio (r_u) for Case 6S

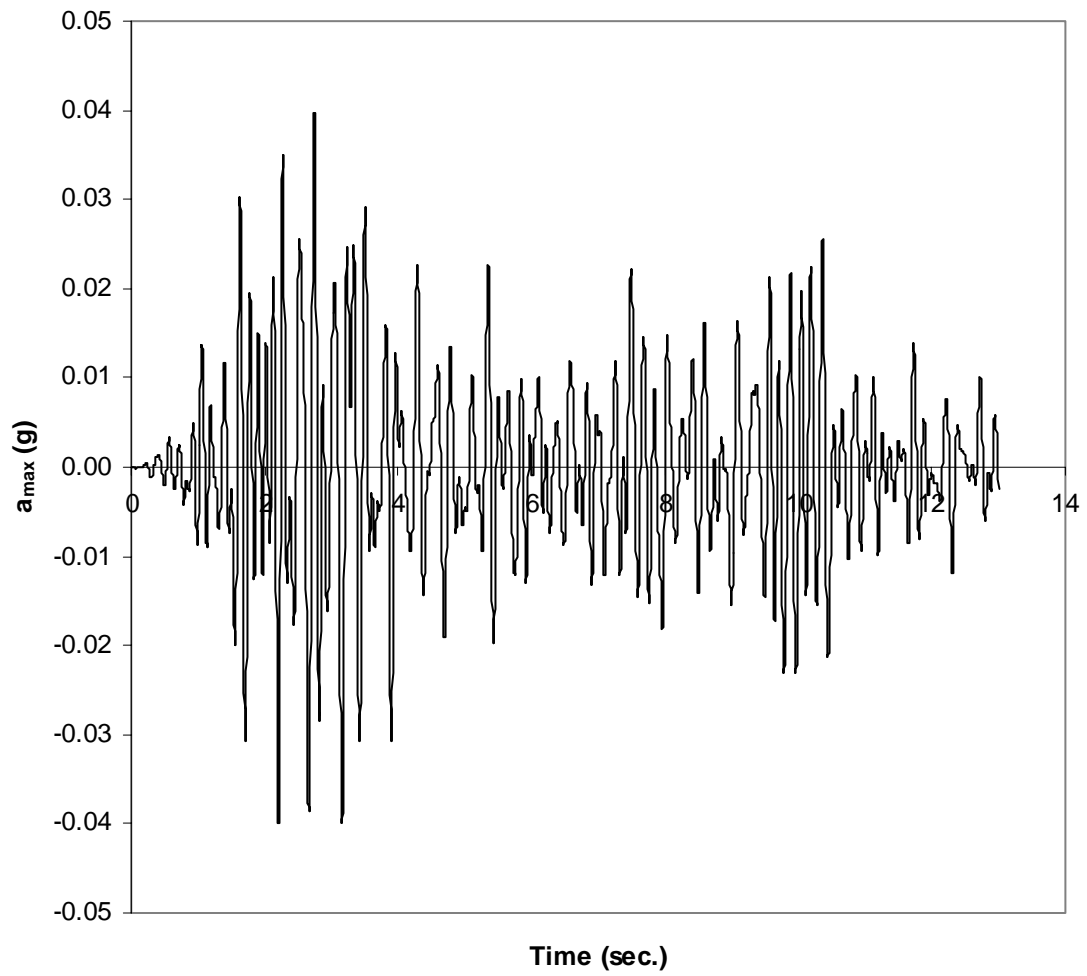


Figure 6.46 Acceleration time history (a_{max}) for Case 6S

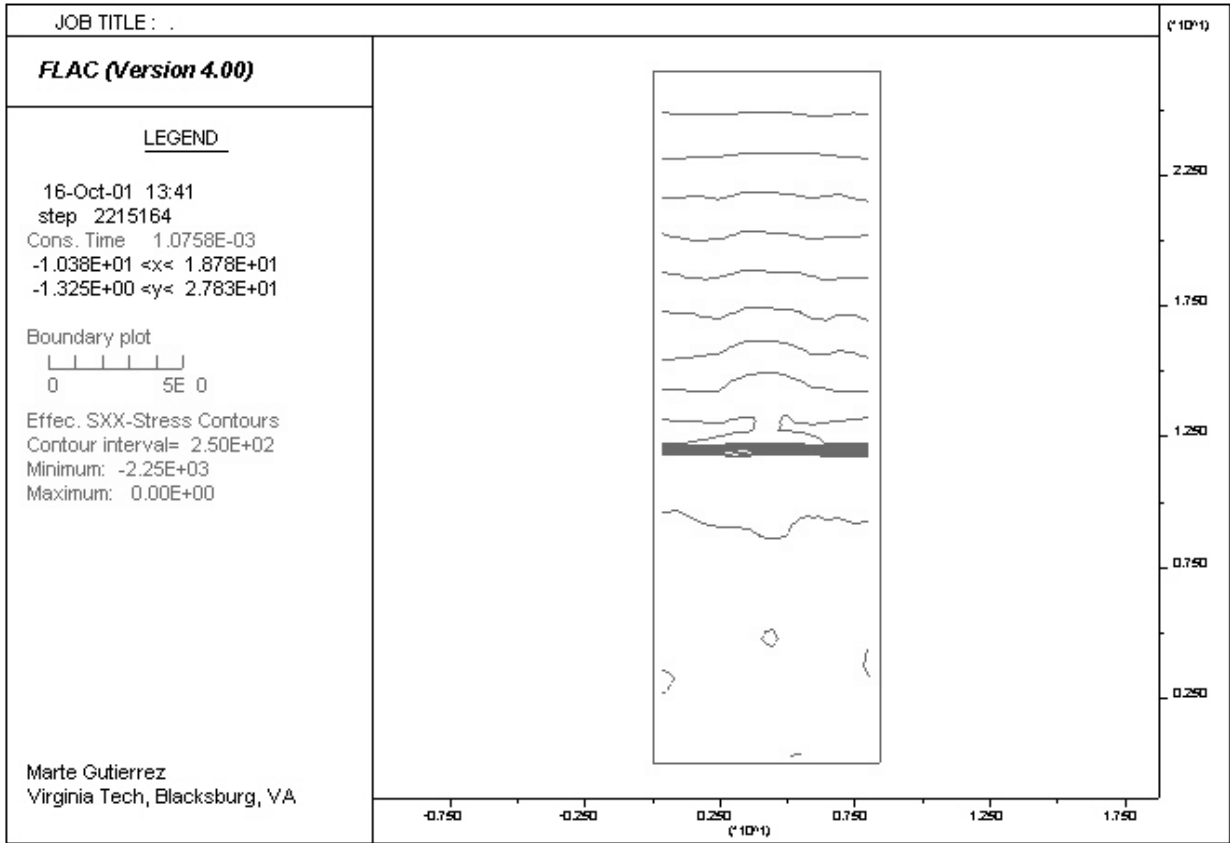


Figure 6.47 Contours of effective horizontal stress for Case 6S

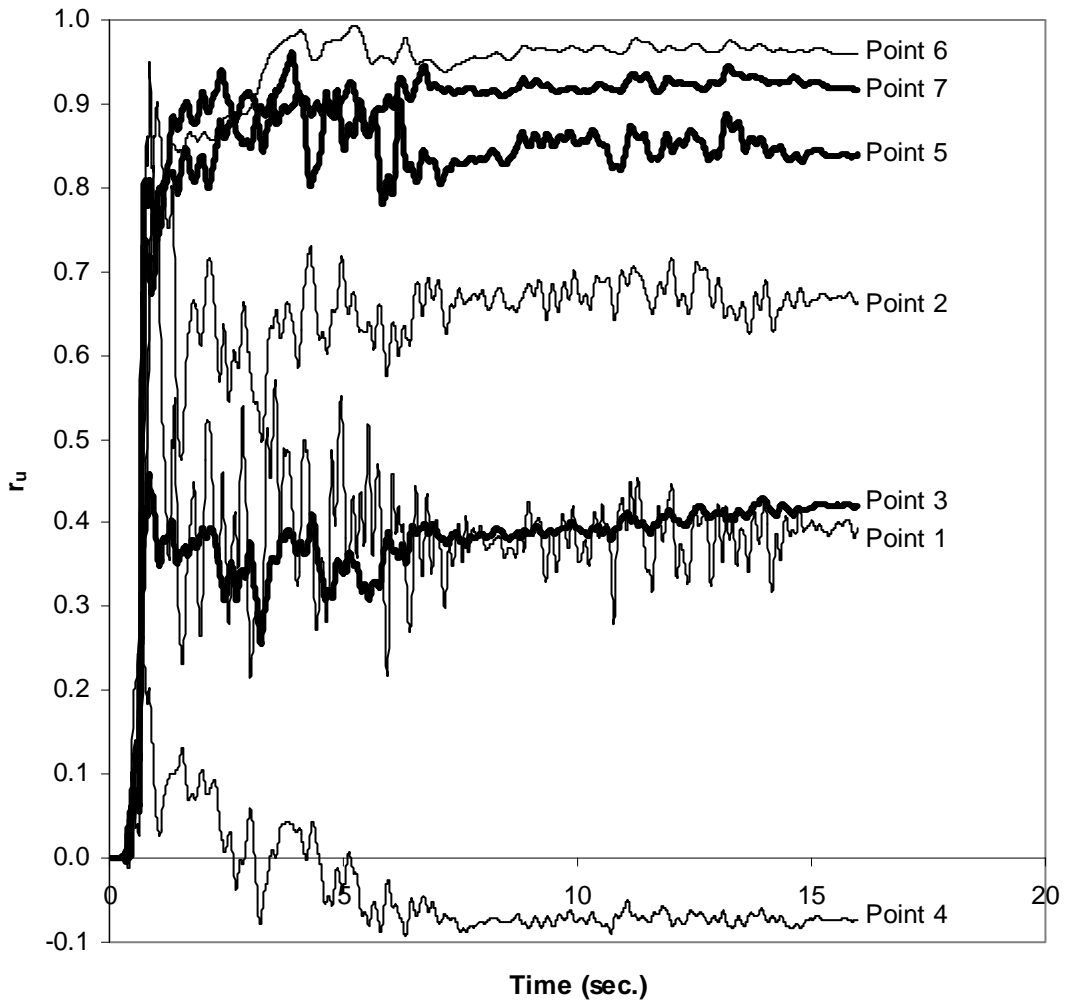


Figure 6.48 History of excess pore pressure ratio (r_u) for Case 8C

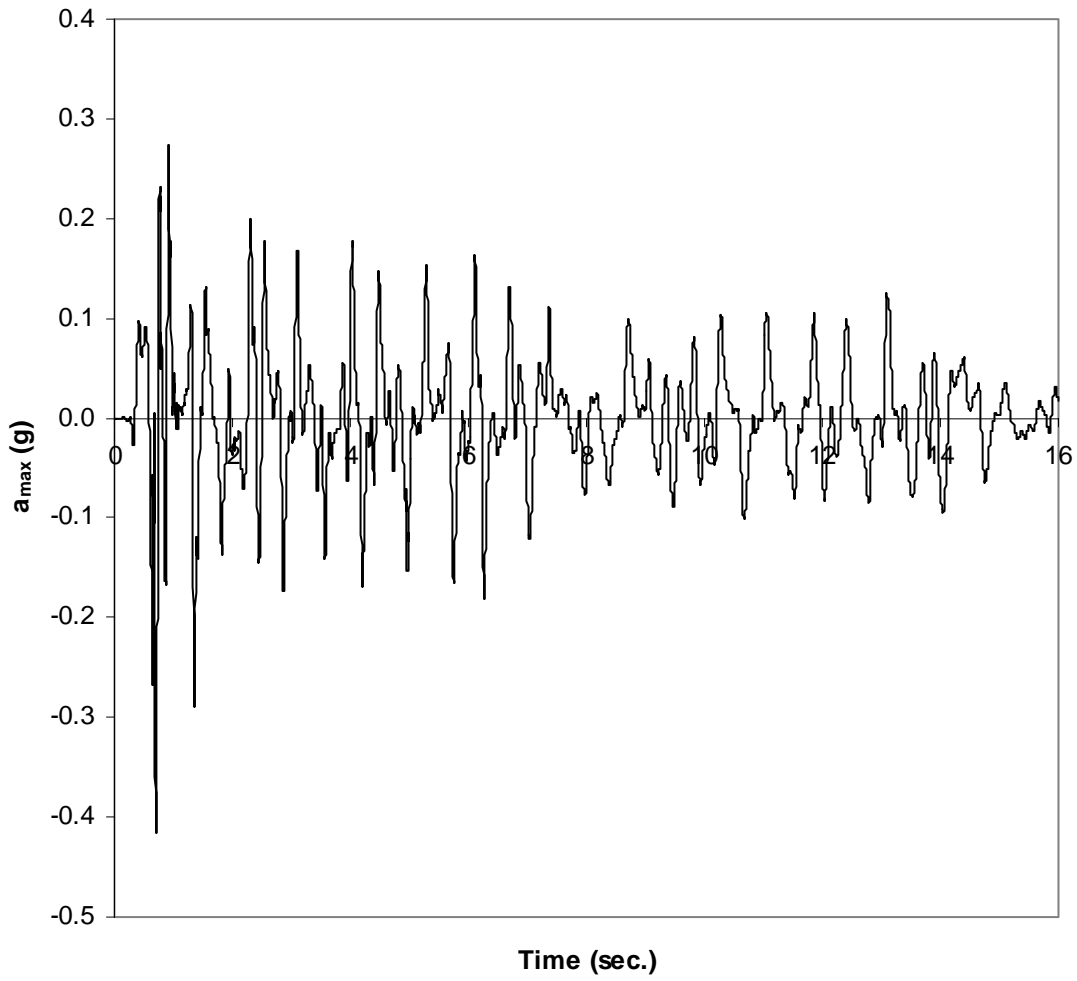


Figure 6.49 Acceleration time history (a_{\max}) for Case 8C

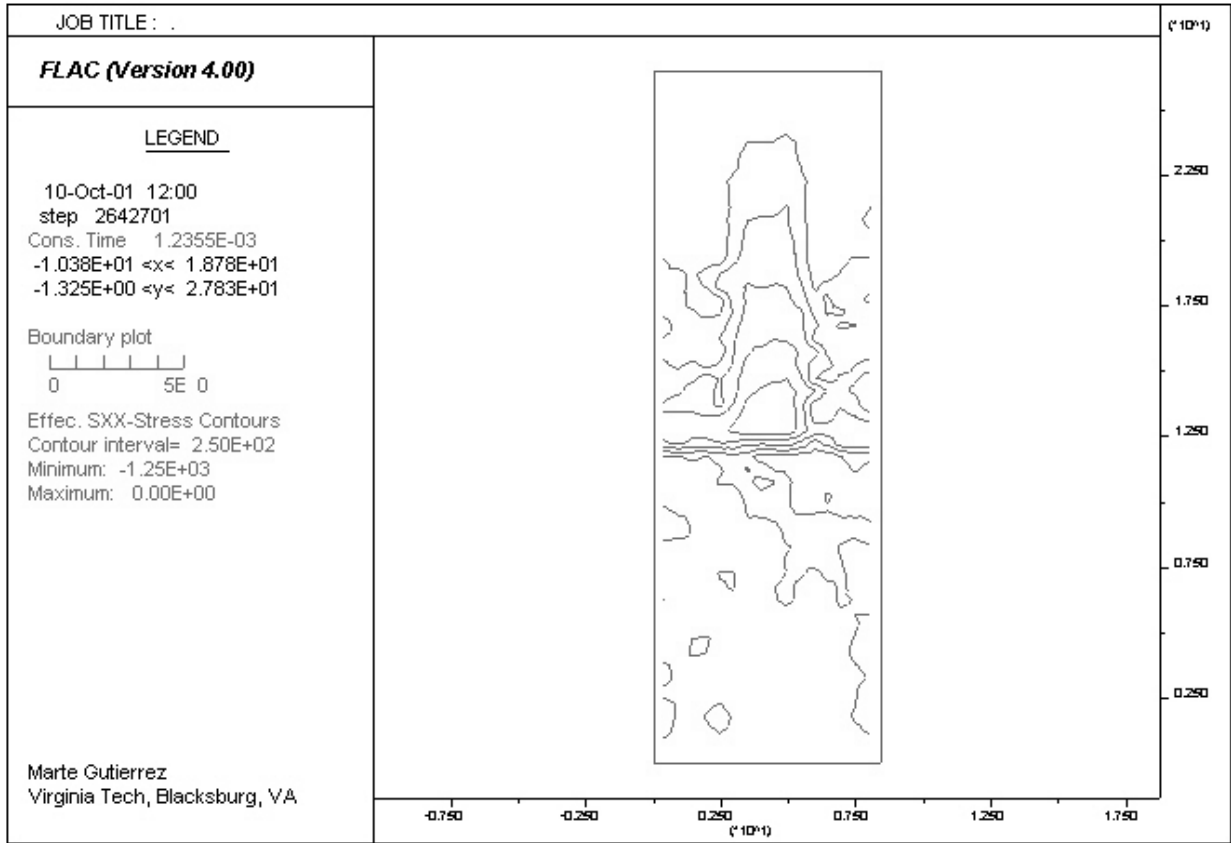


Figure 6.50 Contours of effective horizontal stress for Case 8C

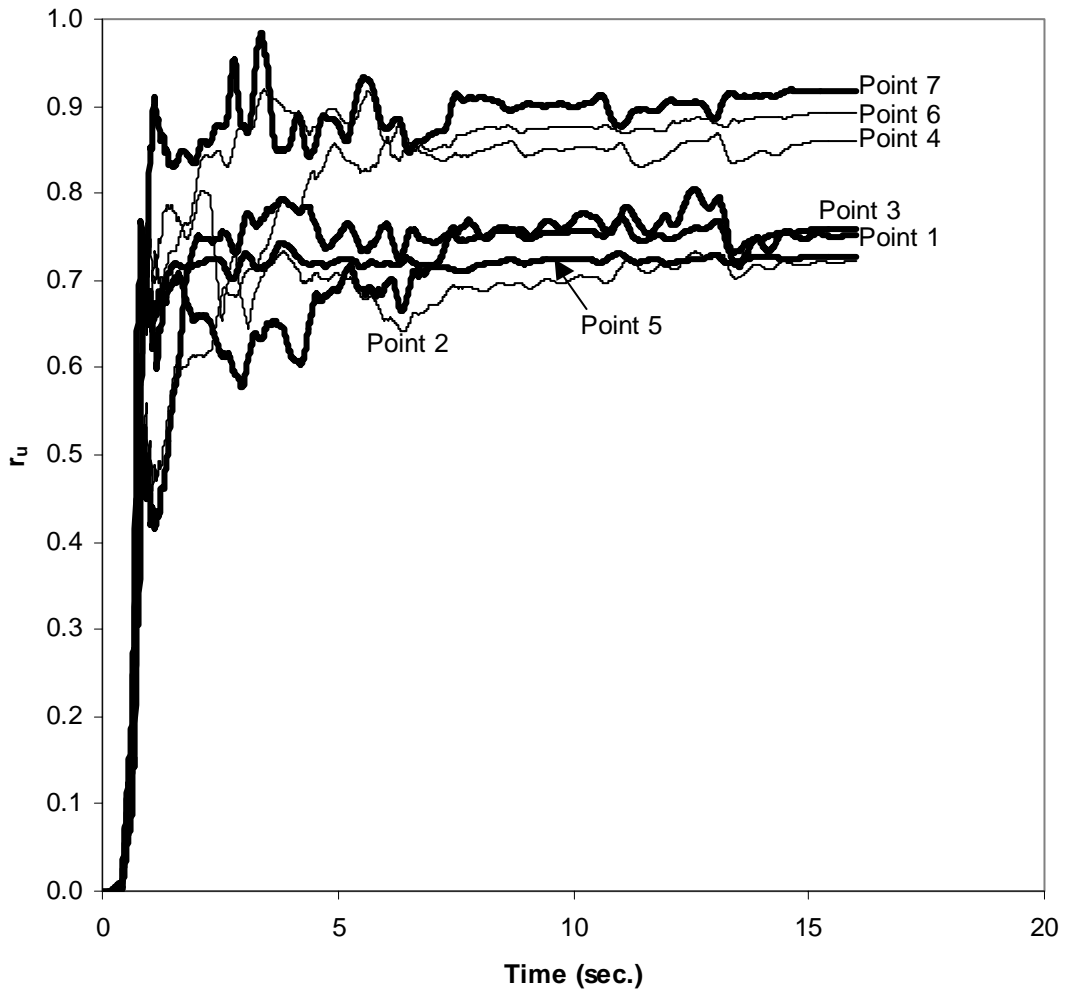


Figure 6.51 History of excess pore pressure ratio (r_u) for Case 7C

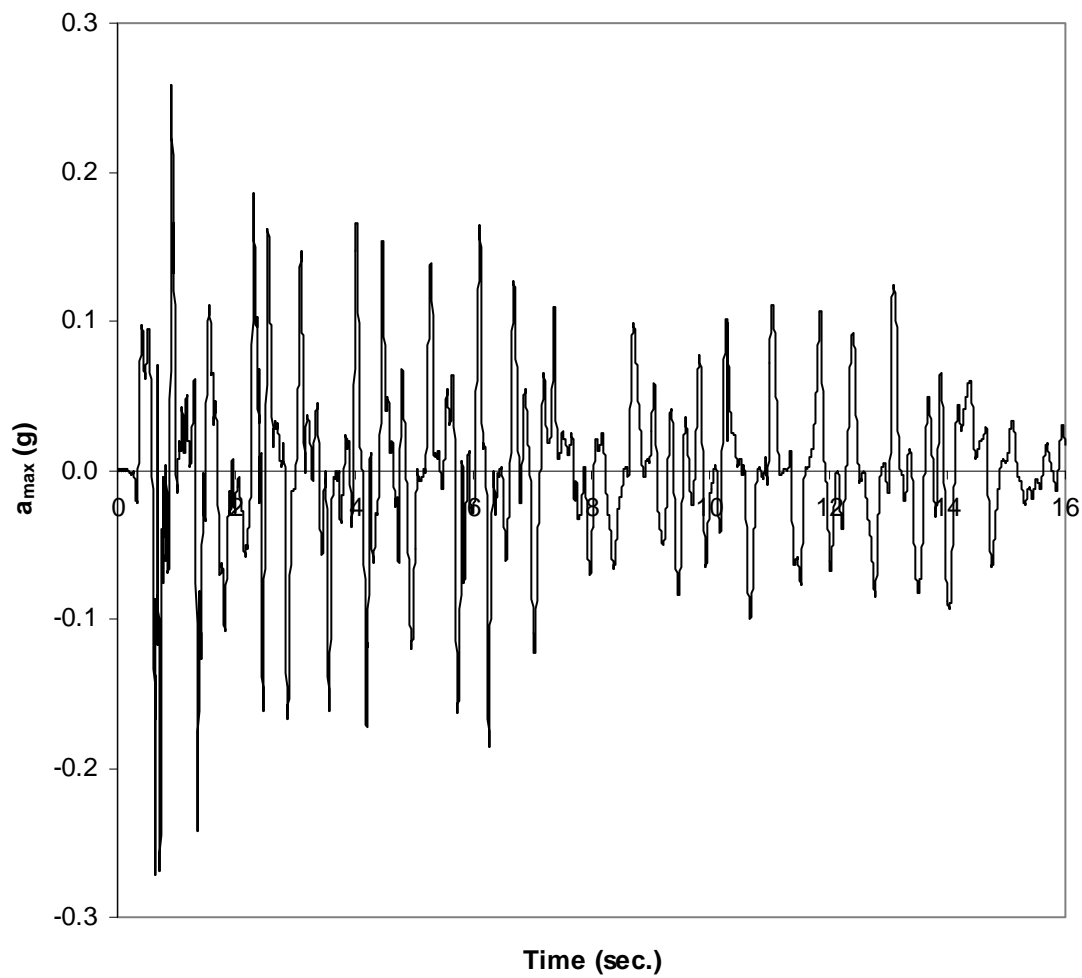


Figure 6.52 Acceleration time history (a_{\max}) for Case 7C

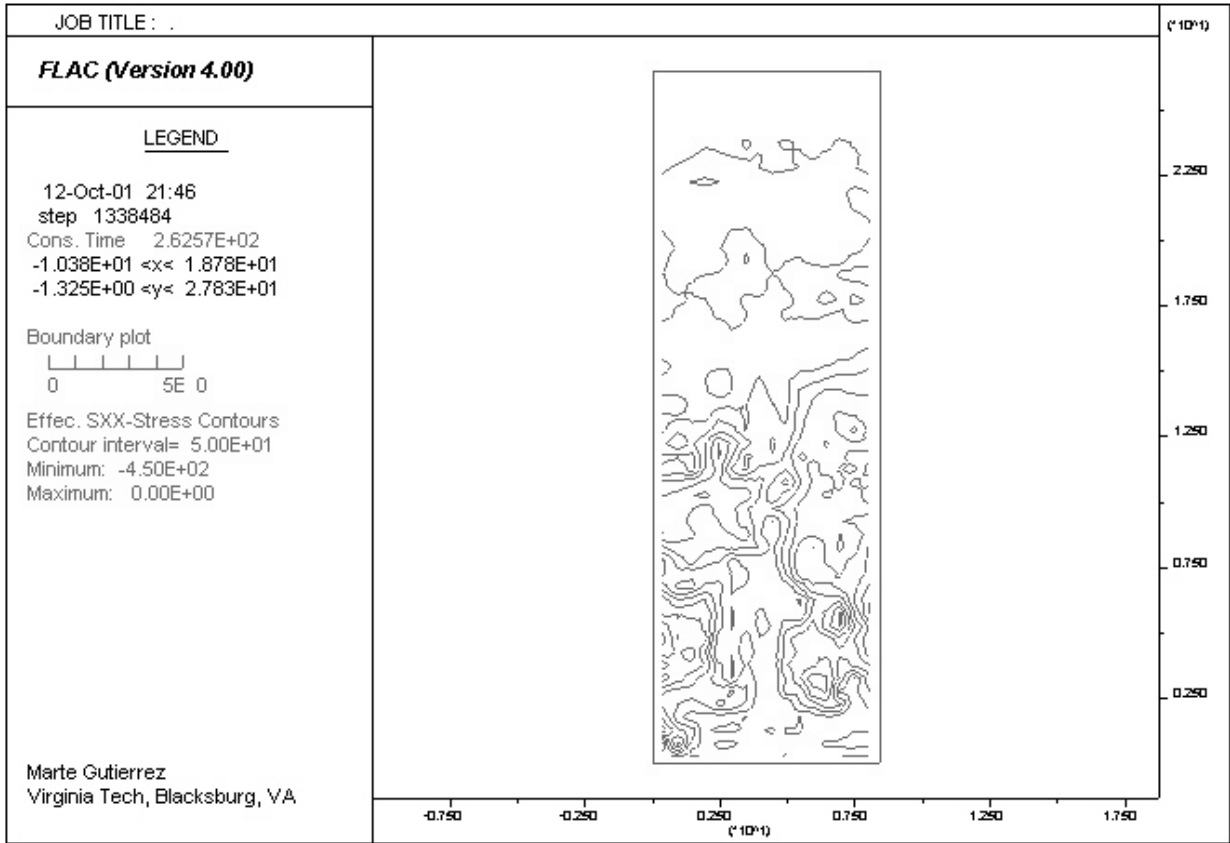


Figure 6.53 Contours of effective horizontal stress for Case 7C

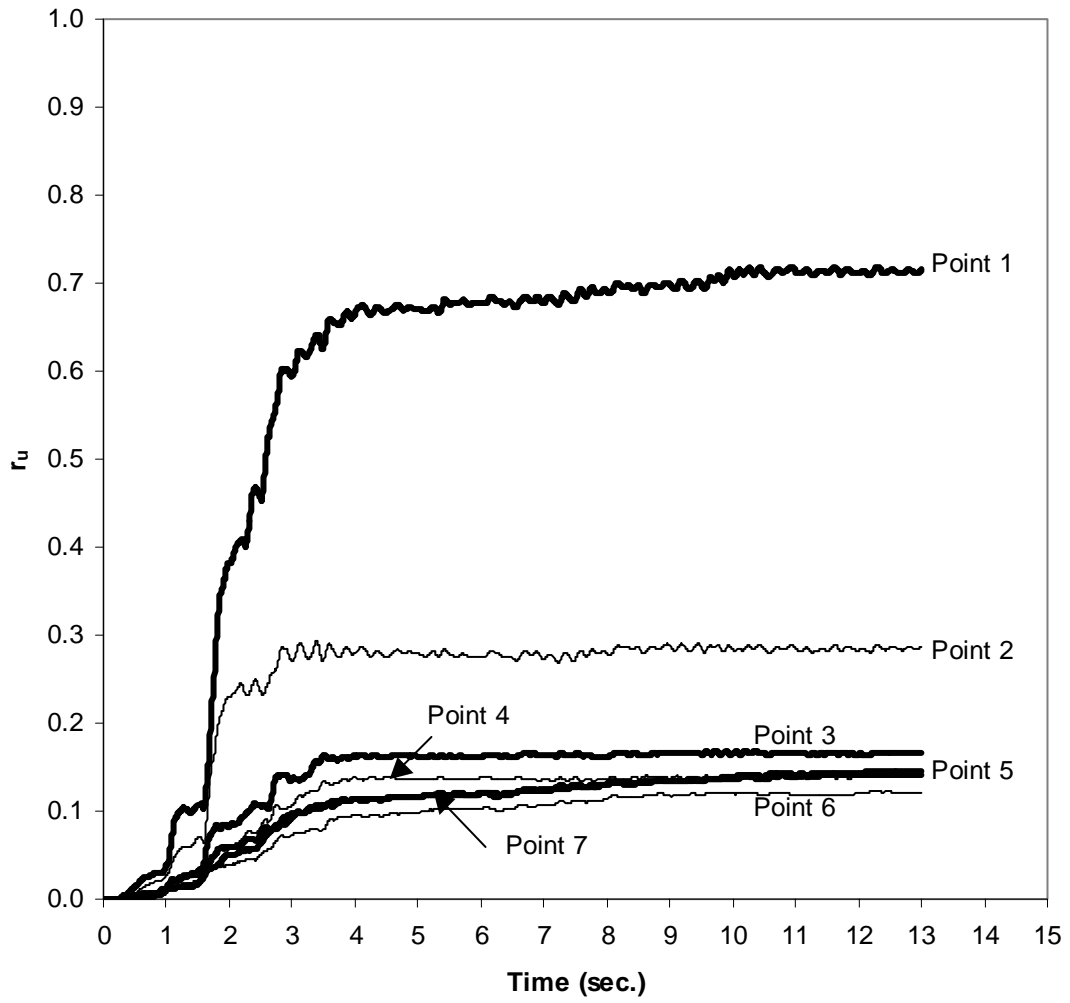


Figure 6.54 History of excess pore pressure ratio (r_u) for Case 8S

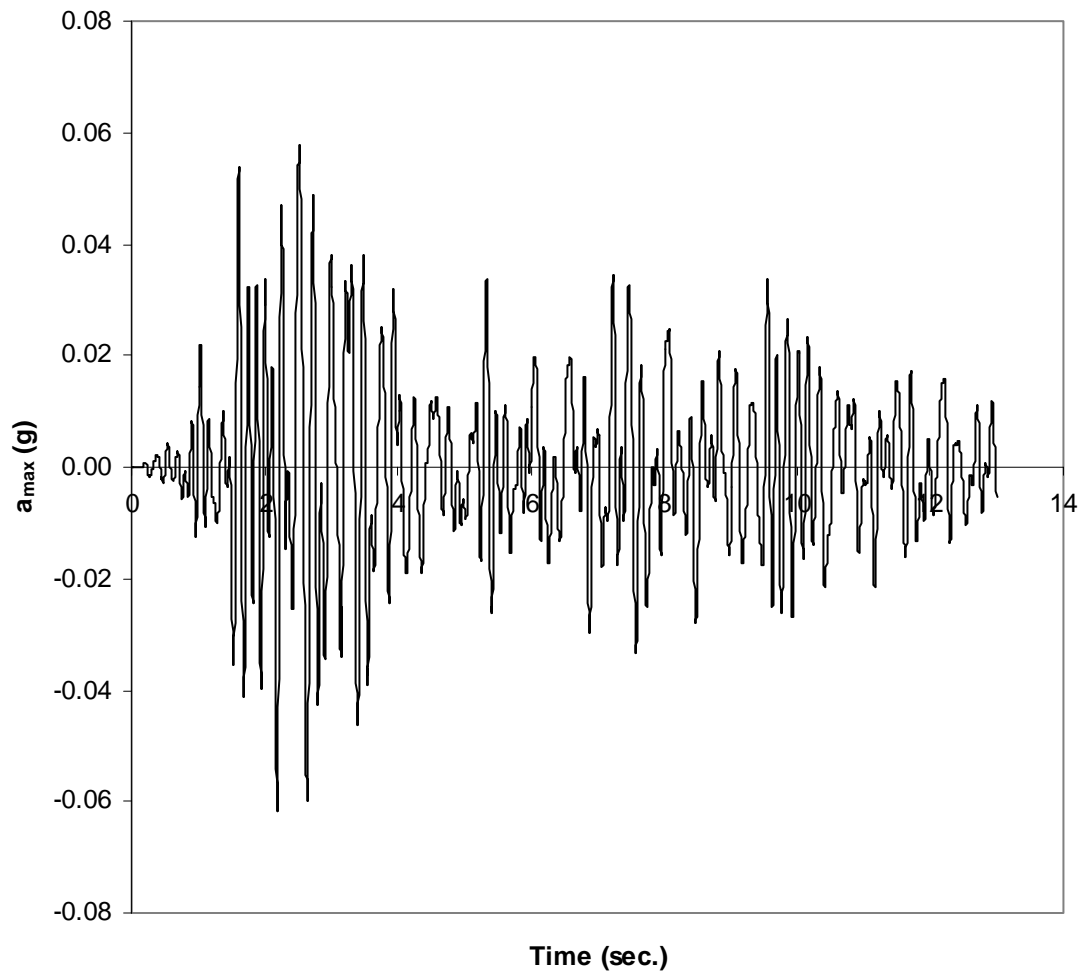


Figure 6.55 Acceleration time history (a_{max}) for Case 8S

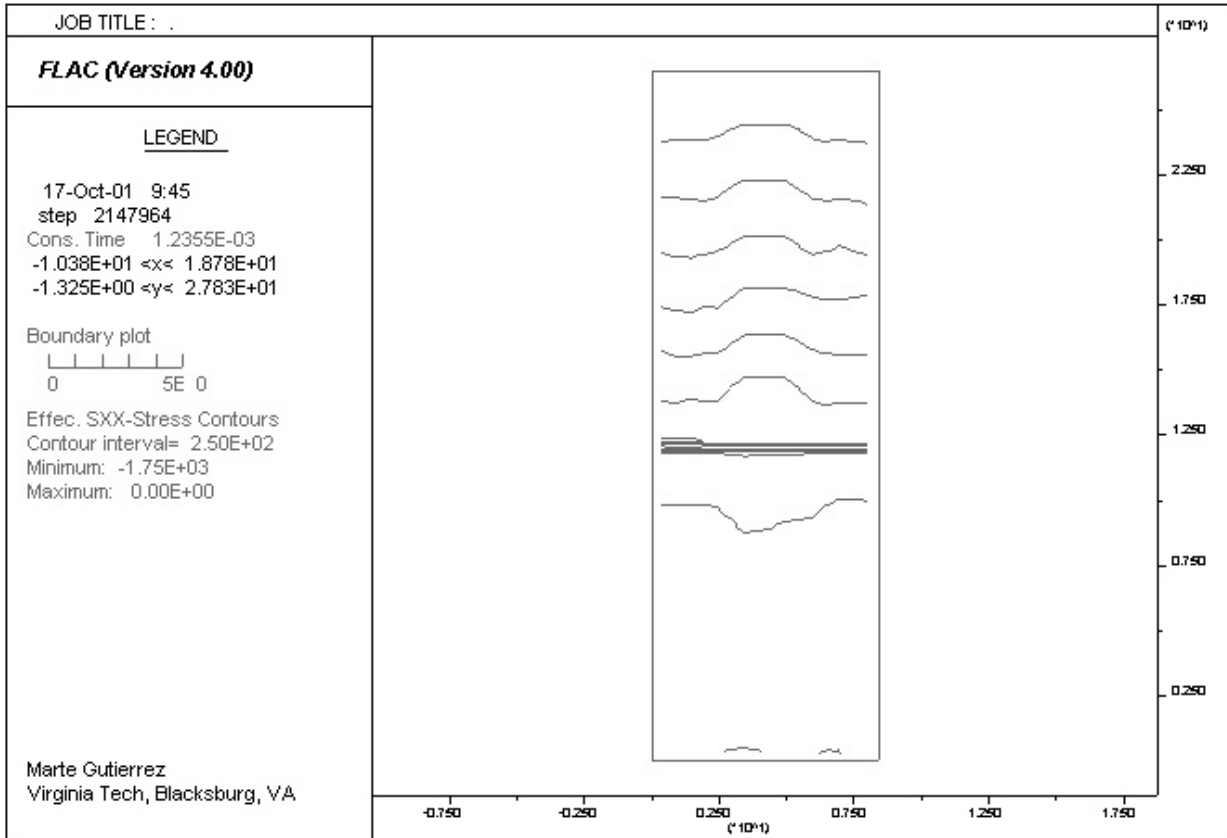


Figure 6.56 Contours of effective horizontal stress for Case 8S

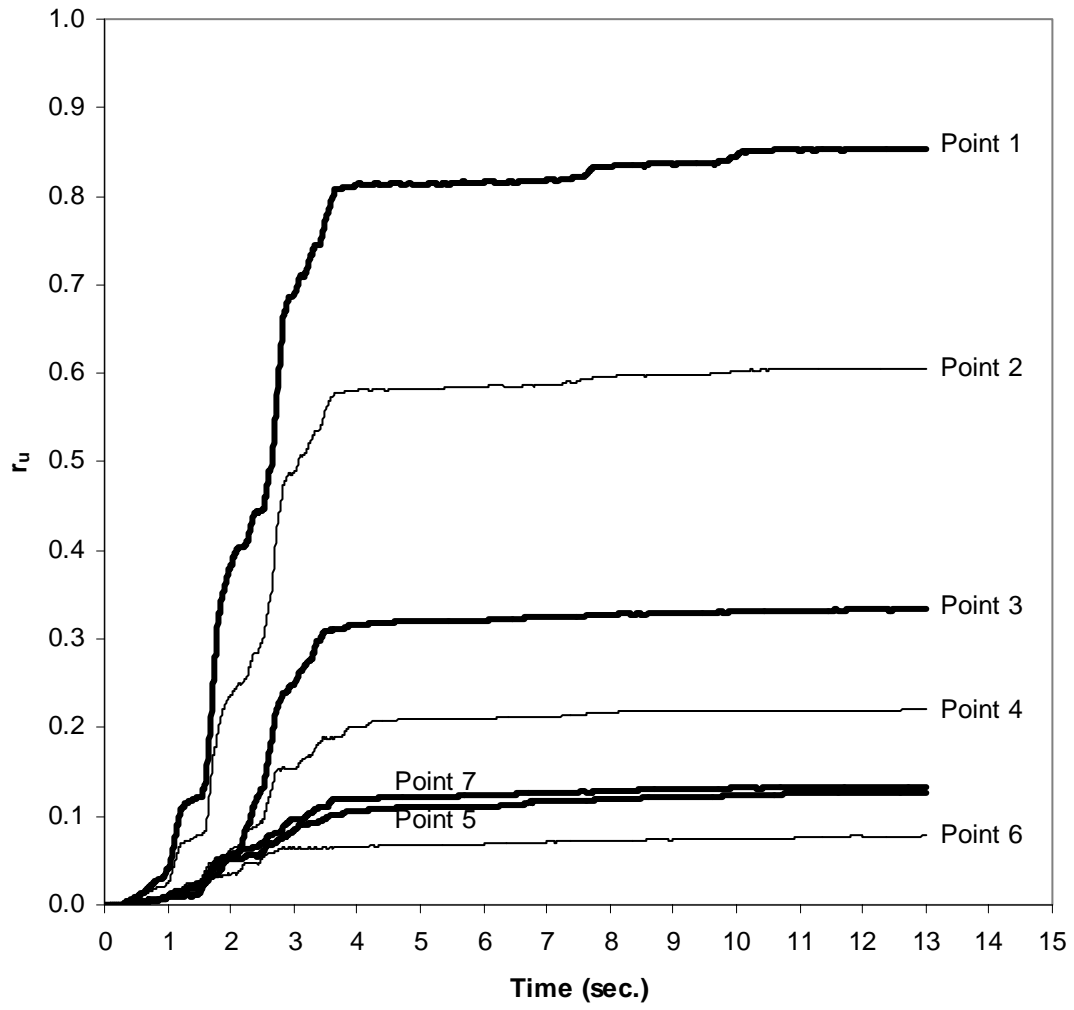


Figure 6.57 History of excess pore pressure ratio (r_u) for Case 7S

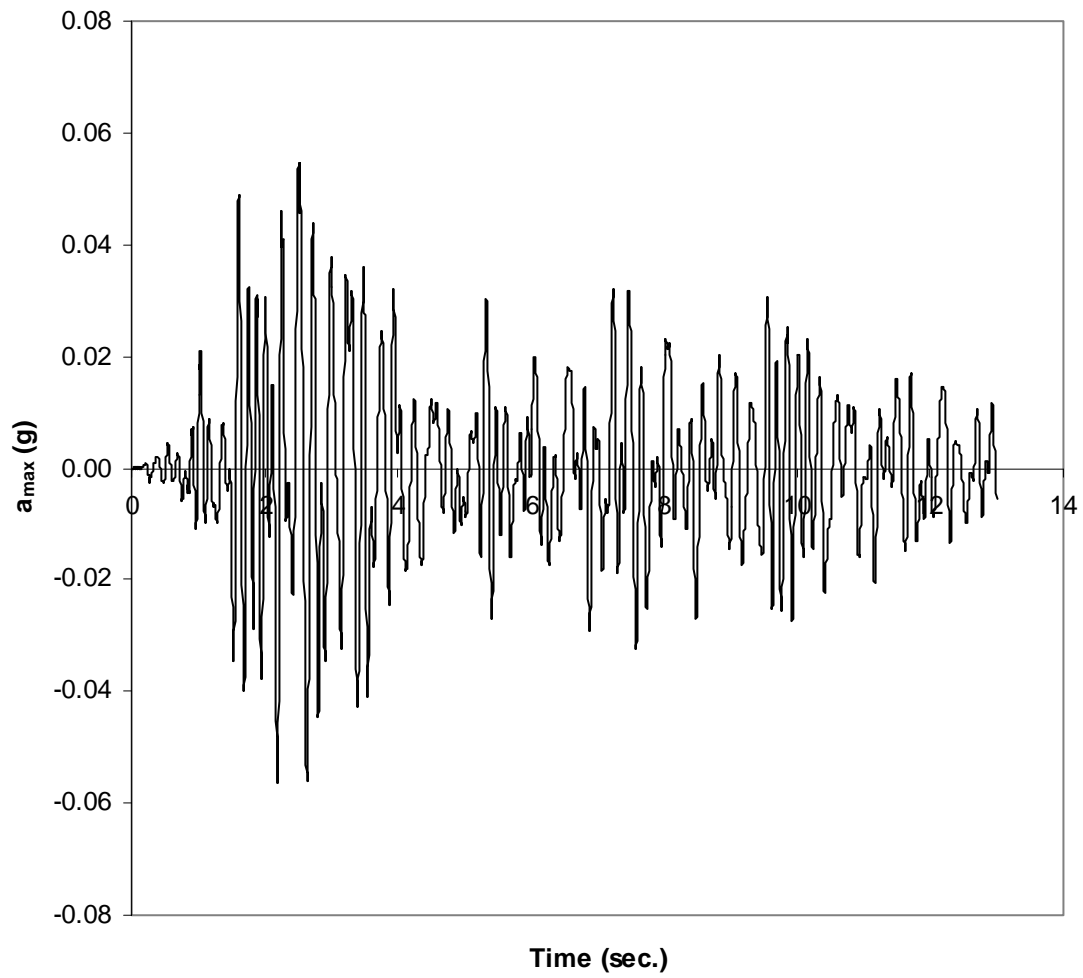


Figure 6.58 Acceleration time history (a_{\max}) for Case 7S

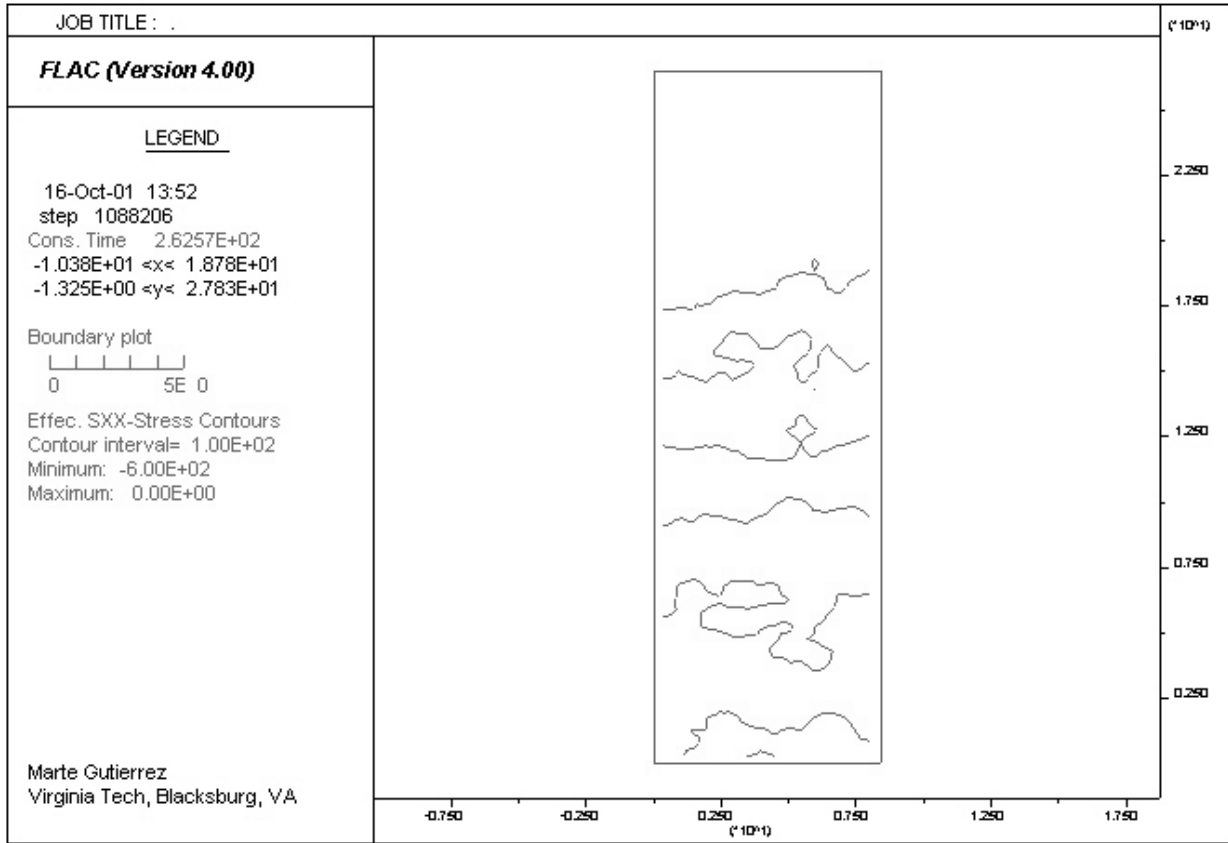


Figure 6.59 Contours of effective horizontal stress for Case 7S

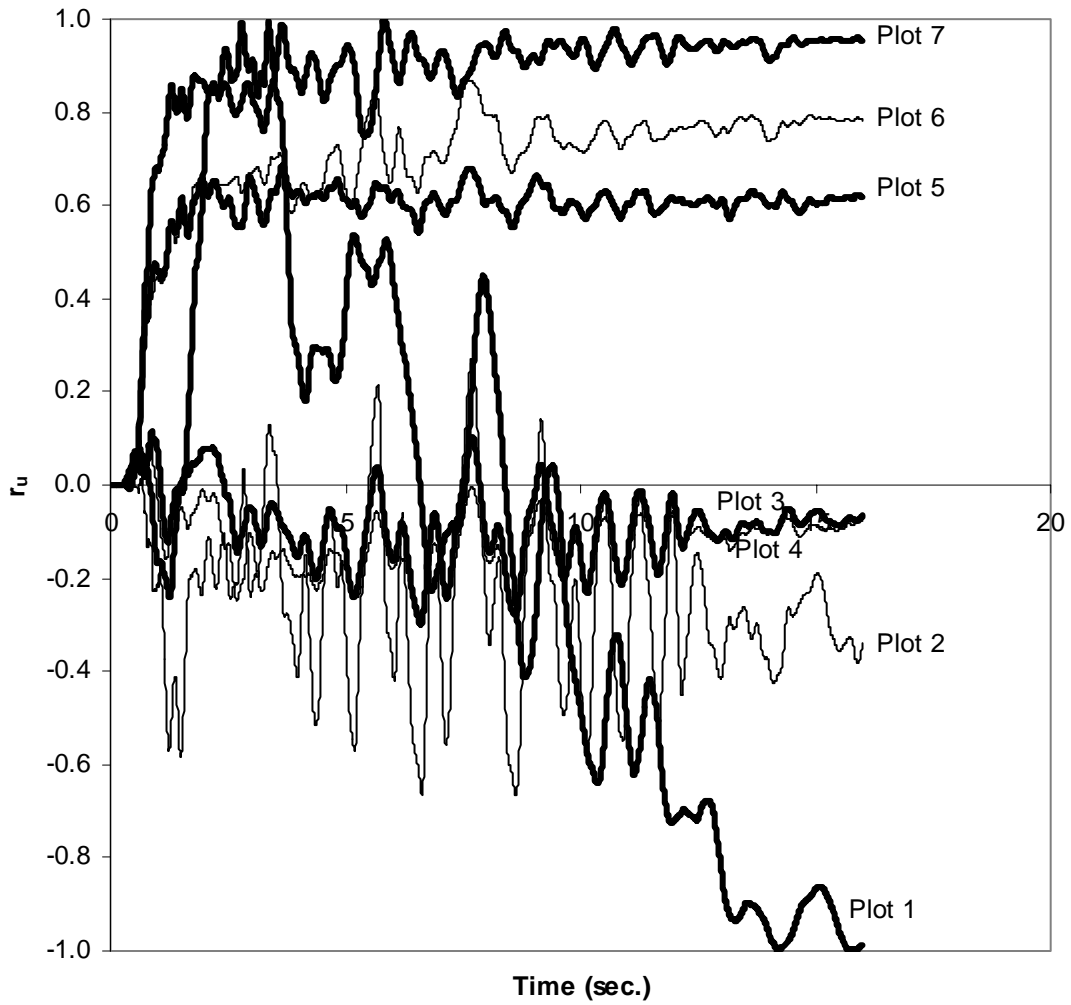


Figure 6.60 History of excess pore pressure ratio (r_u) for Case 9C

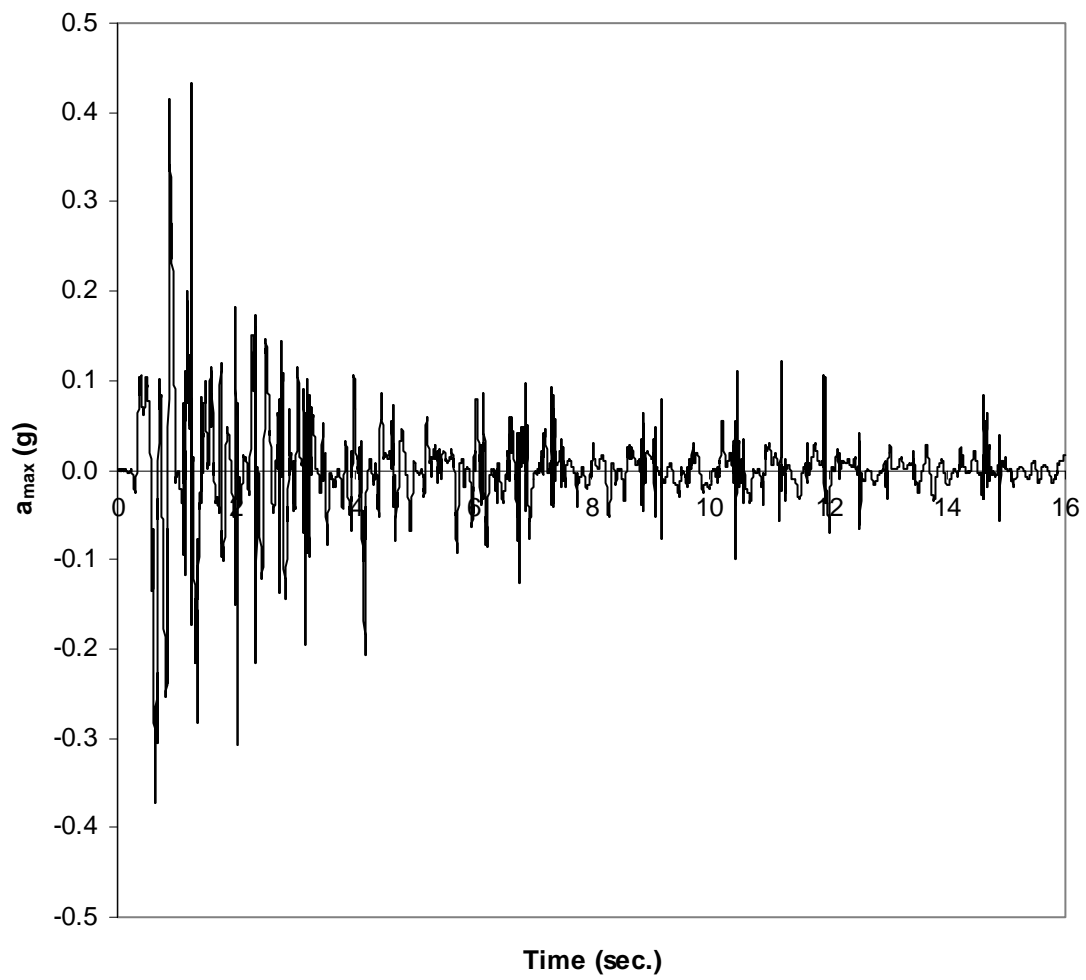


Figure 6.61 Acceleration time history (a_{\max}) for Case 9C

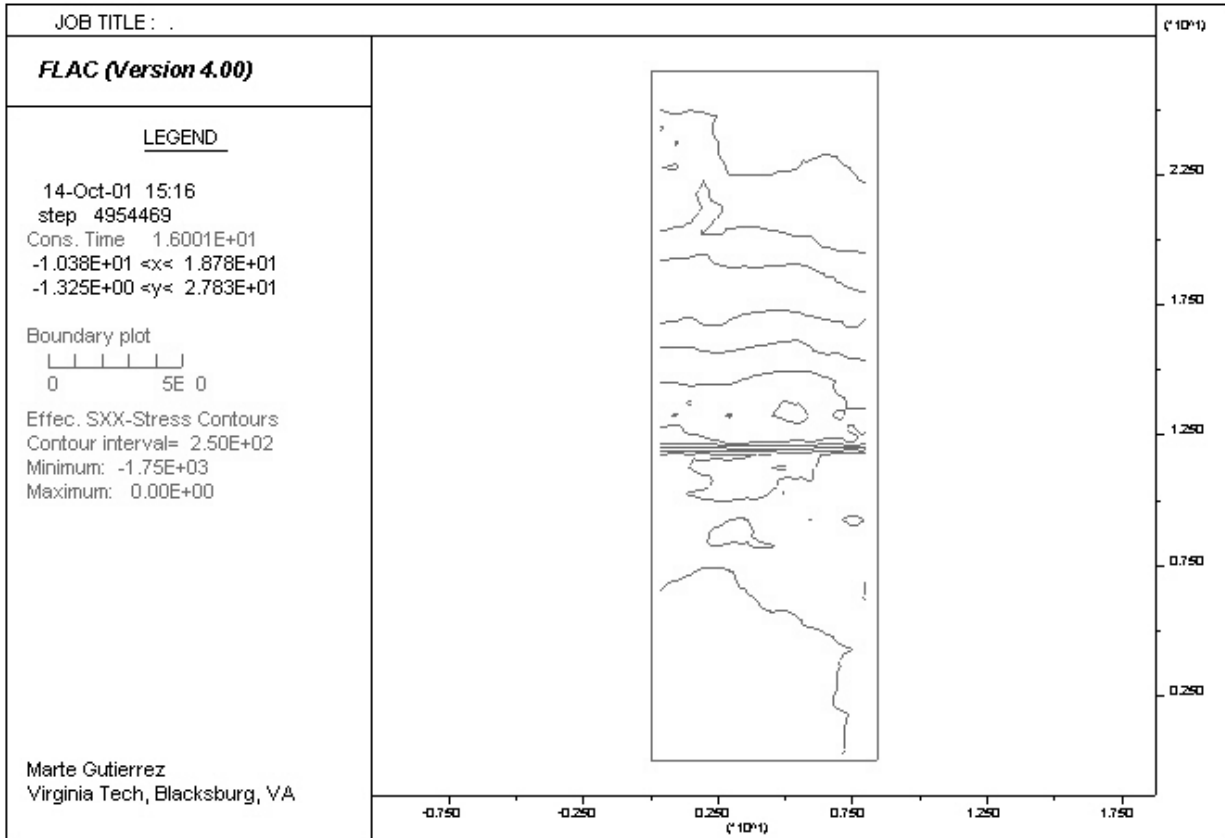


Figure 6.62 Contours of effective horizontal stress for Case 9C

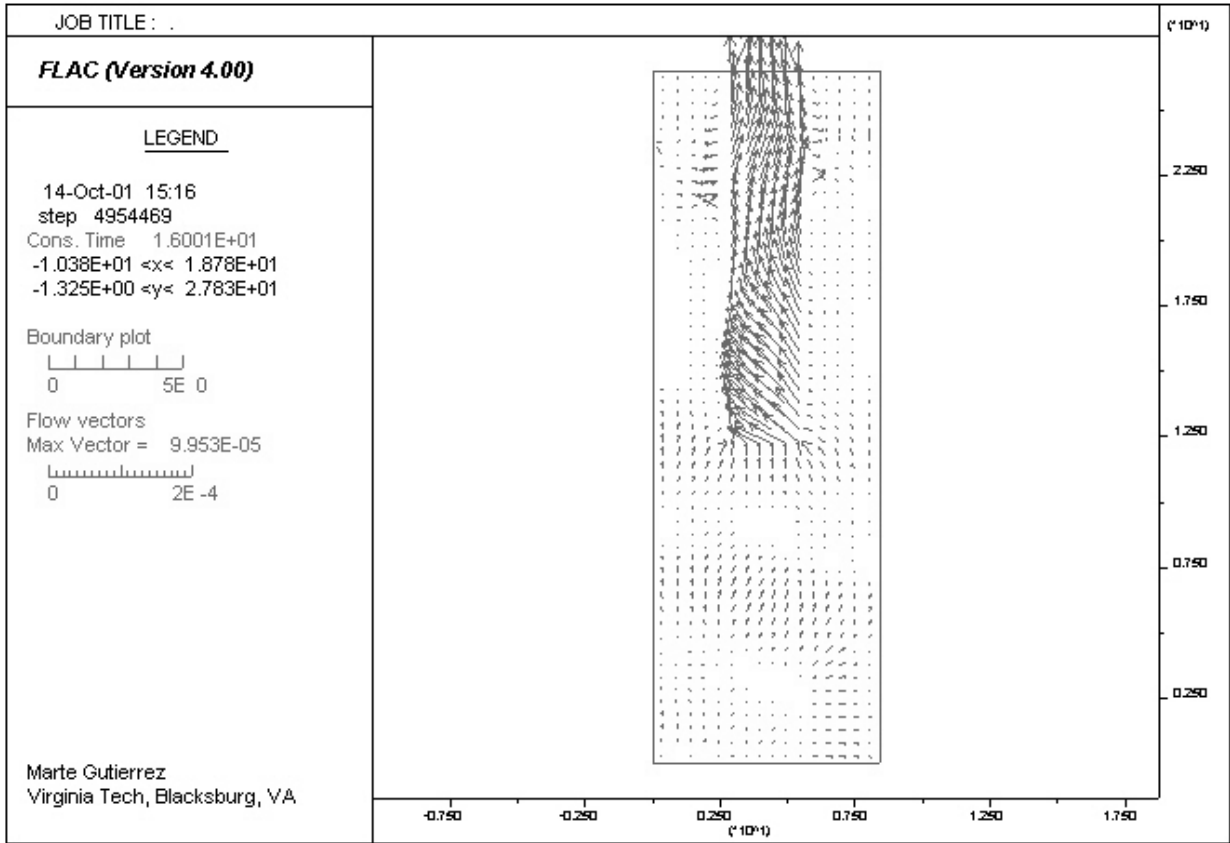


Figure 6.63 Flow vectors for Case 9C

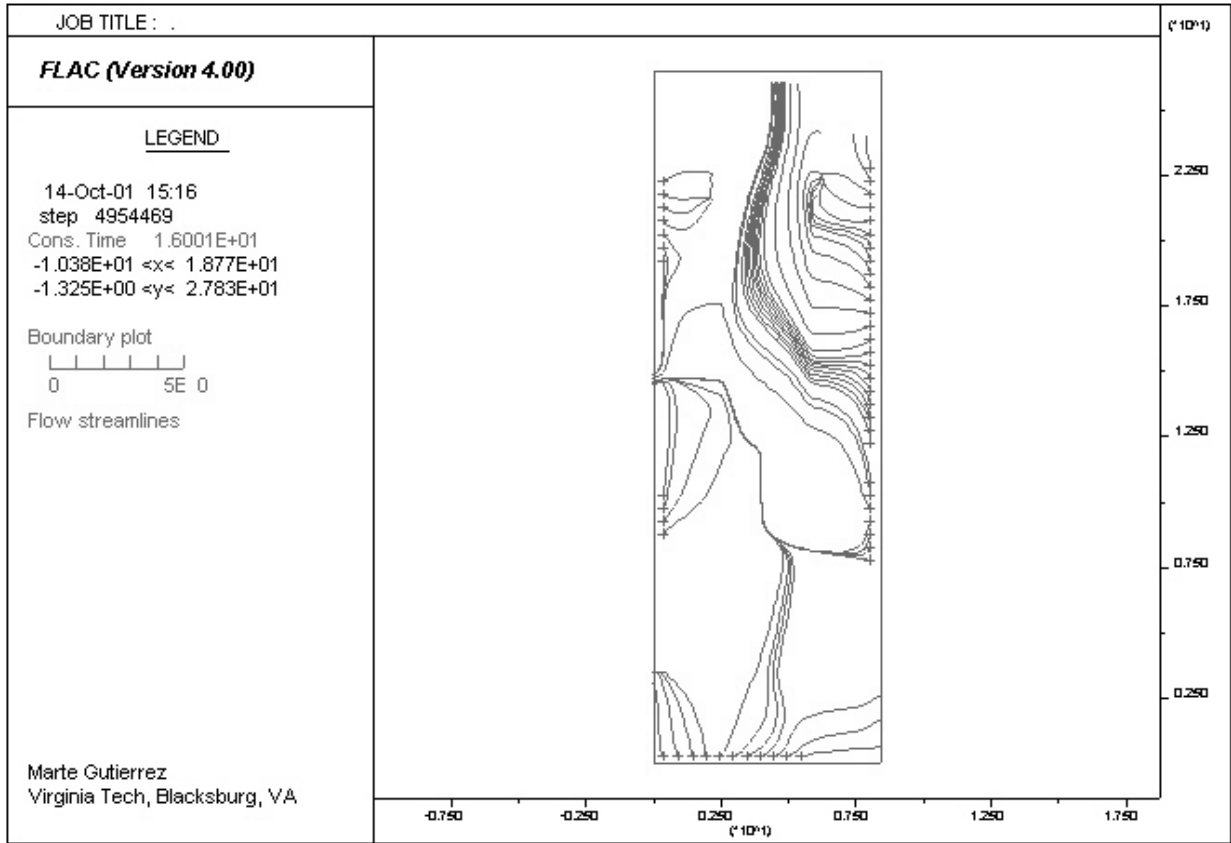


Figure 6.64 Flow streamlines for Case 9C

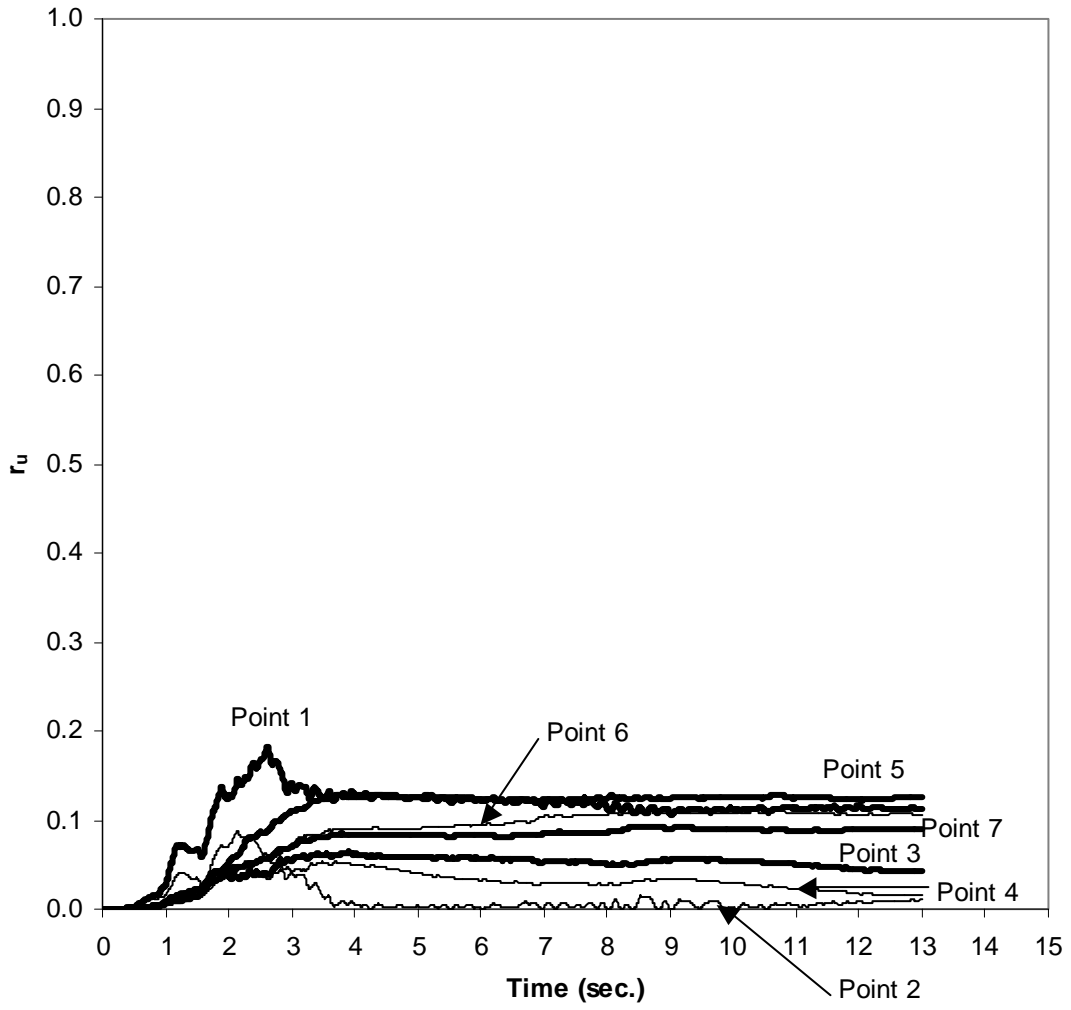


Figure 6.65 History of excess pore pressure ratio (r_u) for Case 9S

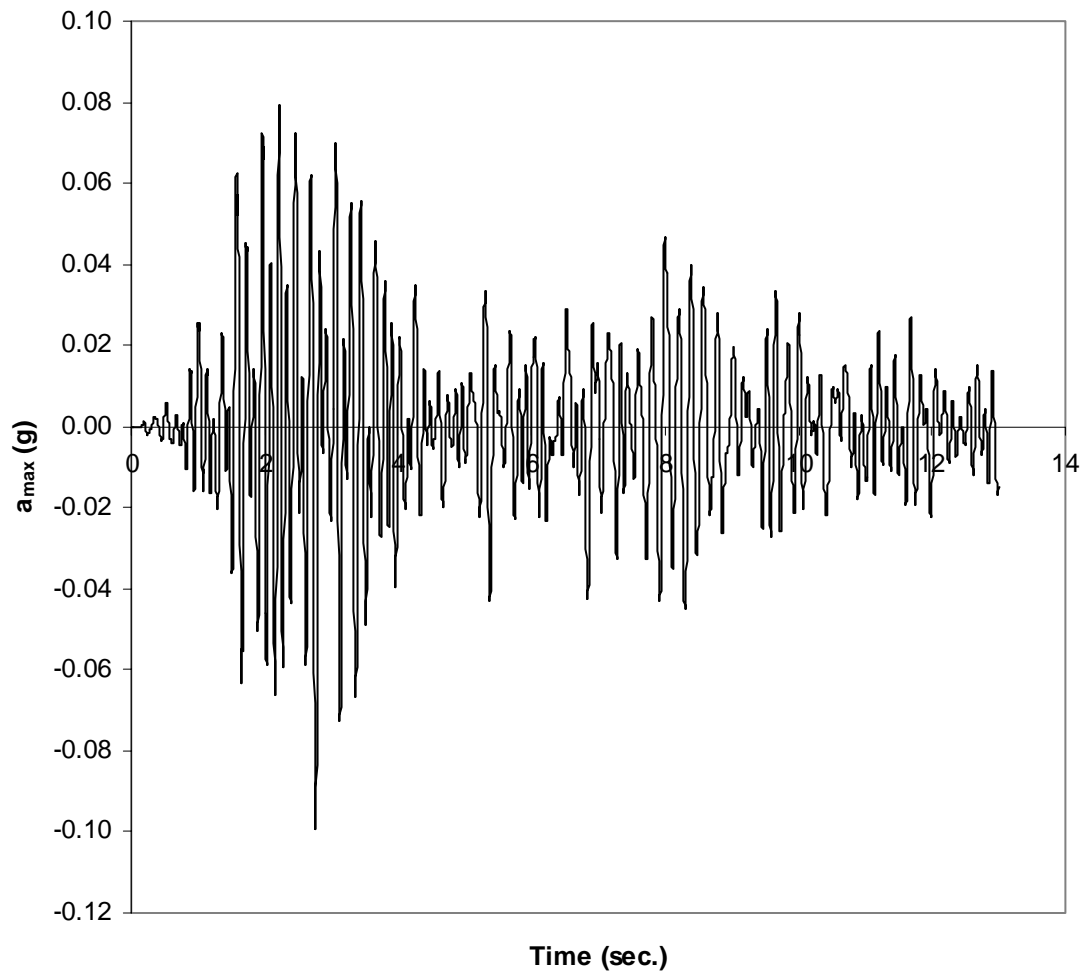


Figure 6.66 Acceleration time history (a_{max}) for Case 9S

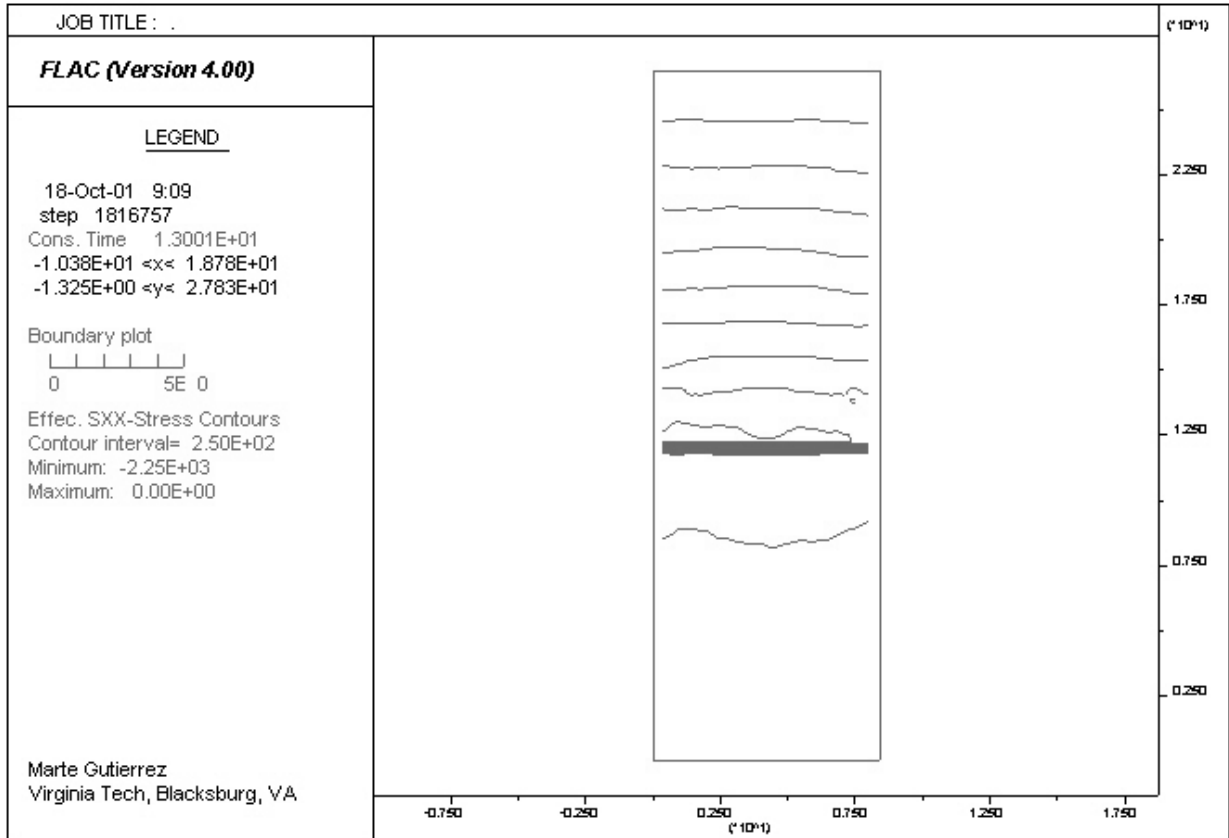


Figure 6.67 Contours of effective horizontal stress for Case 9S

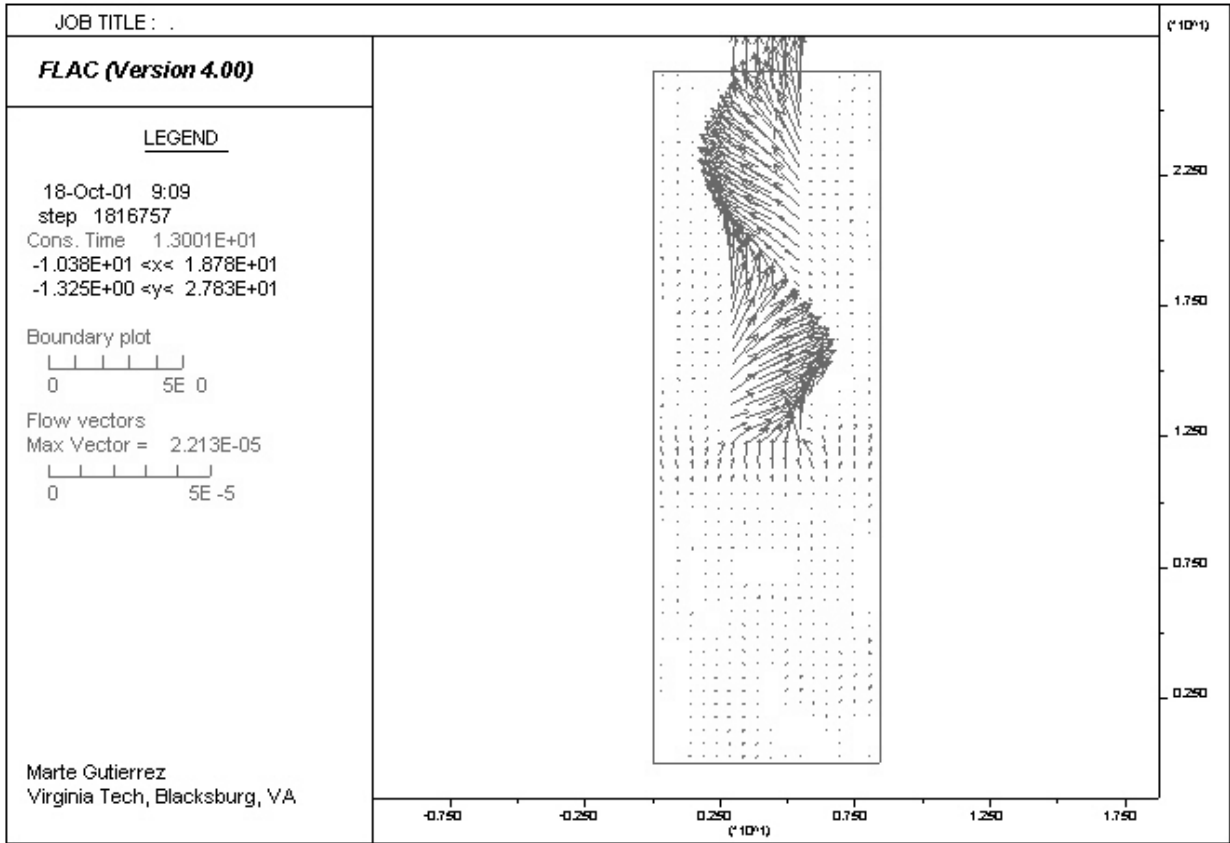


Figure 6.68 Flow vectors for Case 9S

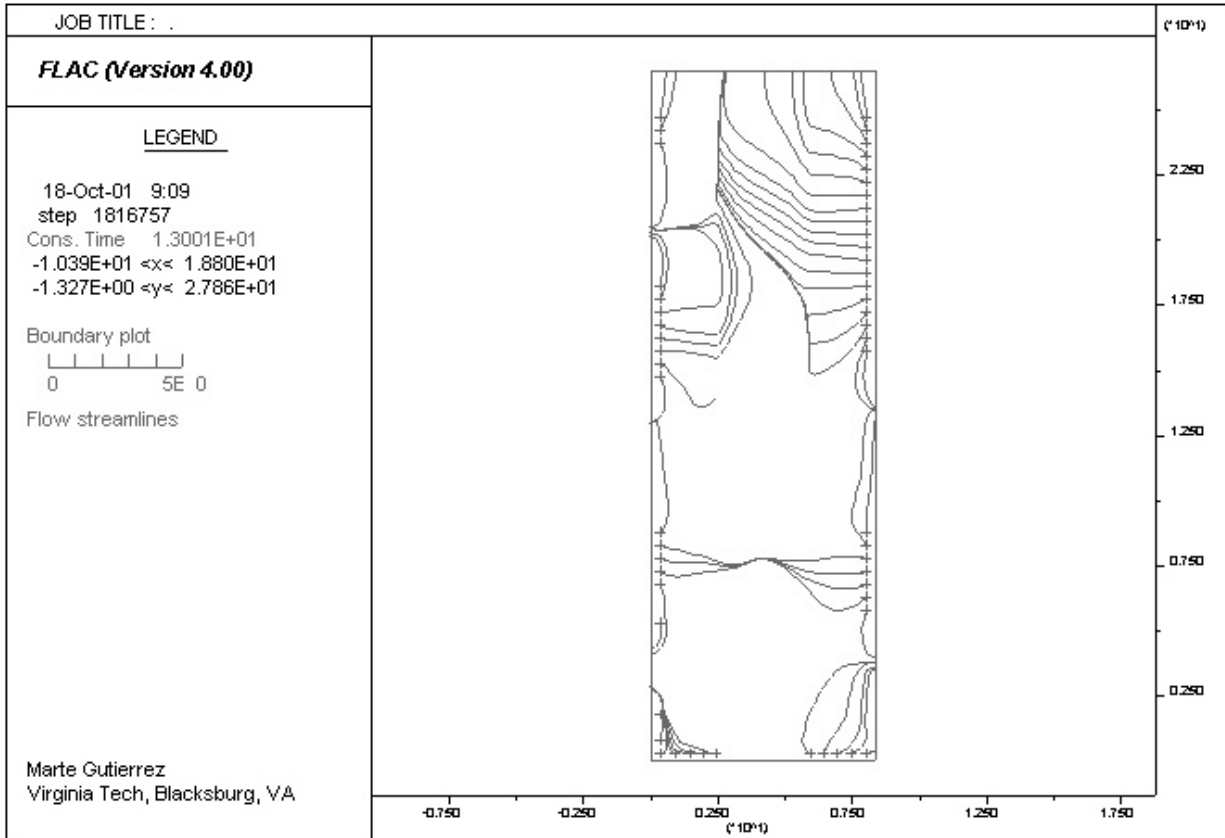


Figure 6.69 Flow streamlines for Case 9S

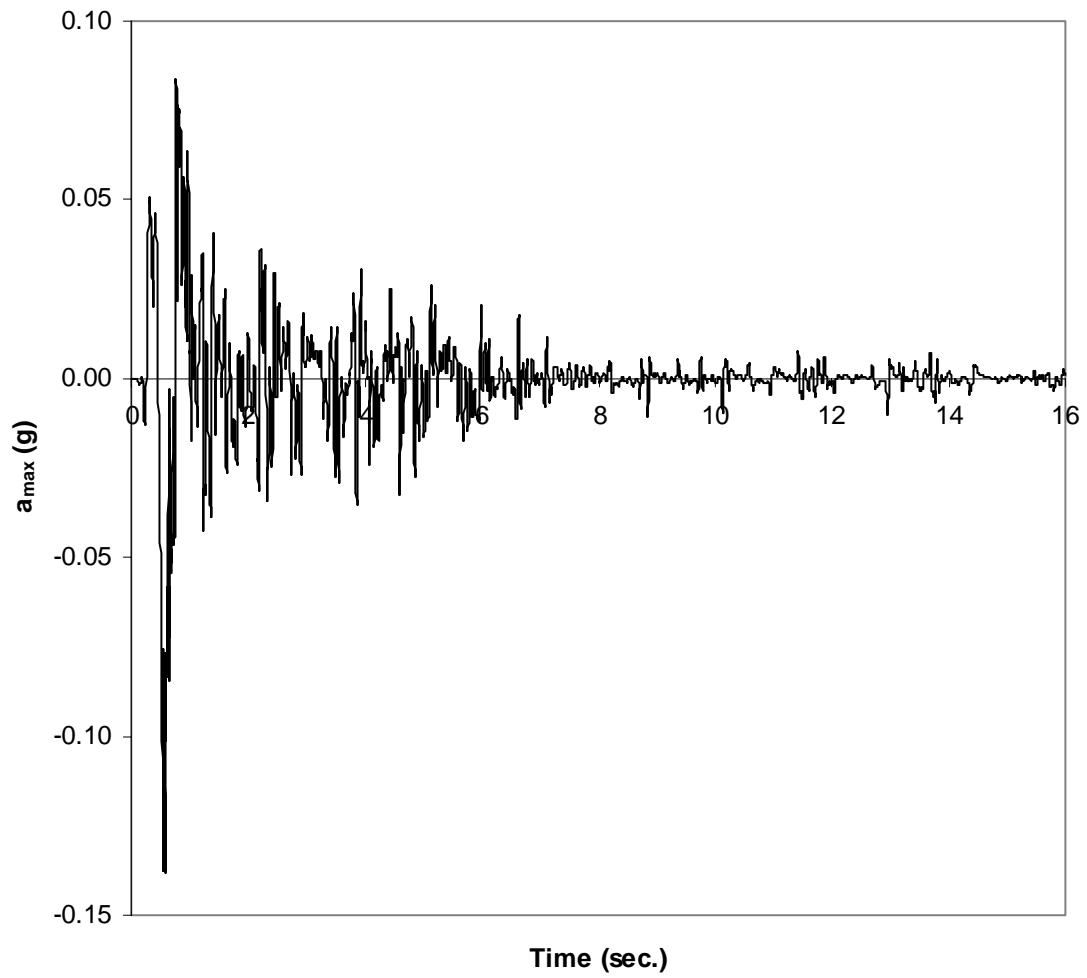


Figure 6.70 Acceleration time history (a_{max}) for Case 1C2

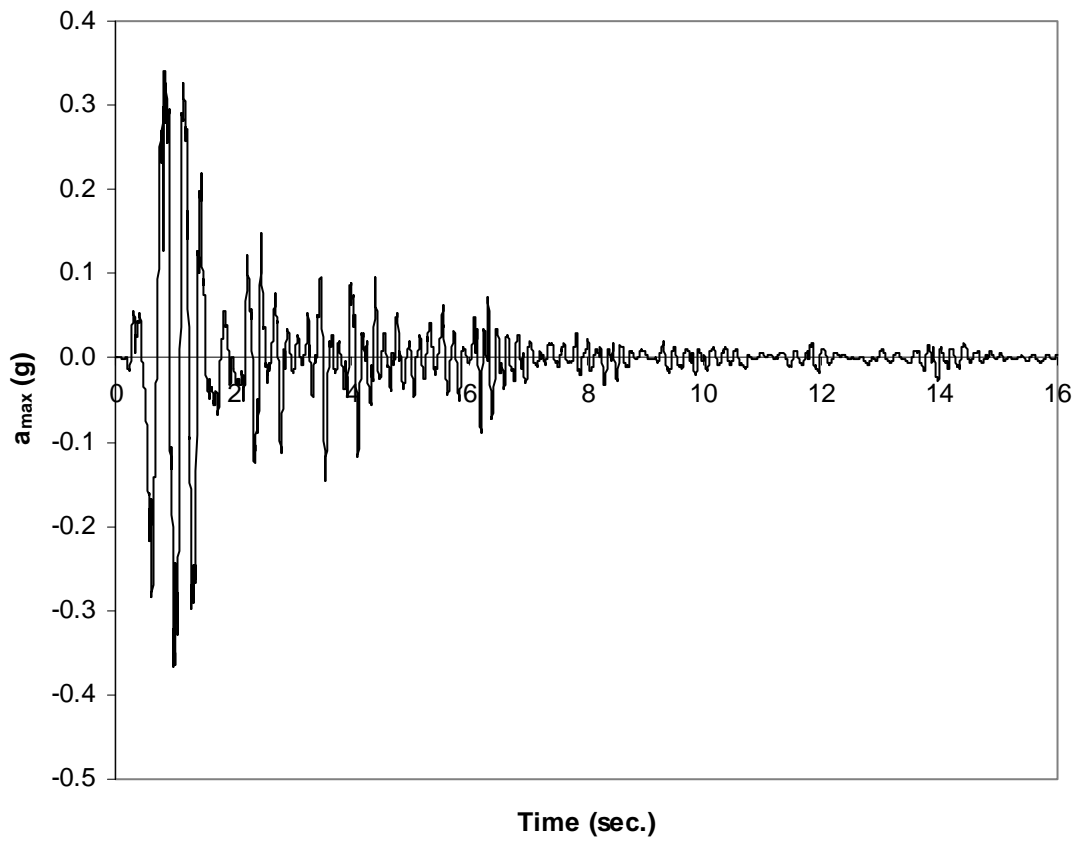


Figure 6.71 Acceleration time history (a_{\max}) for Case 2C2

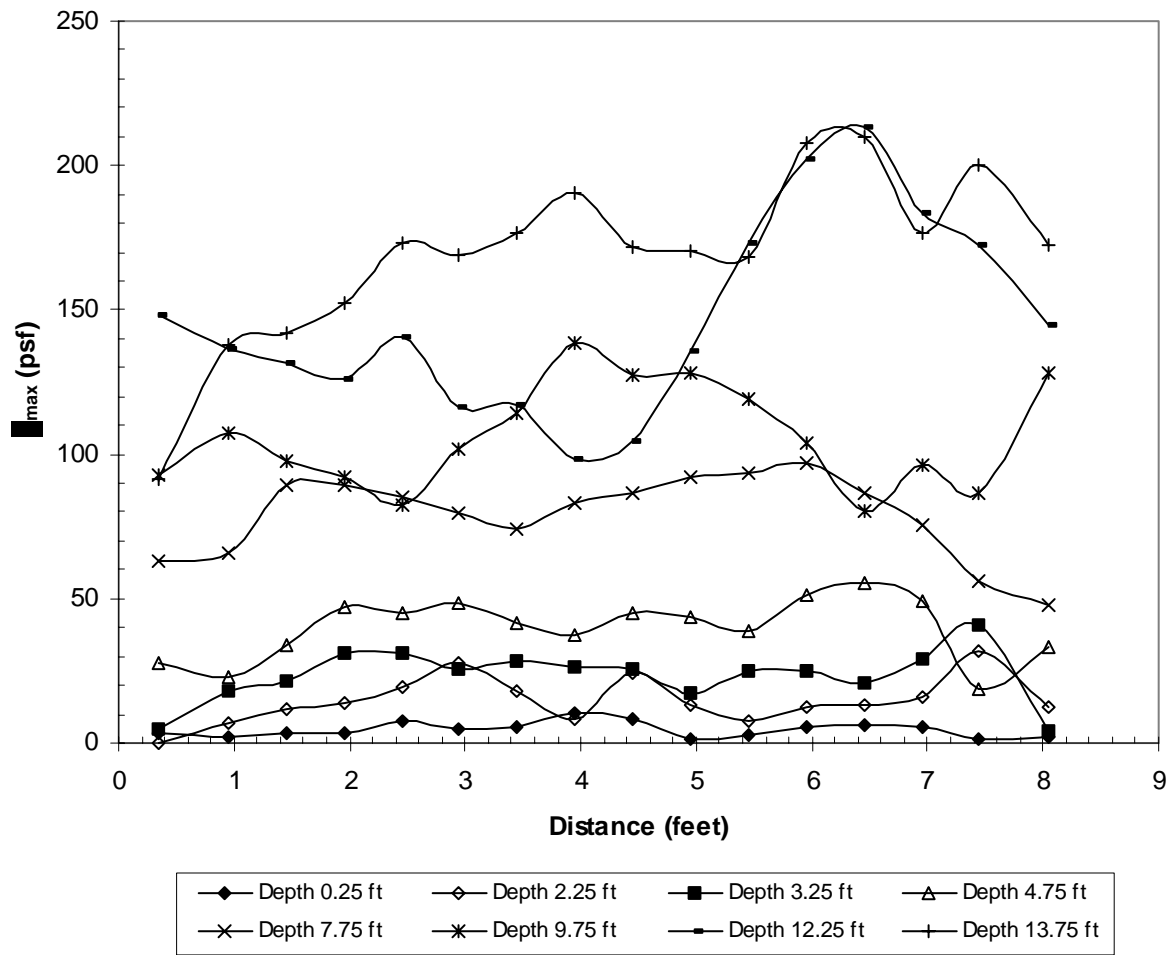


Figure 6.72 Plot of τ_{\max} versus distance for different depths for Case 1C2

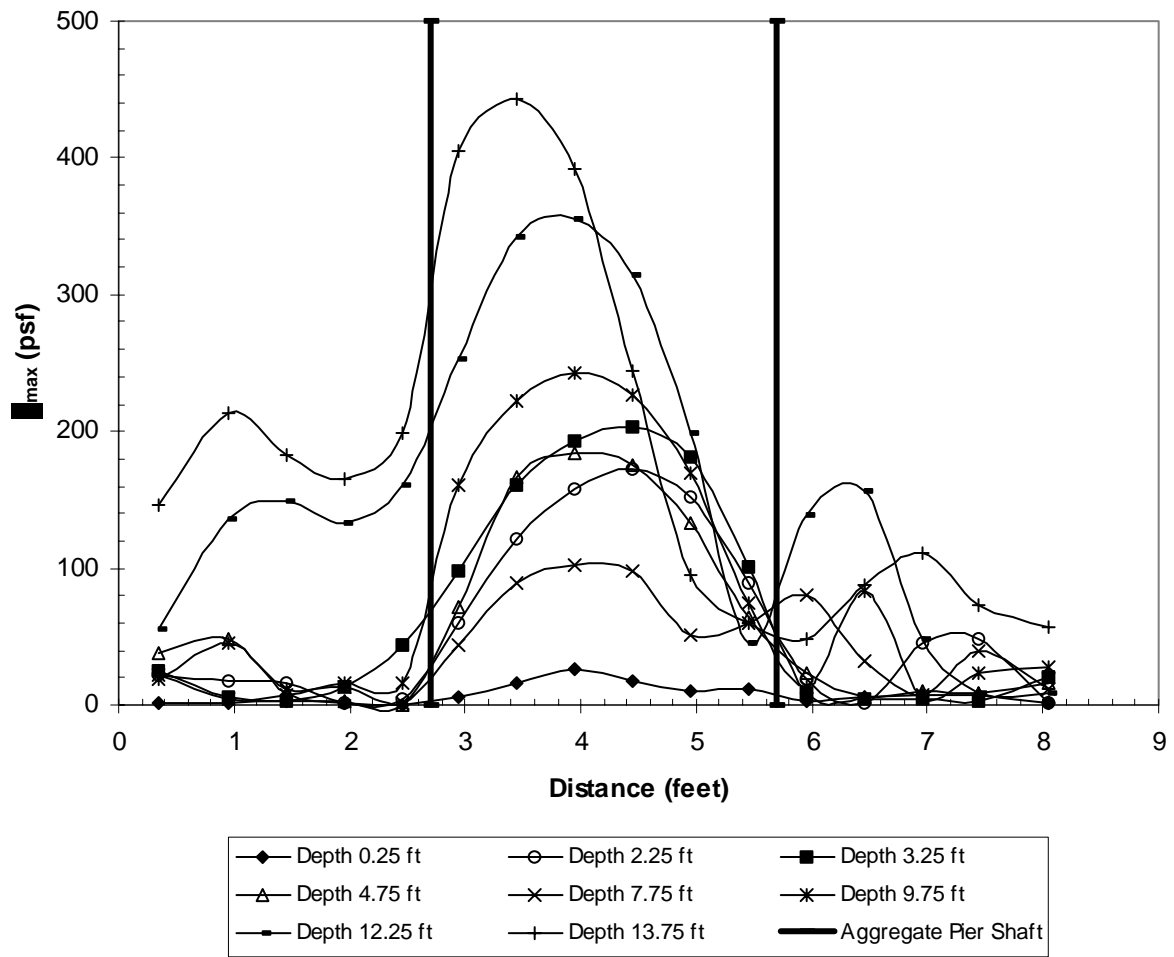


Figure 6.73 Plot of τ_{max} versus distance for different depths for Case 2C2

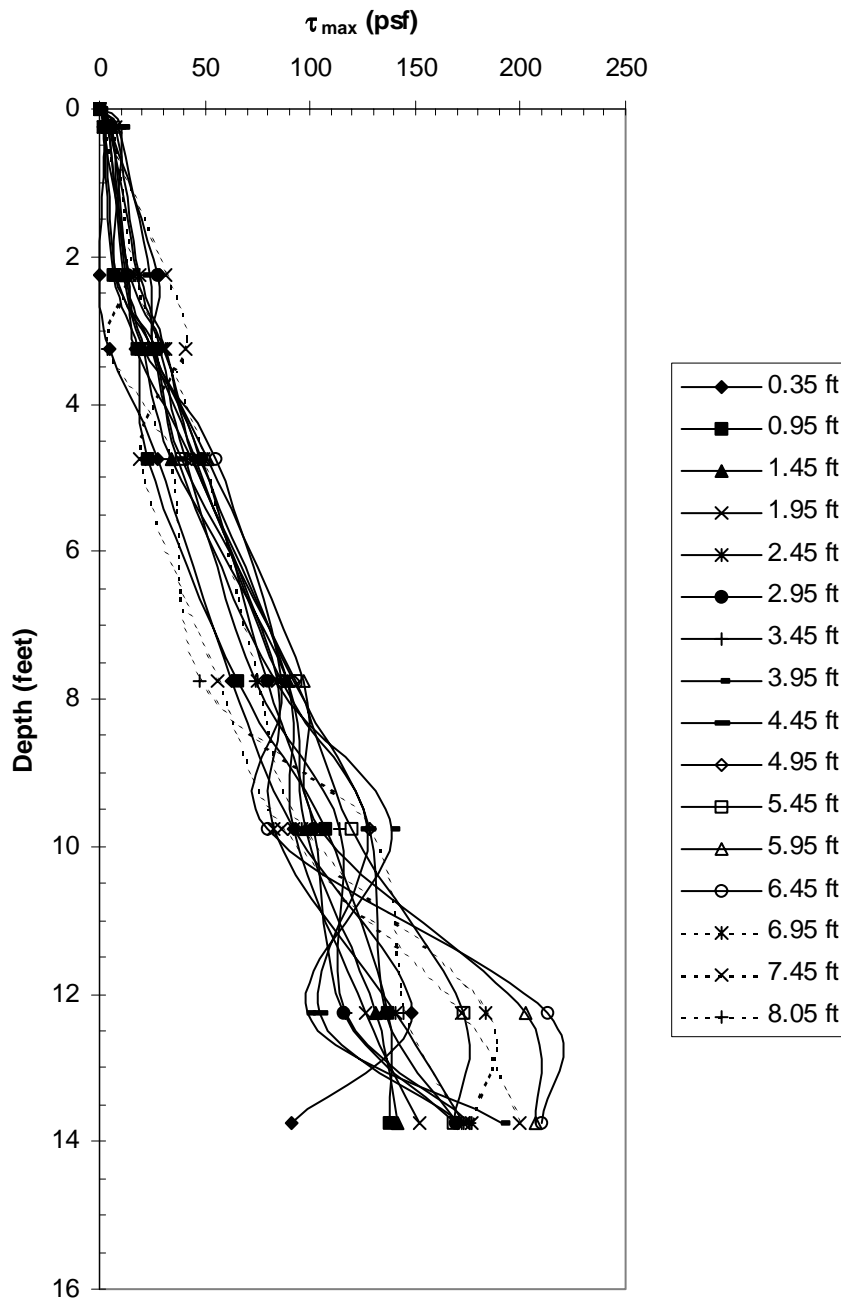


Figure 6.74 Plot of τ_{max} versus depth for different distance for Case 1C2

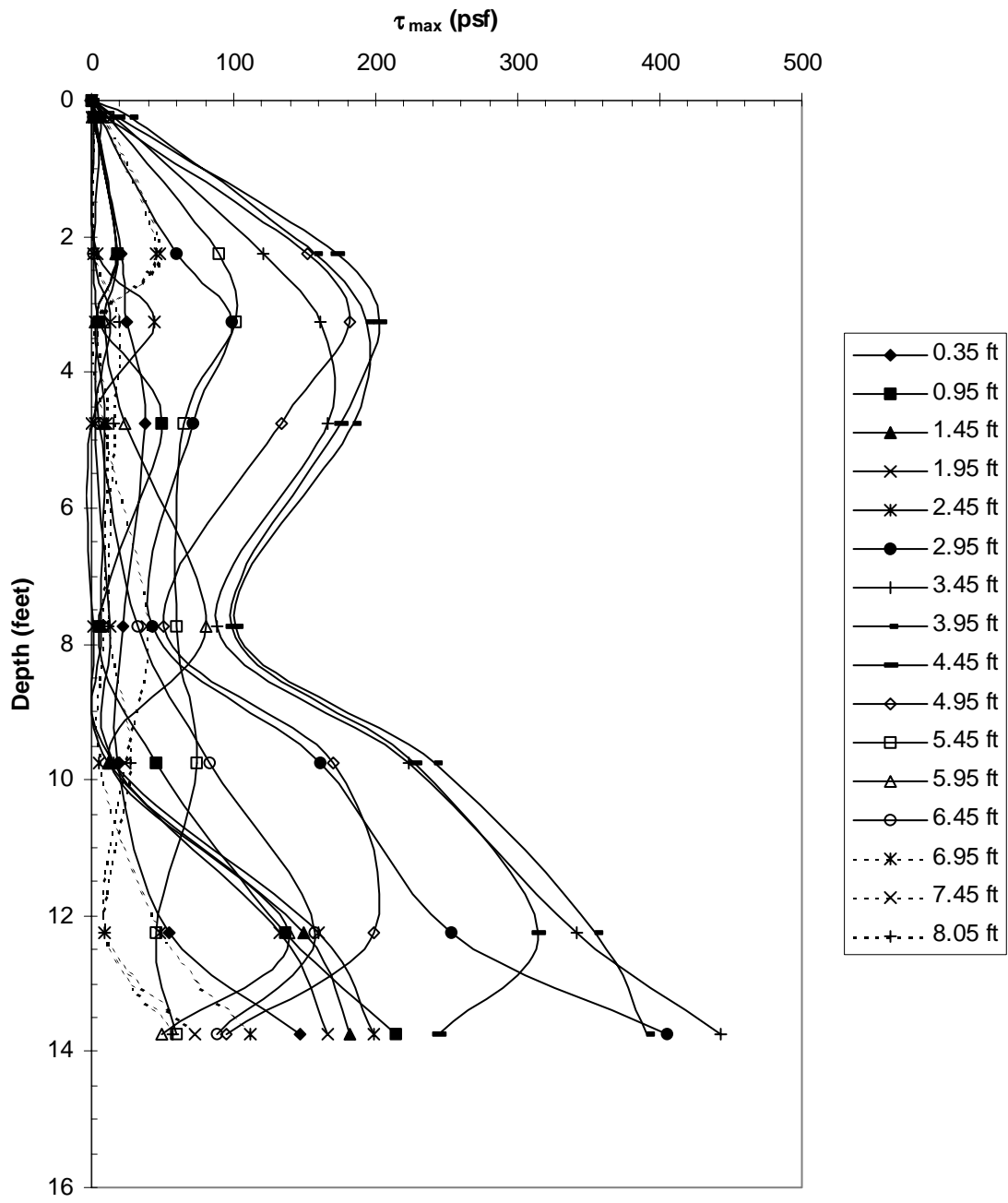


Figure 6.75 Plot of τ_{max} versus depth for different distance for Case 2C2